University of Technology Sydney

Faculty of Engineering and IT

School of Electrical and Data Engineering

Development and Optimisation of Wireless Indoor localisation for the IoT Solutions

Doctoral Candidate: Yu, Zheng yu

CERTIFICATE OF ORIGINAL AUTHORSHIP

I, Zheng yu Yu declare that this thesis, is submitted in fulfilment of the requirements for the award of a degree of Doctor of Philosophy, in the Faculty of Engineering and IT at the University of Technology Sydney.

This thesis is wholly my own work unless otherwise reference or acknowledged. In addition, I certify that all information sources and literature used are indicated in the thesis.

This document has not been submitted for qualifications at any other academic institution.

This research is supported by the Australian Government Research Training Program.

Signature:

Production Note:
Signature removed prior to publication.

Date:

19/07/2020

ACKNOWLEDGMENTS

I would first like to express thanks to my PhD supervisors, Dr Zenon Chaczko and Prof Robin Braun. I have collaborated with my supervisors on several projects for the past four years. Dr Chaczko, you have been more than a supervisor to me all these days, and you have been with me every step of the way throughout this research. Thank you for your kind support during, at times, very stressful moments that I have experienced. I really appreciated your clear guidance and feedback very much.

Also, I appreciate support and help received from the Faculty of Engineering and IT staff and academics, especially that of Prof David McGloin. Thank you so much for organising series of insightful research seminars and providing comments related to my research in those past years. I have learned so much and adopted many of the most up-to-date research information and technology from these presentations.

Lastly, to my family and friends those who always support and encourage me, thank you for being with me all the time. I could not have got this far today without you. I wish for everyone's dream to come true and that you will all lead a happy life.

Contents

List of Figures

List of Tables

Acronyms used in the thesis

ABS	Active Badge System
AoA	Angle of Arrival
AP	Access Point
APS	Ad-Hoc Positioning System
AR	Augmented Reality
BLE	Bluetooth Low Energy
CF	Curve Fitting
CFKF	Curve Fitted Kalman Filter
DV-HOP	Distance Vector Hop
EPG	Electronic Program Guide
FM	Frequency Modulation
GPS	Global Positioning System
HVAC	Heating, Ventilating, and Air Conditioning
IMU	Inertial Measurement Unit
IoT	Internet of Things
KF	Kalman Filter
LBS	Location-Based Service
LSBA	Link State-Based Annulus
MEMS	Micro-Electro-Mechanical-Systems
NFC	Near-Field Communication
NLOS	None Line of Sight
PVR	Personal Video Recorder
QR	Quick Response
RFID	Radio-Frequency Identification
RMSE	Root Mean Squared Error

RP	Reference Point
RSS	Received Signal Strength
RSSI	Received Signal Strength Indicator
RWLS	Residual-Based Weighted Least Square
SSE	Sum of Squares Due to Error
TDOA	Time Difference of Arrival
ToA	Time of Arrival
ToF	Time of Flight
UUID	Universal Unique Identifier
UWB	Ultra-Wide Band
WLAN	Wires Local Area Network
WSN	Wireless Sensor Network

ABSTRACT

Traditional indoor localisation technologies are based on beacon technology, ultrasonics, laser range localisation, or Ultra-Wide Band (UWB) system, and others. Recently, some of these localisation techniques are used in the industry by developers of iBeacon systems for finding the position of an object with Bluetooth sensors. There are various advantages of using the iBeacon-like systems, such as low-cost, a simple signalling process, and the ease of set-up and maintenance. However, using the iBeacon-based system is marked with poor accuracy. With current technology, it is difficult to obtain highly accurate localisation for indoor objects or to perform their tracking. Also, iBeacons are highly susceptible to environmental noise interference and other radio signals. To solve these issues, this research work involves investigation and development of the error modelling algorithms that can calibrate the signal sensors, reduce the errors, mitigate noise levels and interference signals. This thesis presents a new family of error modelling algorithms based on the Curve Fitted Kalman Filter (CFKF) technique. As a part of the research investigation, a range of experiments were executed to validate the accuracy, reliability and viability of the CFKF approach. Experimental results indicate that this novel approach significantly improves the accuracy and precision of beacon-based localisation. Validation tests also show that the CFKF error modelling method can improve the localisation accuracy of UWB-based solutions.

Chapter 1

Introduction

1.1 Background

Currently, the communication technology of Wireless Sensor Networks (WSN) as well as in Internet of Thing (IoT) is developing very rapidly. In particular, the technologies related to the indoor localisation services are in high demand. Indoor localisation technology is becoming more and more popular as a research topic. These days, it is one of the hottest research technology topics related to the domain of localisation.

For some time now, in the outdoor localisation domain, the technology of Global Positioning System (GPS) is being successfully used to achieve the localisation solution. However, the limitation of the GPS technology is that they must have line of sight communication with the satellites. The communication with satellites, however, will be poor, and possibly no signals may be received in the indoor environment. Therefore, it is evident that there are significant differences between the technologies of outdoor localisation and indoor localisation.

Research into indoor localisation began much later than research into outdoor localisation. Nevertheless, the research into indoor localisation has made remarkable headways recently.

At present, there are many various WSN based technologies that are used in the indoor localisation field, such as Bluetooth, ZigBee, Wi-Fi, UWB and Near-Field Communication (NFC). Most of them have indoor positioning network technology to determine the location of the device and the target by utilising particular algorithms with the received signal data.

The applications of wireless technologies have developed rapidly in many areas, including education, healthcare, industry, research, agriculture, and so on. They are essentially benefitting the development of the economy and lifestyle of human society. However, in terms of their accuracy and robustness, most of the indoor localisation technologies reveal weaknesses and disadvantages (see table 1, page 41).

In order to improve these weaknesses, an innovative error modelling solution for indoor localisation is developed and validated in this thesis. Using the related theory of indoor localisation technology, the thesis is focused on the fundamental technology required for the solution of indoor localisation accuracy.

1.2 Scope

Indoor localisation technology is an essential field in the research of WSN. If the location of the sensors is unknown, data from the sensors is not usable.

Currently, the Received Signal Strength Indicator (RSSI) is widely used to measure the range in WSN as it is operated smoothly. In the general indoor area, multipath fading effects impact the location measurement from the RSSI method. People, furniture and objects always interfere with signal transmission. Therefore, the measurement accuracy of the RSSI localisation method is poor. This thesis proposes a new localisation error modelling methodology based on an error modelling filtering adjustment strategy.

1.3 Research Questions

Most of the applications in the WSN use the sensor node localisation method and the range-based localisation method; They must calculate the range between the nearest nodes. Research into the range measurement method between sensor nodes is required. The node localisation method of the WSN generally measures the range from RSSI. At present, several related types of research have been developed in the literature. In this area, this study proposes a designed error modelling calibration and data processing algorithm with a hardware system such as iBeacon and UWB in order to reduce the errors in measurement. Eventually, the solution presents that the result of our curve fitted Kalman filter error modelling is the best for both iBeacon and UWB.

1.4 Research Hypothesis

The research hypothesis for this work is stated as follows:

" It is possible to improve the accuracy and precision of localisation based on the distance measurement for wireless sensor network nodes using a correction mechanism based on the CFKF error modelling algorithm. "

In the CFKF algorithm, the calibration of iBeacon sensors is firstly taken into consideration. Then, error modelling is used to improve the measured sensor data from the iBeacon. Finally, the CFKF error modelling is also used to obtain the optimal sensor data from the UWB anchor. The aim of this research is to perform several experiments that compare traditional approaches for error filtering and to compare these methods with the proposed

CFKF error modelling. The experiment will effectively demonstrate the improvement in accuracy and precision of indoor localisation.

1.5 Research Contributions

In this research work, localisation methods are used to estimate the distance, such as the RSSI method for iBeacon localisation system and the Time of Flight (ToF) method for the UWB localisation system. Most WSN devices can obtain the value of RSSI; however, the estimated distance from RSSI is neither accurate nor robust. Unlike iBeacon, UWB anchor provides higher accuracy, but various errors still occur in the received sensor data. In order to solve these issues, a novel CFKF error modelling is proposed for indoor localisation system. In our publications, we have developed an error modelling for Micro-Electro-Mechanical-Systems (MEMS) accelerometers (Yu et al, 2019), Inertial Measurement Unit (IMU) (Yu et al, 2018), and RFID (Chaczko & Yu et al, 2019) for indoor localisation.

The main contributions of the research work are:

• Improved estimation of distance using orientation awareness calibration

• The calibration and experimental measurements from RSSI method in iBeacon system using the mean fitted and curve-fitting algorithm

• A novel error modelling using the CFKF method has been developed to optimise the estimation accuracy in the experiment and field experiment for both iBeacon and the UWB indoor localisation systems.

• A developed Least Squares algorithm based CFKF error modelling is introduced to improve the accuracy of the distance and coordinate for the UWB moving tag.

The following are publications of my research work:

Book Chapters (Published):

1. Yu Z., Chaczko Z., Shi J. (2020) Low Cost Wireless Micro-Electro-Mechanical-Systems Accelerometers Linear Sensor Model. In: Klempous R., Nikodem J. (eds) Smart Innovations in Engineering and Technology. ICACON 2017, APCASE 2017. Topics in Intelligent Engineering and Informatics, vol 15. Springer, Cham
2. Chaczko Z., Chiu C., Yu Z. (2020) Assessment of a Multi-agent RFID Platform for Industrial Logistic Operations. In: Klempous R., Nikodem J. (eds) Smart Innovations in Engineering and Technology. ICACON 2017, APCASE 2017. Topics in Intelligent Engineering and Informatics, vol 15. Springer, Cham

Papers (Published)

3. Yu Z, Chaczko Z, Optimization of IMU Indoor Localization with Wireless Sensors, 2018 4th IEEE International Conference on Computer and Communications, December 7-10, 2018.
4. Yu Z, Chaczko Z, Jiang J. Development and Optimization of Wireless Indoor Localization Error Modelling, International Conference on Systems Engineering. IEEE Computer Society, 2017:475-479.

1.6 Thesis Structure

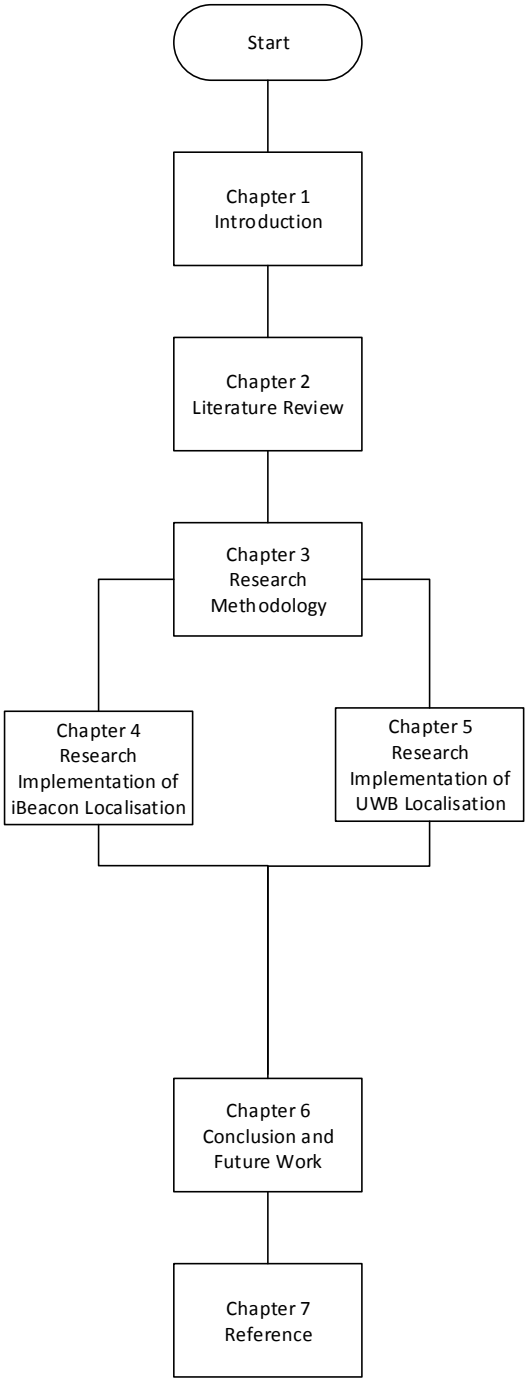

Figure 1 Thesis structure

The structure of the thesis has been presented in figure 1. The details of this structure are explained below:

1.6.1 Introduction

This chapter presents background information and an introduction to the indoor localisation system for this thesis. In particular, various indoor localisation methodologies have been reviewed. The research problem, research hypothesis, research contributions and thesis structure are also stated and explained.

1.6.2 Literature Review

This chapter opens by getting familiar with the research topic and discovering the problems in the area. Literature on indoor localisation techniques and their background is reviewed. Various indoor localisation technologies have also been reviewed such as ultrasonic sensors, iBeacon system, and UWB system.

1.6.3 Research Methodology

This chapter presents many different measurement methods for indoor localisation, such as signal strength spatial mapping, time of flight, Kalman filter, trilateration, triangulation and fingerprinting. The IBeacon structure and protocol have been introduced in the chapter, which includes UUID, Major number, Minor number and advertising interval. Calibration and ranging operations are also discussed as a part of the error modelling. The functional block diagram displays both the processes of system calibration and system error modelling estimation. A novel CFKF error modelling algorithm is introduced in this chapter to generate more accurate and reliable measurement results for the indoor localisation system.

1.6.4 Research Implementation of iBeacon Localisation

This chapter starts from a testbed set up and system calibration for the iBeacon localisation system. The experiments involve a set-up of six iBeacons. During the angel calibration process, different angles of the iBeacon transmit different signal strengths. The value of the received RSSI is slightly different from different angles. The standard RSSI for 1 meter has been calculated with the developed CFKF error modelling to reduce the outliers of the raw data and measured distances. The developed RSSI distance algorithm calculates the values of the distances for transmission. Diagrams are plotted to analysis the accuracy of the localisation method. The field experiment is operated to validate improvement of the accuracy of the CFKF error modelling method in real life. After comparing with other localisation algorithm, the result from CFKF error modelling algorithm with the error rate about 4.5% provide the best accuracy and reliability for the iBeacon localisation system.

1.6.5 Research Implementation of UWB Localisation

This chapter provides the experiment with 3 UWB anchors and 1 tag. The UWB localisation system testbed has been set up and calibrated. Angles calibration has been processed to determine that the distance measurements are various from different angles. Several different algorithms have been used to determine the best method for calibration at the first stage. After the calibration process, the measurement experiments have been processed to determine the estimated distance. The field experiment is a dynamic research, a developed Least Squares algorithm based CFKF error modelling is used to determine the distance and coordinate the moving object. Finally, according to all the records, it is

validated that the results with an error rate (1%-2%) from the CFKF error modelling algorithm are the most accurate and robust method for UWB system.

1.6.6 Conclusions and Future Work

This chapter provides the conclusion to the thesis. It starts with summaries of each chapter. Then the chapter contains thesis contribution, discussion and imitation of the research work and propose future work.

1.6.7 Reference

This chapter presents the reference list.

Chapter 2

Literature Review

This chapter presents literatures on indoor localisation techniques and their background. Various indoor localisation technologies have been reviewed such as ultrasonic sensors, iBeacon system, and UWB system.

2.1 Indoor Localisation Techniques Review

2.1.1 Ultrasonic Sensor-Based Indoor Localisation System[1]

Recently, there has been enormous interest in the Internet of Things (IoT), Industry 4.0 (industrial IoT), Wireless Sensor Networks and Big Data technologies. Most of applications related to these technologies require effective systems for the localisation of objects (i.e., things, humans, entities, events, etc.). Apart of GPS-based solutions, there are many indoor localisation systems that have been used to estimate the distance of objects, such as ultrasonic system, camera system and beacon system (Gatesichapakorn, Takamatsu & Ruchanurucks 2019; Ueda et al. 2011).

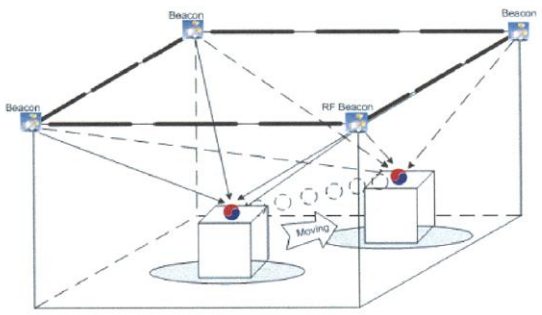

Figure 2 Basic concept of localisation system (Hong-Shik & Jong-Suk 2008)

[1] Published in Yu Z, Chaczko Z, Jiang J. Development and Optimization of Wireless Indoor Localization Error Modelling, International Conference on Systems Engineering. IEEE Computer Society, 2017:475-479.

These indoor localisation solutions have many applications ranging from environment monitoring, multimedia, health services, transport infrastructure and many more. In 2008 Hong-Shik and Jong-Suk introduced an interesting beacon system using ultrasonic media in indoor localisation (Hong-Shik & Jong-Suk 2008). However, due to highly sensitive noises and shocks, it was difficult for ultrasonic sensors, used in the implementation, to generate highly accurate locations for moving objects. To mitigate the problem, the authors designed a band pass-filter solution that isolated targeted frequencies from noises and shocks (Hong-Shik & Jong-Suk 2008). Several researchers suggest implementations of the Unscented Kalman Filter (UKF) technique that allows the optimisation of the indoor localisation system (Sen, Chakraborty & Sutradhar 2015; Zhao & Mili 2019).

2.1.2 RSSI-based Indoor Localisation with High Accuracy[1]

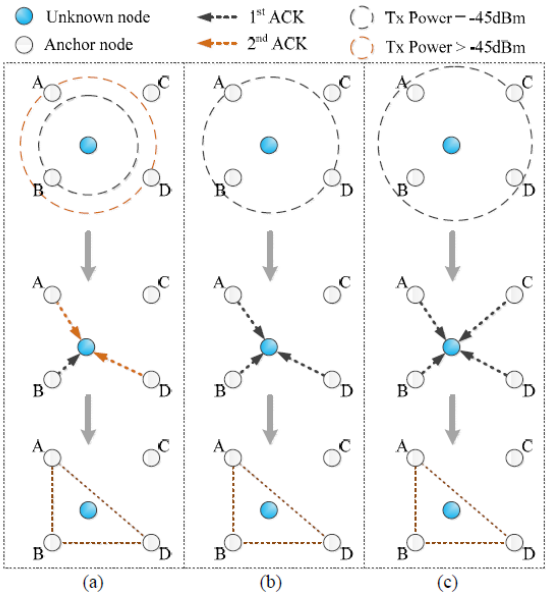

Figure 3 An example of localisation processes (Wang et al. 2012)

[1] Published in Yu Z, Chaczko Z, Jiang J. Development and Optimization of Wireless Indoor Localization Error Modelling, International Conference on Systems Engineering. IEEE Computer Society, 2017:475-479.

In the WSN-based indoor localisation solutions can be realized using groups of collaborating low power sensors nodes that generate radio signals. Wireless nodes in the WSN can include numerous sensors that are integrated with small computing chips. Very sophisticated WSN solutions requiring indoor localisation can be developed by deploying thousands of low power sensor nodes for monitoring environment (Chen et al. 2007), homecare applications (Meltzer et al. 2010), home and building automation (Osterlind et al. 2007), and many more.

However, these solutions often develop serious issues related to security (Ng, Sim & Tan 2006), coverage (Li, Wan & Frieder 2003), reliability, navigation and tracking (Olule et al. 2007). Lately, navigation problems related to WSN and IoT applications received much research attention. Various approaches have been suggested which involve using large groups of collaborating sensors in the navigation industry to provide sensing data, as well as, positioning information.

Traditional GPS receiver based localisation methods are not widely used in large-scale Wireless Sensor Networks applications, as there are many disadvantages of such solutions related to energy consumption and cost (Savvides, Han & Strivastava 2001). Other issues relate to the fact satellite signals have coverage limitations in the indoor environment.

There are many WSN and IoT based solutions where various sensors are used for detecting object positioning with high accuracy in indoor localisation systems. Some of these solutions use ultrasonic sensors (Boukerche et al. 2007), RFID devices (Kumagai & Cherry 2004) and infrared sensors (Moses, Krishnamurthy & Patterson 2003). However, some of those sensors are high cost too. Two kinds of precise localisation methods, range-based and range-free techniques, have been introduced to avoid application of the above localisation methods.

There are some popular range-free algorithms available, such as the Distance Vector Hop (DV-HOP) (Niculescu & Nath 2003), an Ad-hoc Positioning System (APS) (Ji & Zha 2004), centroid, amorphous, and Link State-Based Annulus (LSBA) localisation algorithm (Nagpal, Shrobe & Bachrach 2003).

One of the simplest object localisation methods to implement is the centroid technique which utilises anchor nodes as reference nodes to calculate the localisation of another unknown node. Moreover, one of the most popular methods is DV-HOP which estimates localisation information from reference locations. The hops are counted between corresponding nodes and anchors using an average distance(s) parameter. Nevertheless, the limitation of DV-HOP is on low accuracy, due to the position of all the hops not being identical. Therefore, the localisation accuracy of the range-based algorithm is much higher than the range-free algorithm (Wang et al. 2012).

2.1.3 FM Signals-Based Indoor Localisation[1]

Since its availability in the commercial world, GPS technology has contributed to a range of various solutions in the outdoor navigation area. These days, in a similar way, almost revolutionary changes are taking place in the indoor navigation and localisation area. For example, users in a shopping centre could access their sensor device such as mobile phone, tablet, and smartwatch with an accurate indoor navigation system, to search and navigate the real-time position and direction of any store in that shopping centre. Once the user walks into a shop, the directions could be displayed on the user's mobile device automatically. Meanwhile, the shopping centre could push advertisement and voucher offers into users' mobile devices at their position in the shopping centre, which could

[1] Published in Yu Z, Chaczko Z, Jiang J. Development and Optimization of Wireless Indoor Localization Error Modelling, International Conference on Systems Engineering. IEEE Computer Society, 2017:475-479.

maximise users' interests efficiently. Since GPS signals are not available inside buildings, those scenarios are facing excellent prospects and new application opportunities.

In the absence of GPS signals, the technology of fingerprint-based indoor localisation is becoming the most accurate technology in the indoor localisation area (Bahl et al. 2000; Haeberlen et al. 2004; Youssef & Agrawala 2005). There is no deployment of hardware requirements. Most of the locations have already set up wireless sensor networks, such as Wi-Fi, cellular and Bluetooth with the information of RSSI values (Varshavsky et al. 2007). In the past, due to access points of Wi-Fi being widely set up indoors, and all the mobile devices being designed with Wi-Fi receiver, RSSI value of Wi-Fi sensors have been widely used in the area.

Firstly, the implementation has been utilised to locate people successfully. However, it is limited to detecting the localisation of the room level in indoor environments. Human

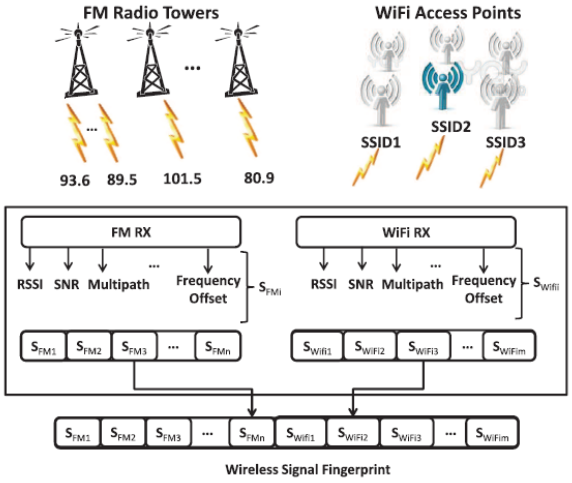

Figure 4 Wireless Signal Fingerprint (Chen et al. 2013)

beings and small objects in a room could interfere with the transmission of the Wi-Fi frequency.

Therefore, localisation error could be generated by the variability of fingerprints records. Secondly, commercial Wi-Fi access points have been deployed in nature. Frequency hopping is employed to improve network reliability, optimisation method. Therefore, observed received signal strength becomes variable due to the optimisation method. Thirdly, the coverage area of the Wi-Fi access point could be smaller inside the building due to the interference from objects, such as walls, metals and the human body (Chen et al. 2013).

Wi-Fi signals for fingerprinting could be replaced by using Frequency Modulation (FM) broadcast radio signals for indoor localisation to improve these limitations of the wireless sensor network. In the US, signals of FM frequency are in the range of 88-108 MHz, which experience less inference from small objects (Alomainy et al. 2006; Karunarathna & Dayawansa 2006). Moreover, FM can transfer over hundreds of kilometres; the coverage is much further than Wi-Fi converge. FM signals are accessible by the majority of mobile devices with an FM receiver; it uses less power consumption and runs at a lower cost than WiFi receivers (Chen et al. 2013).

2.1.4 RSS Fingerprint-Based Indoor Multi-Resolution Localisation[1]

Nowadays, the technology of fingerprint-based localisation which generates localisation information from a mobile device is becoming popular in the research area. Among many approaches, in the fingerprinting area, Received Signal Strength (RSS) from APS has been implemented widely in the Wireless Local Access Network (WLAN) (Bahl et al. 2000;

[1] Published in Yu Z, Chaczko Z, Jiang J. Development and Optimization of Wireless Indoor Localization Error Modelling, International Conference on Systems Engineering. IEEE Computer Society, 2017:475-479.

Honkavirta et al. 2009; Wassi et al. 2005). For a given indoor mapping localisation case, RSS profiles of Reference Points (RPs) are measured, calculated and recorded as fingerprints in a database when it is in an offline environment before mapping. When it is online, a moving object compares the measured offline RSS fingerprints to estimate the actual location.

Most recently fingerprinting localisation methods have been utilising point localisation. The actual location for a moving object can be estimated. The point localisation is still facing some practical limitations, although some algorithms of fingerprinting have been reported to approach outstanding accuracy of localisation (Fang & Lin 2008; Laoudias, Michaelides & Panayiotou 2011; Yin, Yang & Ni 2008). Firstly, fingerprint accuracy is computation intensive. The RPs are calculated with good granularities to generate higher accuracy, for instance, a reference point per square meter. Moreover, when the size if the area increases the number of fingerprints also increases. Hundreds of RPs may be set up in an ample space. Secondly, when many moving objects are seeking the signal of localisation together, the calculation of the real-time location information may be heavy, which may generate some delay information for the moving objects. Finally, in some indoor localisation case studies, some moving objects may not need to be computed localisation precisely. The trace of the record may be enough for the localisation purpose.

A fingerprint clustering method is applied in some works to increase the speed of the localisation process (Chen et al. 2006; Kuo et al. 2007). This idea can be divided into two different phases; online and offline. For the offline phase, according to all the RP's signals, all the RPs are into different clusters, for example, the rule of iteration, the rule of most robust Access Point (AP) and the rule of physical closeness. In the online phase, an object is initially targeted at which cluster it is into, and then those fingerprints are compared in the particular cluster. Those clusters can reduce the calculation process and increase the computation speed (Zhou et al. 2012).

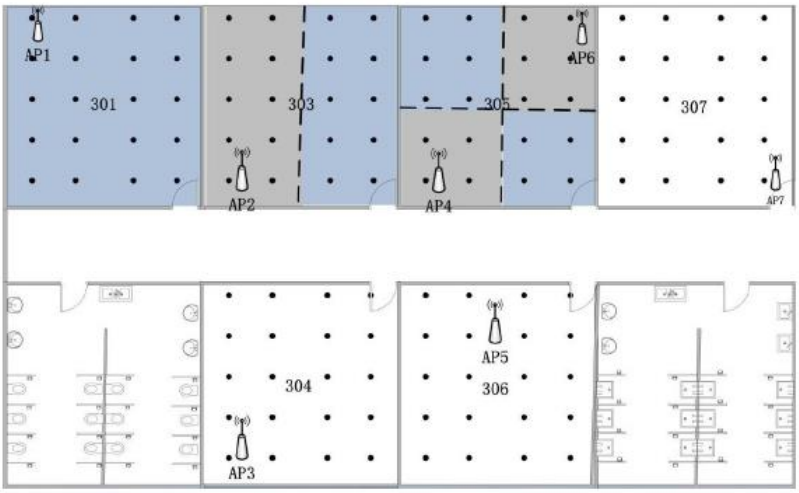

Figure 5 The Next Generation of the Internet Access System (Zhou et al. 2012)

2.1.5 Fingerprint-Based 3D Indoor Localisation in Wireless Sensor Networks

The research in the applications of WSN is led by the technology of the development of the wireless sensor network. Localisation is one of the applications to measure the localisation of a target object. WSN is operated as the network of sensor nodes (Akyildiz et al. 2002). There are two central well known technologies for indoor localisation, for example, a fingerprint-based technology and a range-based technology. Indoor localisation research in 2-dimensions have mentioned the methodology to compare fingerprint technology and rang-based technology (Cherntanomwong & Suroso 2011). The system can determine whether the object is moving or static. The result has determined that the fingerprint-based technology provides better accuracy than the accuracy from the range-based technology. Therefore, fingerprint localisation is considered in the next stage of research.

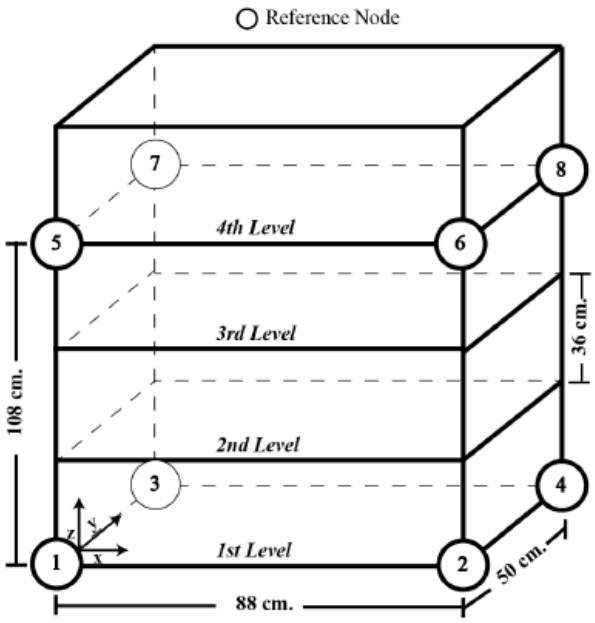

Figure 6 Illustration of the experiment system (Chuenurajit, Phimmasean & Cherntanomwong 2013)

In a real-time case study, a 3D environment is a big challenge, as more accuracy is calculated for height and altitude. For instance, when targets are in the same building, the 3D localisation will identify the differences in the height on the same floor plan to determine the different locations of the objects. According to the signal pattern with the information of recorded known signal location, the fingerprint technology can detect the location of the object. In some cases, the ZigBee standard (IEEE 802.15.4) wireless sensor is setup as reference nodes or target nodes (Cherntanomwong, Takada & Tsuji 2009). ZigBee has many strengths, including low-cost, low energy, more security, low data rates and reliability (Chuenurajit, Phimmasean & Cherntanomwong 2013).

2.1.6 RSS-based Fingerprinting in Indoor WLAN Localisation

Location-based service (LBS) has been introduced recently (Bellavista, Küpper & Helal 2008); it has widely attracted most attention in the telecom market. It integrates localisation technology, positioning information and wireless sensor data. LBS provides customers with the service of geographic location. For example, the provider of the LBS can send customers some information, such as retail shops, traffic, hotels in terms of calculated position information of smart devices. In indoor localisations, many fields are utilising LBS such as areas of entertainment, indoor mapping, logistics and so on. The satisfaction of the LBS service relays on the calculation of the localisation information. Therefore, accurate localisation technology plays an essential role in the improvement of the LBS industry. In outdoor environments, GPS has been widely used. However, GPS signals are unavailable in an indoor area (Chen et al. 2013). The accuracy of the localisation technology is low because of the propagation of None Line of Sight (NLOS).

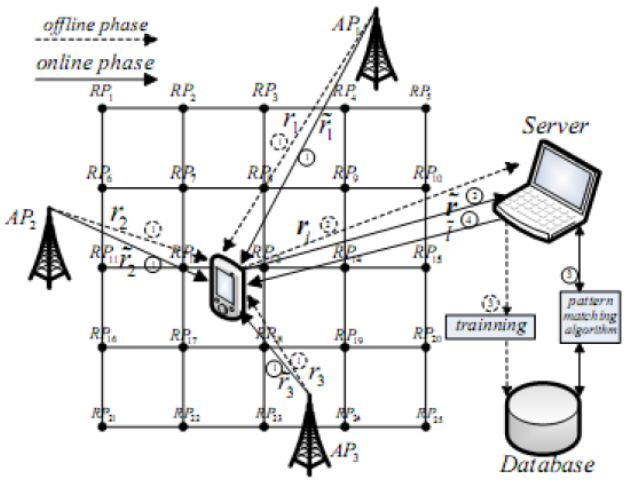

Figure 7 Fingerprinting localisation system (Ding et al. 2013)

Therefore, the popular techniques that have been introduced into indoor localisation research are radio frequency (Arnitz, Muehlmann & Witrisal 2012), wireless networks (Fang, Lin & Lee 2008), and ultra-wideband (Wymeersch et al. 2012). The standard localisation methods contain three different groups: trilateral method, triangulation method, and fingerprinting method. There are complex NLOS propagations in indoor environments. The trilateral method and triangulation method are facing significant estimated localisation errors, whereas the fingerprinting method may estimate better accuracy in an indoor localisation environment. Since wireless networks such as WIFI has been widely set up in offices, shopping centres, hospitals and so on, the localisation of the hotspots and RSS can be smoothly calculated by WIFI APs. Thus, fingerprinting becomes a hot research technique in the indoor localisation area recently.

There are two different phases in fingerprinting methods, the offline localisation calibration stage, and the online estimated localisation stage. In the offline stage, a map of radio is generated by the collection of the value of RSS from all the APs and at every Reference Point (RP). In the online stage, the target position would be calculated by algorithms of pattern matching to compare the difference of sets of collected data of real-time fingerprint with the radio map (Ding et al. 2013).

2.1.7 Hybrid Techniques in Indoor Localisation Environment

There are several categories of localisation research, among them are: radiofrequency, GPS, an infrared network, cellular networks, and indoor localisation techniques. The Active Badge System (ABS) approach is one of the new techniques in a localisation aware system (Want et al. 1992). In the system, a unique Infrared Signal could be broadcasted every 10-seconds by the badge. Sensors are set up in known locations to detect unique identifiers which are operated by location software. The method provides accurate information about the

location. However, it has some disadvantages, such as the limitation of the range of Infrared Signal, the high-cost of installation and maintenance, as well as, the presence of sunlight. In the cellular system, location techniques have been introduced such as the Time Difference of Arrival (TDoA), the Angle of Arrival (AoA) and signals attenuation (Tekinay 1998). The method generates outstanding results in the outdoor area. However, due to the multiple signal reflections from Radio Frequency sensors in the indoor environment, this method has limited accuracy. The GPS has been widely used in the outdoor environment with its highly accurate results. However, it has minimal accuracy in an indoor environment due to the lack of signals from satellites, as buildings and walls block GPS signals (Misra & Enge 1999). Mobile WIFI is an alternative localisation technique which uses signal strength to detect the location of the object (Bahl et al. 2000); this technique has been called triangulation.

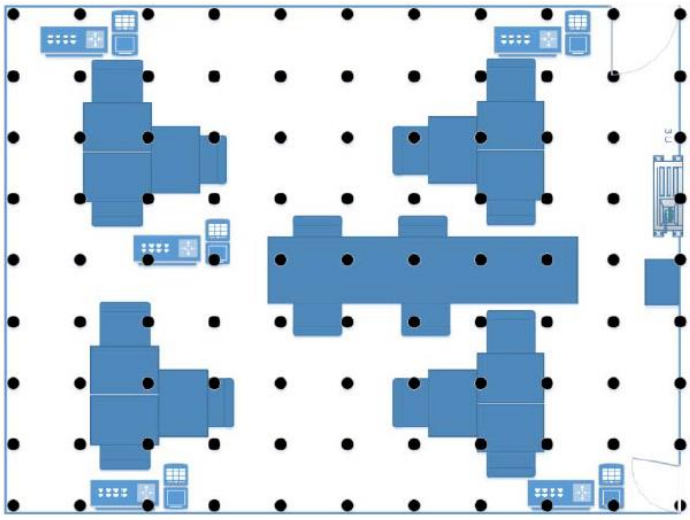

Figure 8 Floor Map of Testbed (Kharidia et al. 2014)

The example of this technique is the RADAR system, which is a radiofrequency system for detecting and tracking objects in the buildings. In the environment with multiple base stations, the strength of the signal from the RADAR-based is recorded and calculated. The

standard solution using the RADAR-based technique can handle range of about 2 to 3 meters; these are the sizes of a small room. This research is focusing on detecting various available radio frequency-based wireless network in the indoor environment. According to the deployment, scalability, range, and maintenance, networks of Radio Frequency (RF) can provide several advantages over the infrared network (Kharidia et al. 2014).

2.1.8 Wireless Optical Indoor Localisation System

In wireless network systems, in terms of their limited mobility functions, the indoor localisation technique is highly demanded (Borah et al. 2012). A wireless optical technique using in indoor localisation is introduced. The localisation technique could be determined by implementing the AoA information or detected optical signal strength. Experiment results present that about 4cm range of accuracy could be detected by the RSS method. It can be developed to about a 3cm range of accuracy by using the AoA method (Wang et al. 2016).

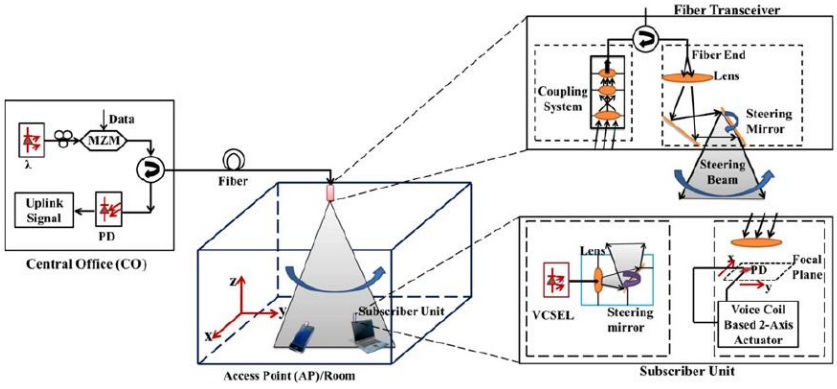

Figure 9 Architecture for both data transmission and user localisation (Wang et al. 2016)

Moreover, according to research in the transmission power level of the system, the results of the input optical signal display that the accuracy of localisation improves when the transmission power level increases. Also, a novel 3D indoor localisation technique with height measurement is introduced with the method of RSS and AoA information.

Experiment results display that the accuracy of localisation is about 7cm, whereas the error of the height measurement is less than 6cm (Wang et al. 2016).

2.1.9 Bluetooth-Based Indoor Localisation System

Since GPS-based implementations play a significant role in an outdoor environment, indoor localisation is proposed to play an essential role in our life. For personal implementations, the indoor navigation is an essential technique in indoor localisation. Museum visitors, exhibition attendees, or shopping centre visitors would not be missing or lost with accurate indoor navigation (Wang et al. 2015).

Localisation of an object is another essential implementation. Objects can be detected precisely with a highly accurate indoor localisation technique. Therefore, personal belongings could be watched securely. Once the personal belongings are missing, their location can be easily detected. For business implementation, indoor localisation can be used to analyse customers habits and interests. In terms of analysing customers' behaviours, retailers can adjust their strategy to satisfy the consumers.

There are wireless sensor network techniques, such as Wi-Fi, that are available in indoor localisation. In this research, Bluetooth Low Energy (BLE) technology is selected due to its energy efficiency and adopted functions. The BLE enables the object to last long during the operations. The adopted functions encourage indoor localisation to be used in many different systems (Wang et al. 2015).

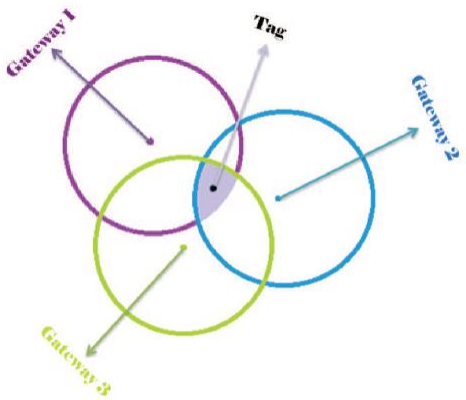

Figure 10 Tag within the Transmission Range of Multiple Gateways (Wang et al. 2015)

2.1.10Wi-Fi Fingerprint-Based and Trilateration Techniques in Indoor Localisation

Recently, as the provider of outdoor localisation services, GPS communicates with mobile devices, such as the mobile phone and mobile device. GPS outdoor localisation has been widely used by the public, however the indoor equipment poses limitations for the individual, because of the high cost for the setting up in an indoor environment (Misra & Enge 1999). The purpose of the research is to develop a low-cost indoor positioning system using WIFI network. Two different WIFI localisation methods have been used in the research. The first method is the fingerprint method which uses RSS to match the distance from proximity Access Points (APs) to the object. The second method is distance-based trilateration technique, which uses three coordinates AP to calculate the distance of the object. Accuracy of the indoor positioning could be improved based on the combination of two methods. This combination enables LBS to be communicated more effectively. The RSS mapping could also improve the network coverage of the locations where WIFI is unavailable. The result displayed in the research provides a combination of indoor and outdoor positioning to generate a gapless transmission network for users (Chan & Sohn 2012).

2.2 iBeacon Localisation Techniques Review

2.2.1 Beacon Code Extension Structure

iBeacon is a system that integrates a localisation technique of iOS7 with the BLE technique. It is used to detect situations when the object comes or goes the measured position and then calculates the range between object and iBeacon. The measurement of distance is calculated based on signal transmission and RSS from Bluetooth which includes the Universally Unique Identifier (UUID), iBeacon packet, Major information, and Minor information. The UUID is unique to each different company. The information of Major and Minor is specific for each set of related iBeacon.

For instance, UUID specifies the company name of the department store. Major information specifies the name of the group of the department store. Minor information is the name of the store. (Kim & Lee 2014)

The code area, which can be implemented, is 4 bytes in iBeacon. It can only be used to indicate an area inside the building. It is impossible to indicate every object in the building (Kim & Lee 2014).

2.2.2 iBeacon-based TV Companion Applications

A smartphone application from the manufacturer can control the modern connected TV. The applications range from the simple remote control to other featured media centres which contain PVR programs, interactive EPGs and video from TV to mobile phone. Moreover, the next generation of companion devices can communicate with the large screen and provide mobile applications with functions to extend or mirror the display of the mobile phone (Bassbouss, Güçlü & Steglich 2014).

Today, single devices and screens are the standard application models, whereas multi-screen applications experience some challenges. For example, synchronisation, communications between applications, devices discovery, the launch of applications and so on are the main challenges. New protocols, concepts, and technologies are developed to address these challenges. However, issues and limitations are still evident between different platforms and devices. For example, for controlling a companion device with the iOS platform and Android platform, two different limitations and capabilities must be considered (Bassbouss, Güçlü & Steglich 2014).

2.2.3 A Bluetooth-based iBeacon Indoor Localisation Networks

Bluetooth is a wireless low-cost sensor technique for short-range communication. For example, Bluetooth can connect a computer with a mouse, keyboard and headphone. It has successfully replaced cable communication in many implementations, industries, and applications, because of the design for continuous and streaming data applications. Recently, the increasing usage of mobile equipment increases the usage of low-cost wireless sensor devices. Attached coin-cell batteries for the power source have introduced a new industry for wireless sensor applications, for example, the Internet of Things (IoT), however, as the original Bluetooth consumes high level of power, it does not meet the low power communication designed by those applications. In 2010, the Bluetooth Version 4.0 has been developed and named BLE (Varsamou & Antonakopoulos 2014).

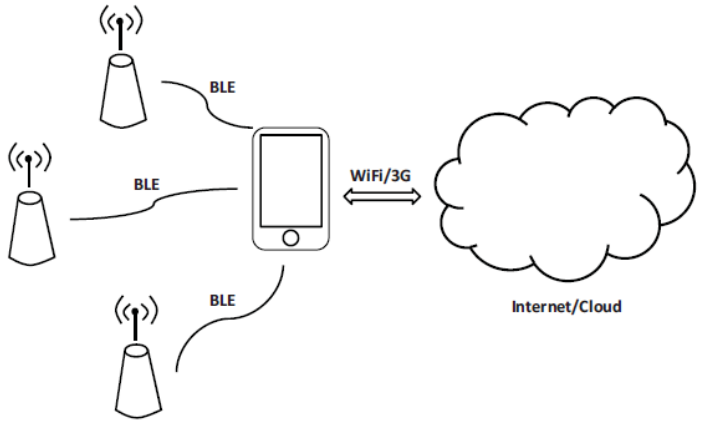

Figure 11 A star topology of BLE network (Varsamou & Antonakopoulos 2014)

Most of the components are reused from the previous version of BLE. However, a redeveloped physical layer is introduced. and it is upgraded to decrease energy usage as well as enabling asynchronous communication. After the improvement, the BLE energy consumption, in standby mode, is extremely low, and the pow consumption of the operating mode has been significantly decreased. It is suitable for apps which require communications of a low amount of data. The BLE could be implemented in a range of industries. Proximity sensing is used in another type of application, which is powered by one or more coin-batteries communicating with a host device. It allows the host device to either detect the objects missing from sight or to send a notification when a target moves farther than the specified range from the host. RSSI from the receiver calculates the physical measurement. According to the transmission distance, the transmission of the signal decreases non-linearly in signal strength. RSS could be estimated from the signal receiver. The movement of the object could also be estimated after a few measurements of direction have been calculated. In WSN, RSS is a common technique for measurement (Ilyas & Mahgoub 2004).

The devices with BLE sensing capabilities have encouraged Apple to develop an indoor localisation system. In 2013, Apple introduced “iBeacon”, a BLE based indoor localisation

technique, which enables a smart device, such as iPhone, iPad and iPod to communicate the date of the location by detecting how far it is. Every iBeacon transmits data packets of short identification periodically which are communicated by other smart equipment. The range between the iBeacon and the smart device is measured according to the estimated RSS value. The more accurate the RSS values received, the more efficient the indoor proximity system is. However, RSS values are strongly error-prone affected by the transmission platform used and surrounding environments, such as receivers, antennas, and other communication devices (Ilyas & Mahgoub 2004). To obtain accurate positioning information from the mobile device, during the installation of the system in the venue, an analysis of the RSS scene should be arranged.

2.2.4 Smart Building Managed by iBeacon

Today, more and more buildings are becoming more intelligent with the installation of sensors and actuators in the localisation aspect. This progress is an evolution of the construction industry, as they make customers more comfortable, safe and provide low energy consumption (Davis, Diegel & Boundy 2009). The fundamental technique of this system is to obtain information about the position of the users in the building. For example, there is an efficient way to avoid wasting energy by the HVAC technique when it is necessary. The management of an efficient lighting system is another case of the benefits of users. In the smart building, it can detect the user's position and switch the lights in terms of user actual needs; this improves the efficiency of building energy consumption.

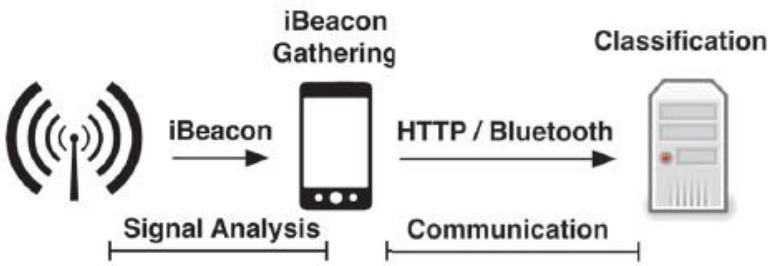

Figure 12 Main aspects of the proposed solution (Corna et al. 2015)

In terms of the previous research (Conte et al. 2014), different technologies have been used in detecting building occupancies, such as RFID (Hahnel et al. 2004), infrared sensors (Want et al. 1992), WiFi (Jiang et al. 2012), GSM/3G (Otsason et al. 2005) and Bluetooth (Pei et al. 2010). Nevertheless, none of the technologies satisfies all advantages from low cost, low energy, reliability and simplicity. Therefore, the solution is still open to be found (Corna et al. 2015).

2.2.5 iBeacon Technology Implemented in Location-based Services

IBeacons are the new technology to communicate with the hardware. iBeacon is using BLE to send a specific format signal. It is like a light tower which sends light to all the boats in the sea. For example, when people wait for their luggage at the airport luggage reclaim, they have no information where they can find their luggage. However, if the luggage is iBeacon attached, it is possible to track the luggage. They will receive a notification about location information of the luggage before people can see it. This case is only one example of iBeacon solutions. It can also be used in a shopping mall or home (Koühne & Sieck 2014).

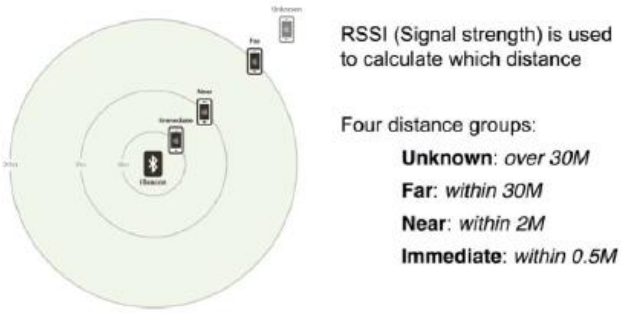

Figure 13 Distance calculations with iBeacon (Koühne & Sieck 2014)

2.2.6 iBeacon Deployment for Mobile Devices in Indoor Positioning

Recently, Location Based Services (LBS) have been widely implemented in many industries; the localisation sensor networks play an essential role in people's lives. In general, there are two parts of positioning technology, indoor positioning, and outdoor positioning. Currently, in the mobile device industry, indoor LBS research has become more popular, as most of the time, people are staying inside buildings, such as shopping centres, hospitals, and universities (Fard, Chen & Son 2015). In terms of the research report, people spend about 70% of the time indoors, which is essential information for indoor LBS. Therefore, indoor positioning research and applications have become more and more popular. However, there are still some significant challenges and difficulties in indoor positioning (Fard, Chen & Son 2015). For instance, GPS signals are unavailable in an indoor environment; indoor LBS could be an alternative way to approach the poisoning result. The indoor positioning usually contains RFID, WIFI, ZigBee and BLE. In the research area of indoor localisation, a newly introduced BLE technology in iBeacons is gaining a lot of momentum. This is due to its low energy consumption footprint. Low energy consumption is the most crucial advantage of iBeacon. It is possible to deploy a small sized device quickly that only requires to be powered by a small battery and avoid the needs of the current infrastructure (Fard, Chen & Son 2015).

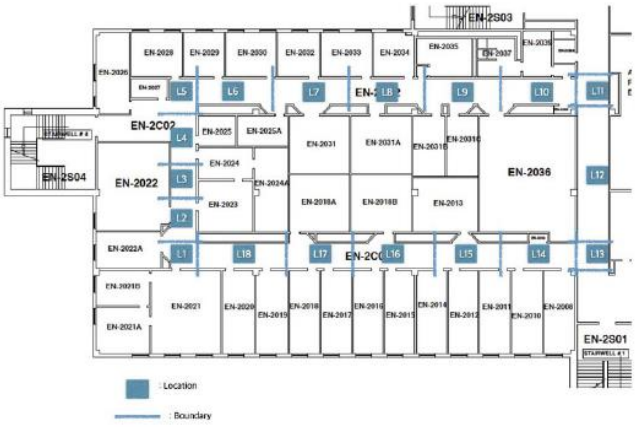

Figure 14 Partitioning of space into locations (Fard, Chen & Son 2015)

2.2.7 iBeacon Interaction System in a Museum

In a museum, applications of improved IoT have made signal roaming better. Studying the history information in a museum hall or from the website is becoming more popular today. Visitors need to be onsite or go online to experience information. Applications make this easier to approach the knowledge in the museum. Research based on how to learn more information in the museum is enable visitors to find something more interesting in the exhibition. Quick Response (QR) code is one of the hottest methods to share data, introduction, images, and web links. Visitors can receive information on specific collections from smart devices with attached cameras to scan the QR code. The website would turn up on the mobile device to introduce the collections to visitors when the network is used in the museum. Augmented Reality (AR) is also introduced in the museum to raise interests of visitors in a collection. The Taipei Palace Museum has designed software to enable visitors to pick a part of the artwork. The collections can be rotated clockwise and counterclockwise by visitors to discover more details (He et al. 2015). The development of an online museum has been focused on by other researchers. The information would be displayed behind the collection overall. In this case, more information will be received by visitors from their mobile devices and other computers in the museum. This would enable visitors to absorb

more interesting information from the collection, moreover, it interactively connects visitors and collections. However, those research technologies are passive, such as an online museum, QR code, and AR. Information is waiting for the user to discover it. Visitors must scan the QR code using the mobile device to get more information with the internet which is available whenever they would like to know about a collection in the museum. However, they need to download the AR application on the mobile device to experience the information of the collection with AR technology (He et al. 2015). Alternatively, they must go to the computer and browse the information about the collection on the internet. The biggest disadvantage of the existing methods is that they are passive technology. To absorb more information, visitors must actively participate. They may find it hard to find some impressive collections easily without paying attention or if they have only an information leaflet or no idea about these collections. However, there are some automatic solutions by positioning technologies to notify visitors. Indoor positioning technology can use Bluetooth, ZigBee, WiFi, etc. iBeacon, a proximity location technique, could improve the case above (Liu et al. 2007).

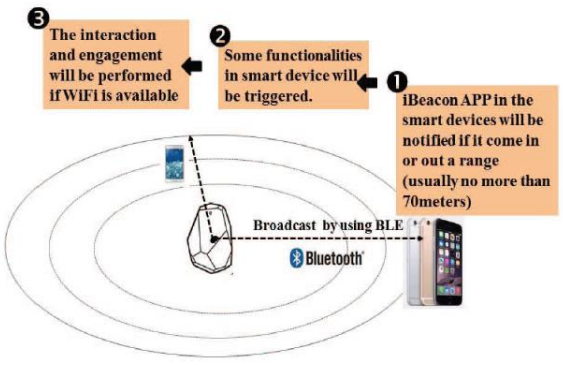

Figure 15 Working process of iBeacon technology (He et al. 2015)

2.2.8 iBeacon Implementation in Internet of Things Environment

IBeacon is a new low cost, low powered indoor positioning system, which could send information of presence to the IOS 7 devices (Dilger 2013). It is also available on and applicable to the Android system. Through this positioning system, the iBeacon device can receive notification from the iBeacon device nearby. iBeacon contains BLE, which is Bluetooth 4.0 or intelligent Bluetooth. By using iBeacon, shops can provide the visitor with notification about promotion information, as they can detect the visitors' position. Furthermore, we can pay automatically without using a wallet or credit card. This technology could be a competitor of NFC (Dilger 2013). RFID was an earlier stage of IoT before. Objects and people should be managed and filed by computers if they are attached to an identifier. Also, to use RFID, things may be tagged by some technologies, such as QR codes, barcodes, NFC and digital watermarking. Daily life could change if all objects in the world are attached with an identifier. For example, shops would no longer run out of stock, as the centre control system would notify which goods are needed and used (Evans 2011).

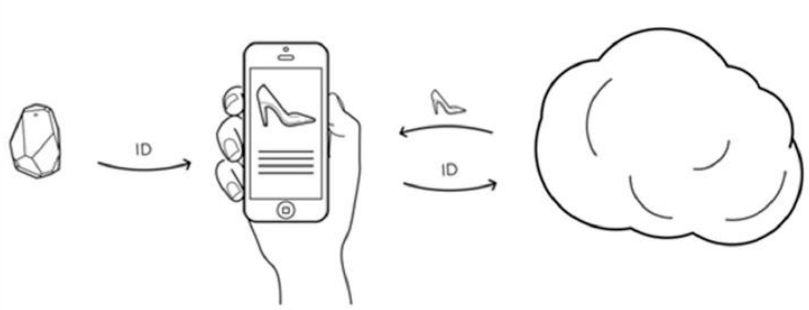

Figure 16 App communicates with iBeacon (Burzacca et al. 2014)

2.2.9 An Extended iBeacon System Proposed in Indoor Localisation

Recently, in the smart device industry in the world, new services using close-range wireless network technology such as WIFI and Bluetooth have been explored. The most recent accessible research is in iBeacon from Apple (Gast 2014). It is a wireless communication

technology by using BLE (Townsend, Cufí & Davidson 2014). It generates communications between beacon device and mobile phone with low power consumption. The beacon device broadcasts BLE radio frequency to automatically trigger mobile device users nearby about information of an existing application. The usual use of iBeacon in-store is to transfer data automatically for couponing and advertising. The indoor positioning system is also used in terms of localisation information from the beacon device and the measurement of the Received Signal Strength Indicator from a mobile device.

IBeacon also can analyse what it sends by sensing a mobile phone user. It would detect where the user is. This technology can be used for localisation and navigation, which can be applicable to search the potential visitors to a store.

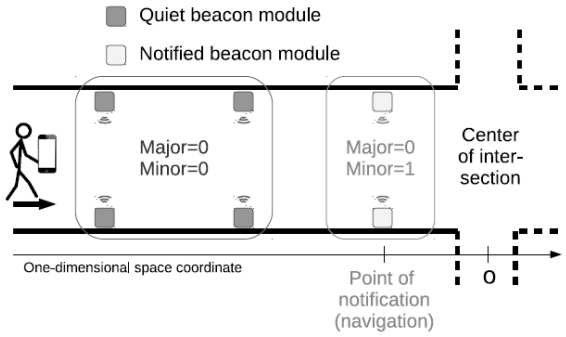

Figure 17 Multiple beacon modules for indoor route guidance (Fujihara & Yanagizawa 2015)

Fujihara and Yanagizawa (2015) propsed an iBeacon based indoor route navigation system. The indoor route navigation image resembles a car route guidance system. Before arriving at the next intersection, the system notifies the user about the next route to follow with the correct timing and direction. In this case, the beacon device can be divided into two types: the silent beacon and the activated beacon. These two kinds of beacons are placed along the passageways in the building to navigate the users to their destination (Fujihara & Yanagizawa 2015).

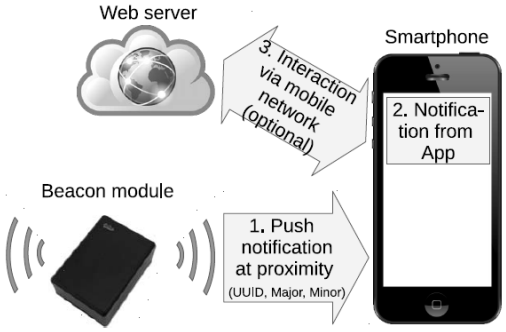

Figure 18 A design of iBeacon (Fujihara & Yanagizawa 2015)

2.3 UWB Localisation Techniques Review

2.3.1 Optimised UWB-Based Localisation in IoT

In 2001, Adams et al. proposed an embedded optimized localisation method for the IoT application. The devices in the system are computing the required measurements by using UWB signals across vast distances. The UWB technique provides measurements from Time-of-Arrival (ToA) with decimetre error range (Adams et al. 2001). In an indoor environment, especially, in wireless sensor network covered environment, UWB localisation technique also provides feedback control for IoT applications. Hence, a two-way ToA method with a non-linear least-square optimised localisation is introduced in a real-life 3D environment. This

approach provides a signal to detect the location itself by ToA technique from the UWB device (Gezici et al. 2005). These devices are named anchors. A sensor which is aimed to detect the location named tag is required for at least first three anchors which are not in line, and the rest of the anchor should not be installed in the same plane generated by the previous three anchors to determine the localisation of the tag (Beuchat et al. 2019).

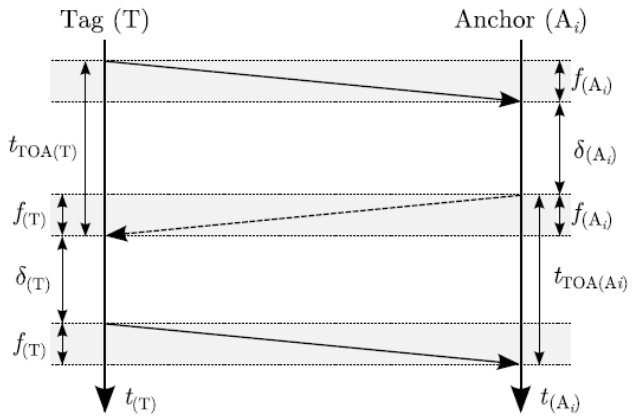

Figure 19 Double-sided two-way ranging between tag and an anchor (Beuchat et al. 2019)

2.3.2 UWB Multi-User in Indoor Localisation System

At present, the UWB technique plays a vital role in the environment of indoor localisation, such as mine communications, security rescue, and other areas. As a new technology of wireless communications, UWB has lots of advantages, such as high accuracy, strong anti-multipath ability, high transmission rate, and nanosecond time resolution (Shang, Champagne & Psaromiligkos 2014). There are many different localisation algorithms developed for UWB. They include the ToA, RSSI, Angle of Arrival (AoA) and Time Difference of Arrival (TDoA). Due to the advantages of high localisation accuracy, the method of ToA and TDoA algorithms are more prevalent in the new UWB localisation system (Ding, Qian & Wang 2010; Li & Cao 2014). In the traditional method, the absolute time of signals propagation between the moving tags and reference anchors are measured by a one-way ToA estimation algorithm. Thus, the anchors and tags have to be synchronised. A developed TDoA estimation algorithm has been introduced to measure the related time of the signal propagation between different anchors and the same tags. The TDoA estimation algorithm is required to communicate with all the reference anchors to maintain time synchronisation (Wang et al. 2013).

In the UWB localisation system, the time synchronisation is the main problem. There are some other algorithms introduced to solve this problem. An estimation algorithm of single round-trip transmission localisation is developed (Kang et al. 2006). It is based on the ToA estimation equation. The error model of clock between different reference point corrects the clock error to improve the accuracy of the localisation. However, the algorithm has two disadvantages. First, the clock offset correction is not applied in the clock error model for each reference point. Second, the system needs communication of two-way bidirectional between anchors and tags. However, the system may not be stable when the amount of the detected objects changes. A UWB antenna array method is developed to solve this issue. There are

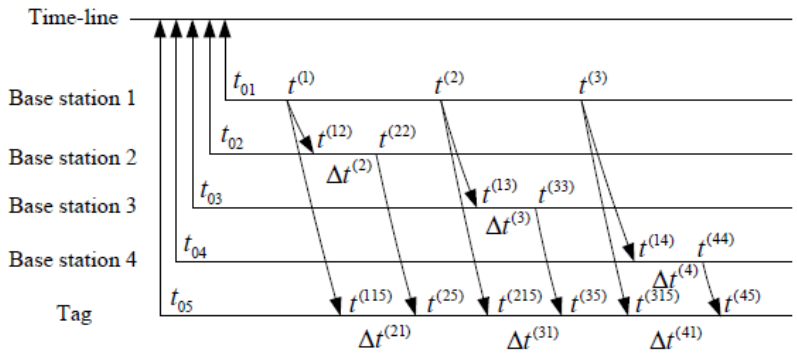

Figure 20 Pseudo-time synchronisation localisation scheme schematic (Wang et al. 2017)

four array antennas implemented at reference anchors. The UWB signals transmitted from an unknown position reference point are received by each antenna (Xiong et al. 2010). Four equal length optical fibres antennas transmit the data to the computer for calculation. The system can solve the time synchronisation issue. There is no strict synchronised time between anchors and tags. However, when the quantity of the tag changes, the algorithm of the processing unit changes. For solving the time synchronisation problem and measure a limited quantity of tags in the system, a developed pseudo-time-synchronised algorithm is introduced (Wang et al. 2017).

2.3.3 3-Tier UWB Technology for Indoor Localisation System

A 3-tier UWB sensors indoor localisation method is proposed (Li, Dehaene & Gielen 2009). This localisation system contains a few numbers of low-cost transmit-only tags, a few numbers of hubs as relay stations and a few anchors. ToA algorithms of UWB pulses are used at reference nodes to determine the localisation (Porcino & Hirt 2003). The proposed 3-tier UWB-based localisation system can be extended by adding new hubs which care to replace the anchors on a large scale to reduce the system cost. At least four hubs communicate the tag signal to determine the tag transmitting time and the location for the 3D environment.

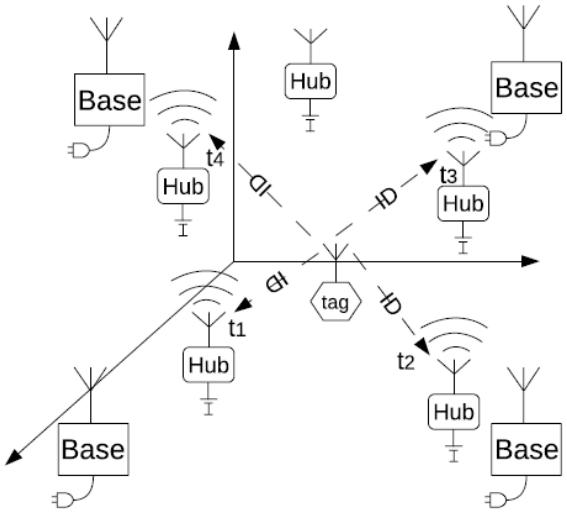

Figure 21 3-Tier UWB Technology for Indoor Localisation System (Li, Dehaene & Gielen 2009)

2.3.4 Low-Cost UWB System using Linear Bayesian Filter for Mobile Device in Indoor Localisation Environment

A UWB based indoor localisation technique is developed by using Bayesian Filtering method. There are two critical points in the name system (Zhang et al. 2018). Firstly, a highly updated rate of UWB signals with the linear regression modelling is used to reduce the noises of the

measurement. Secondly, Bayesian filters can be used to improve the accuracy of the localisation.

The measurements from both odometry and UWB sensors are used to calibrate the position of anchor and tag to minimise the error from the noise and vibration. The proposed technique contains three key points:

1. Modules of Low-cost UWB using the model of linear regression are developed to minimise the errors of the measurement (Aiello & Batra 2006).
2. The development of Bayesian filters with the anchor and tag (Zhang et al. 2018).
3. A nonlinear measurement transform leading to linear filters is developed (Alarifi et al. 2016).

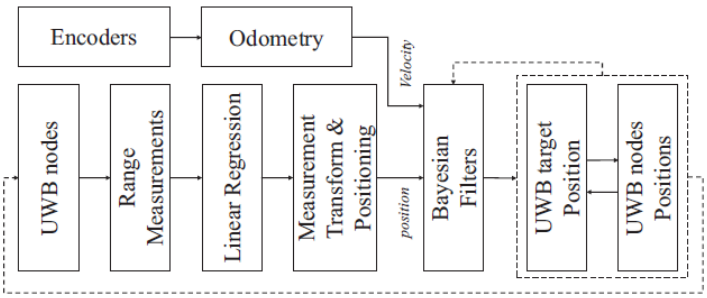

Figure 22 Flowchart of low-cost localisation system diagram (Zhang et al. 2018)

2.3.5 Bluetooth/UWB using Weighted LSA for Indoor Localisation

Recently, a need for low-cost and high accuracy LBSs is developing. However, the current methods are either with low accuracy with a low cost or high accuracy with high cost. The first study for indoor localisation contains Bluetooth, Wi-Fi, UWB and so on. Bluetooth and UWB are the most popular localisation technologies in recent years. The Bluetooth 5.0 version supports indoor navigation and positioning. The topaz location technique is one of the more popular Bluetooth localisation methods, which determines localisation information with an error of around 2 meters (Yang & Wang 2017).

There are several advantages in Bluetooth technology, such as low energy consumption, overall low cost and responding speed. It is important to note that the accuracy of the Bluetooth localisation technology is low, whereas the UWB sensor is more accurate, which has a detecting range of 50-100 meters with an error of only 15 cm. Although the UWB localisation technology has high accuracy in cm-level, the cost of the system is too high (Gu, Lo & Niemegeers 2009). Moreover, the UWB localisation system provides extendable coverage on an extensive indoor area. A novel localisation algorithm named the residual-based weighted least square algorithm (RWLS) has been developed to integrate the high accuracy of UWB technology and the low-cost Bluetooth technology. The feasibility of a UWB and Bluetooth integrated indoor localisation system is proposed (Yang & Wang 2017).

2.4 Summary

The table below has discussed the most popular localisation techniques in this chapter:

Table 1 The advantages and disadvantages of the most popular localisation techniques

Popular Localisation Techniques	Advantage	Disadvantage
GPS localisation System	*The GPS has been widely used in the outdoor environment with its highly accurate results.*	*It has minimal accuracy in indoor environment due to the lack of signals from satellites as buildings and walls block GPS signals.*
Cellular system localisation	*The method generates outstanding results in an outdoor area.*	*In the cellular system, due to the multiple signal reflections from Radio Frequency sensors in the indoor environment, this method has limited accuracy.*
RADAR system localisation	*RADAR system, which is a radiofrequency system for detecting and tracking objects in the buildings. It uses signal strength to detect the location of the object.*	*RADAR system needs multiple base stations, the strength of the signal from the RADAR-based is recorded and calculated. The standard solution using the RADAR-based*

		technique can handle range of about 2 to 3 meters; these are the sizes of a small room.
Ultrasonic Sensor-Based Indoor Localisation System	*Easy installation.*	*Due to highly sensitive noises and shocks, it was difficult for ultrasonic sensors, used in the implementation, to generate highly accurate locations for moving objects.*
FM Signals-Based Indoor Localisation	*FM can broadcast radio signals for indoor localisation to improve those limitations of the wireless sensor network. In the US, signals of FM frequency are in the range of 88-108 MHz, which has less inference affected from small objects. Moreover, FM can transfer hundreds of kilometres; the coverage is much further than Wi-Fi converge. FM signals are accessible by the majority of mobile devices with FM receiver; it is less power consumption and lower cost than WiFi receivers.*	*This method needs the deployment of hardware requirement. The installation and deployment cost could be high.*
RSS Fingerprint-Based Indoor Multi-Resolution Localisation	*Some algorithms of fingerprinting have been reported to address accuracy of localization.*	*It is still facing some practical limitations. Firstly, fingerprint accuracy is computation intensive. The RPs are calculated with good granularities to generate higher accuracy, for instance, a reference point per square meter. Moreover, when the area size increases the number of fingerprints increase. Hundreds of RPs may be set up in an ample space. Secondly, when many moving objects are seeking the signal of localisation together, the calculation of the real-time location information may be heavy which may generate some*

		delay information for the moving objects. Finally, in some indoor localisation case study, some moving objects may not need to be computed localisation precisely. The trace of the record may be enough for the localisation purpose.
Infrared Signals in Indoor Localisation Environment	*In the system, a unique infrared signal could be broadcasted every 10-seconds by the badge. Sensors are set up in the known locations to detect unique identifiers which are operated by location software. The method provides accurate information about the location.*	*Infrared Signal, it has some disadvantages, such as the limitation of the range of Infrared Signal, the high-cost installation and maintenance, as well as, the presence of sunlight.*
WIFI-based Indoor Localisation System	*There is no deployment of hardware requirement. Most of the locations have been already set up wireless sensor networks, such as Wi-Fi, cellular and Bluetooth with the information of RSSI values.*	*It is limited to detect the localisation of the room level in indoor environments. Human being and small objects in a room could interfere with the transmission of the Wi-Fi frequency. Therefore, localisation error could be generated by the variability of fingerprints records. the coverage area of the Wi-Fi access point could be smaller inside the building due to the interference from objects, such as wall, metal and the human body*
Bluetooth-Based Indoor Localisation System	*Bluetooth Low Energy (BLE) technology is selected due to its energy efficiency and adopted functions. The BLE enables the object to last long during the operations. The adopted functions encourage indoor localisation to be used in many different systems.* *There are several advantages from Bluetooth Low Energy (BLE) technology, such as low*	*Bluetooth is a wireless low-cost sensor technique for short-range communication. The original Bluetooth consume high power, which does not meet the low power communication designed by those applications. The accuracy of the Bluetooth localisation technology is low.*

	energy consumption, low cost and dispose of quickly.	
iBeacon Localisation Techniques	*This is due to its low energy consumption footprint Low energy consumption is the most crucial advantage of iBeacon. It is possible to deploy a small size device quickly that only required to be powered by a small battery and avoid the needs of the current infrastructure.* *IBeacon is a new low cost, low powered indoor positioning system, which could send information to the IOS 7 devices of the information of presence nearby. It is also available and applicable by the Android system. Through this positioning system, the iBeacon device can receive notification from the iBeacon device nearby. iBeacon contains BLE, which is Bluetooth 4.0 or intelligent Bluetooth.*	*This technique is a short-range communication. RSS values of iBeacon are strongly error-prone effected by the transmission platform used and surrounding environments, such as receivers, antennas, and other communication devices.*
UWB Localisation Techniques	*UWB has lots of advantages, such as high accuracy, strong anti-multipath ability, high transmission rate, and nanosecond time resolution. the UWB localisation system is extendable on an extensive coverage indoor area.*	*Although UWB localisation technology has high accuracy in cm-level, the cost of the system is too high, Moreover, In UWB localisation system, the time synchronisation is the main problem.*

Chapter 3

Research Methodology

In this chapter, in terms of determining the indoor location of the object and reference point, the device may use one or more different measurement methods for indoor localisation. The recent measurement methods for indoor localisation are presented here. iBeacon specification and protocols are introduced in this chapter, including UUID, major number and minor number. A calibration process is used at the first stage of the experiment to initially correct the accuracy. A functional block diagram displays the calibration and the error modelling process. Finally, a new CFKF error modelling is designed and presented to improve the accuracy of the system.

3.1 Indoor Localisation Method

3.1.1 Signal Strength Spatial Mapping

The method introduces a collection of a multitude of signal strength measurements in an area. A spatial grid is mapped in this area by using a (Feldmann et al. 2003) RSSI from a wireless sensor device to measure the distance. This method develops a simple localisation system to determine the distance (Feldmann et al. 2003).

As mentioned, the technique method contains the utilisation of empirical measurements, this method is utilised to determine the distance using RSSI. However, the theoretical model, such as the long-distance path loss model is for outdoor localisation. It does not include interference in an indoor environment, such as wall reflections (Feldmann et al. 2003).

3.1.2 Time of Flight (ToF) Method

ToF is the method used to measure the propagation time of signals transmitted between two reference nodes; the estimated distance can be measured (Dahlgren & Mahmood 2014). Notably, the signal propagation time can be calculated between the initial time of signal sending and the time of signal arrival. The signal speed is close to the speed of light in a vacuum environment (Schauer, Dorfmeister & Maier 2013), the distance can be determined by using speed of light and time. This method relays on the synchronicity of both the time of sender and time of the receiver. Errors will be introduced when a small gap of timing is calculated (Dahlgren & Mahmood 2014). This high-level precision is not available in the standard Wi-Fi equipment; specialized components are introduced to implement this technique. Nevertheless, comparing with signal strength spatial mapping, ToF technology has fewer complications from others (Schauer, Dorfmeister & Maier 2013).

3.1.3 Kalman Filter Method in Position Measurement

As recursive linear filtering, the Kalman filter can be used to reduce the noise effects in position measurements (Zhao, Yang & Kyas 2011). The historical measurements are calculated to limit the random deviations from calculations (Bulten 2015).

The current state (Xt) is a combination of a previous state (Xt-1) and noise (Et). The measurement model of the current state (Zt) consists of the current state and the measurement noise (δt).

3.1.4 Trilateration and Triangulation Techniques

Trilateration is one of the most widely used methods for position measurement. Three or more distances and reference points are measured in this technique (Liu et al. 2007). Those reference points can be recognised, as the centre of the several measurements and the distance can be recognised as the radii (Feldmann et al. 2003; Papamanthou, Preparata & Tamassia 2008). It is observed that the shortest dimensions of this three-circle model can be calculated to determine the position (Dahlgren & Mahmood 2014).

In some case, reference points from Wi-Fi or Bluetooth beacon, have been particularly calculated either with the method of signal strength or ToF to determine the distance(Dahlgren & Mahmood 2014). A high precise calculation should be applied to avoid a negative effect on the accuracy of the calculation.

Triangulation is another well-known positioning technology. It is operating with a similar method to trilateration. At least two measured positions of reference points are used, and two known AoA of the signals from the reference points are measured. In this case, the 2-dimensional position can be calculated from the information collected above (Liu et al. 2007).

Moreover, the trilateration technique is also suitable for the triangulation in the three measured positions case (Dahlgren & Mahmood 2014). It is calculating a triangle and using the shortest dimensions method on the equations. The measured angles are merely replacing the measured distances in the equation. With Wi-Fi and Bluetooth beacon, developed equipment is necessary for determining the accurate AoA (Dahlgren & Mahmood 2014). The lack of hardware precision development could generate an inaccurate result.

3.1.5 Fingerprinting Signal Mapping

Fingerprinting is a new method in the indoor localisation field by using signal properties (Iglesias, Barral & Escudero 2012). Signal strength is mapped at the known positions which are like a database of unique signal strength, called fingerprint cells (Dahlgren & Mahmood 2014). Those fingerprint cells divide the spatial area for sub-cells to increase the accuracy of the positioning (Dahlgren & Mahmood 2014). When the information of the cells is enough to be identified, they can be recognised uniquely on the segment of the area (Iglesias, Barral & Escudero 2012).

There are two different sequential phases in this technique, which are offline phases and online phases (Costilla-Reyes & Namuduri 2014). In the offline phases, characterisation data such as average signal strength value is produced on the target cell and is saved to a database of fingerprints. This process generates a map of fingerprints to identify an area (Costilla-Reyes & Namuduri 2014). In the online stage, the device will be active to measure the RSSI by comparing with the produced database of fingerprints to calculate the positioning.

3.2 Bluetooth Low Energy (BLE) Beacons

In BLE, the proximity specification is essential technology in order to enable iBeacon. BLE is also called Bluetooth Smart. It improves the specification of the existing Bluetooth for a low-power operation design. The beacons with BLE transmit the information of identification to detect the location where the beacons are set up. The dual-mode BLE devices called “Bluetooth Smart Ready” are compatible with both BLE and traditional Bluetooth.

iBeacon is a kind of BLE beacon. All iBeacons belong to BLE beacons family, they are all BLE devices. However, some BLE devices are not beacons, and some beacons are not using Bluetooth technology. If using low transmission power, the consumption of power for a beacon is low. Generally, the beacons are able to operate for months or years depending on the life of the battery.

Beacons do not require other networks to access the function. The protocol of beacon is easy to understand. An application can embed beacon protocol to operate without internet access.

3.3 The iBeacon Protocol

3.3.1 The Universal Unique Identifier (UUID)

Usually, UUID is a 128-bit unique identifier, it is transmitted by iBeacons. UUID contains the organization information of the iBeacon. For instance, the UUID can identify that the iBeacon is used by a particular company.

In Bluetooth specification, some devices use UUID as a unique element identifier. UUID in iBeacons is a proximity UUID, it is different from other UUIDs belonging to some Bluetooth device. The UUID is located at the top hierarchy level, it is utilised to identify iBeacons for common management.

The UUIDs in some networking protocols, for example, 802.11, are not managed to avoid conflicts centrally. In the Bluetooth protocol, the UUIDs should be unique. Unlike other networks, such as IEEE 802, the Bluetooth does not have centralized calculation to produce uniqueness. It has designed a 128 bits identifier generator to randomly select unique numbers. Applications of iBeacon configuration can always generate a random unique UUID.

3.3.2 Major Number in BLE

In the specifications of Bluetooth and iBeacon, the major number identifies the information of the major group of the beacons which belongs to a specific entity. For instance, if there is a chain of stores, the major number is used to identify the specific store where a group of beacons are located.

3.3.3 Minor Number in BLE

The minor number identifies the lower hierarchy level of the group beacons. For instance, there is a chain of stores, the minor number is used to identify an individual product or beacon in the particular store.

3.3.4 Advertising Interval

In the Bluetooth specification, the advertising interval is usually set at 100ms. The life of the battery will last longer if the advertising interval is set longer. However, the longer the advertising interval is set, the less signal transmission in the communication process. Therefore, the balance should be adjusted between advertising internally and the purpose of implementation.

3.4 Ranging

The ranging operation is to determine the distance between a device and an iBeacon. In order to determine the distance, the receiver can calculate the signal power based on the signal transmission strength and the system calibration.

It is a high-power consumption operation to determine the range as the beacon requires a strong signal to distinguish it from others. This operation also requires a high advertising interval rate for most of the moving receivers. The ranging operation usually is used to detect the nearest iBeacon to the receiver.

3.5 Calibration and Ranging Accuracy

Calibration constant, “measured single power” is the key settings to determine the ranging accurately. In order to measure the range, the mobile receiver calculate the received signal power with the calibration constant.

In the process of the calibration, iBeacon is assumed to be located in a free space. The inverse-square fading will be the major effect of the signal loss. In the experiment, the measured range always bounces around due to the interference from multipaths when the radio signal transmits in multiple paths from the iBeacon to the receiver, the energy from the radio can interfere with the radio transmit in other paths. In some case, the radio signal becomes stronger as the interference is constructive. In another way, the radio signal becomes weaker as the interference is destructive. Multipath interference usually happens when the iBeacon is set up close to the selling or barrier, the radio signal reflects when the signal transmits towards to the celling or barrier.

3.6 Functional Block Diagram

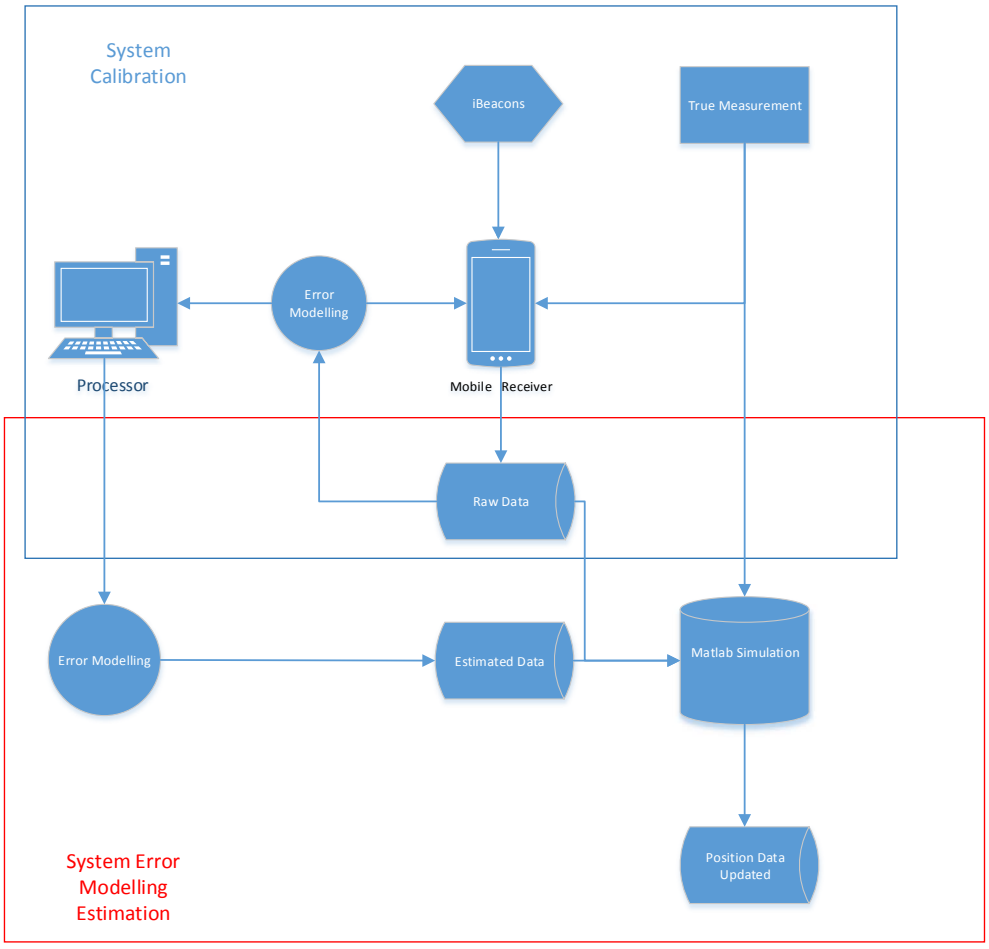

Figure 23 System calibration and error modelling estimation

On the system calibration stage, the experiment focuses on initialising the RSSI at a 1-meter distance. In the experiment, iBeacon broadcasts the raw data signal; a smart mobile phone is used as a mobile receiver; the Bluetooth on the phone can communicate the signal transmitting with iBeacon. During the signal transmitting, raw data is logged as a file which is saved on the phone. After the experiment, a computer is used to read the raw data from the phone. The raw data contains information such as time (ms), UUID, Major ID, Minor ID, RSSI (dBm) and Device ID. The equation is implemented below to calculate the distance measured from iBeacon:

$$\mathrm{A} = |RSSI| - [\mathrm{n} \cdot 10 \ln(D)] \qquad (3.1)$$

In equation 3.1,

D stands for distance

RSSI stands for Received Signal Strength Indication

A stands for expected RSSI at a distance of 1 meter.

N stands for propagation constant, free space n =2.

According to the equation, to calculate the value of distance, we need to determine the value of RSSI, and the value of A. RSSI is readable, which is from the raw data from the mobile receiver. The value of A can be calculated when the iBeacon is placed in 1 meter away from the mobile receiver. This is the step of calibration of the iBeacon. Errors and noise occurs during signal transfer. In order to minimise the noises and error, raw data has to be processed on the computer by an error modelling algorithm such as Curve Fitting (CF), KF and CFKF, and the estimated data has been generated by the error modelling. In order to align the RSSI at 1 meter, the value of RSSI needs to be compared with using a different algorithm to generate the optimised value. This value is used to recalculate the distance with the value of A from the first calculation. N stands for propagation constant. n =2; generally, if the environment does not change, we do not change the value of N. The value of N may change due to the different environments. In order to calculate n when the environment changes, the following equation can us used:

$$n = \frac{|RSSI| - A}{10 \ln(D)} \qquad (3.2)$$

After calculating the estimated data, updated data is plotted on the Matlab figure. Error rates are calculated from the system, it can determine that the CFKF is more accurate than

another algorithm, and the calibration stage should be done. Different iBeacon may contain different errors due to different manufactory process. Each iBeacon needs to be calibrated individually.

In the next stage, to determine a distance other than 1 meter by using RSSI, we need to use the results from the previous stage, value A should be used in the equation to determine the distance. The equation being:

$$D = 10^{\left(\frac{|RSSI|-A}{10\times n}\right)} \quad (3.3)$$

Distance is calculated in different ranges by different algorithms. They are plotted on Matlab to determine the best accurate algorithms.

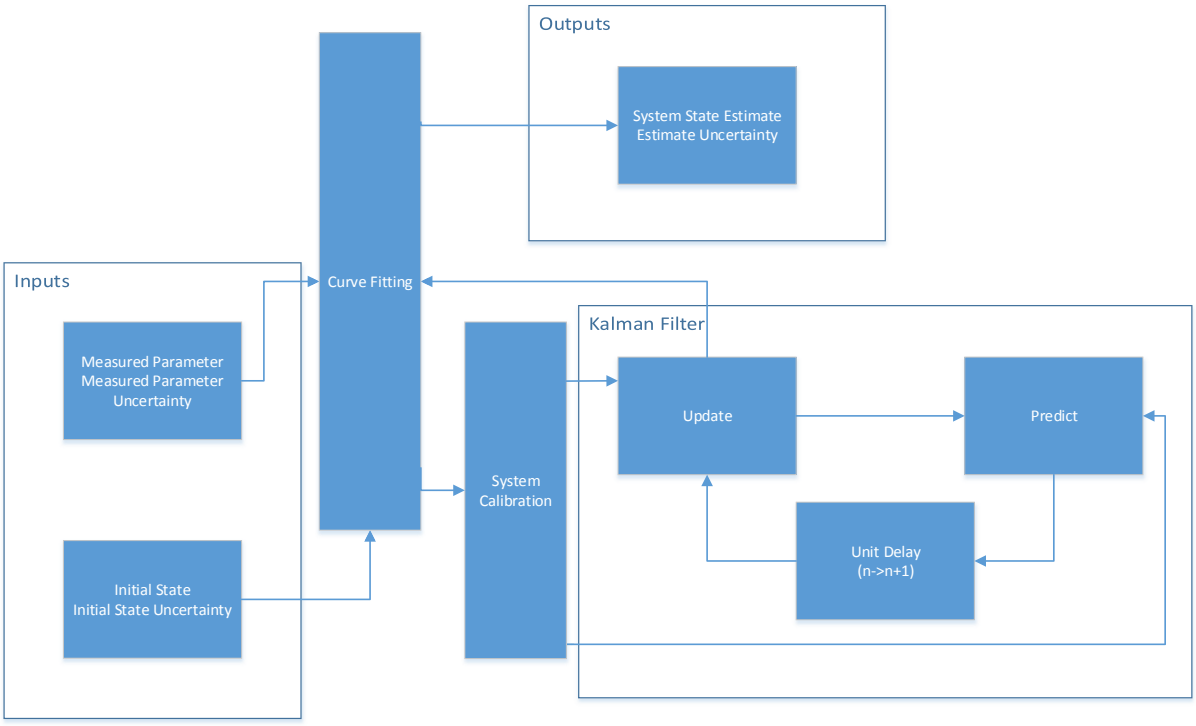

Figure 24 Curve Fitted Kalman Filter Error Modelling

In figure 24, the diagram of curve fitted Kalman filter error modelling, inputs are the raw data from the iBeacon; they contain information such as time (ms), UUID, Major ID, Minor ID, RSSI (dBm) and Device ID. The measurement is calibrated and processed by CF algorithm to determine the value of the expected RSSI at a distance of 1 meter and then is calculated by KF algorithm to improve the accuracy of the system, finally the results are processed by the CF algorithm again to optimise the output from KF, the equations are below:

$$y_i = a_0 + a_1 x_i + a_2 {x_i}^2 + \cdots + a_k {x_i}^k + \varepsilon_i (i = 1, 2, \ldots, n) \qquad (3.4)$$

$$\begin{bmatrix} y_1 \\ y_2 \\ y_3 \\ \vdots \\ y_n \end{bmatrix} = \begin{bmatrix} 1 & x_1 & x_1^2 & \vdots & x_1^k \\ 1 & x_2 & x_2^2 & \vdots & x_2^k \\ 1 & x_3 & x_3^2 & \vdots & x_3^k \\ \vdots & \vdots & \vdots & \ddots & \vdots \\ 1 & x_n & x_n^2 & \vdots & x_n^k \end{bmatrix} \begin{bmatrix} a_1 \\ a_2 \\ a_3 \\ \vdots \\ a_k \end{bmatrix} + \begin{bmatrix} \varepsilon_1 \\ \varepsilon_2 \\ \varepsilon_3 \\ \vdots \\ \varepsilon_n \end{bmatrix} \qquad (3.5)$$

a stands for scale factor error of the system

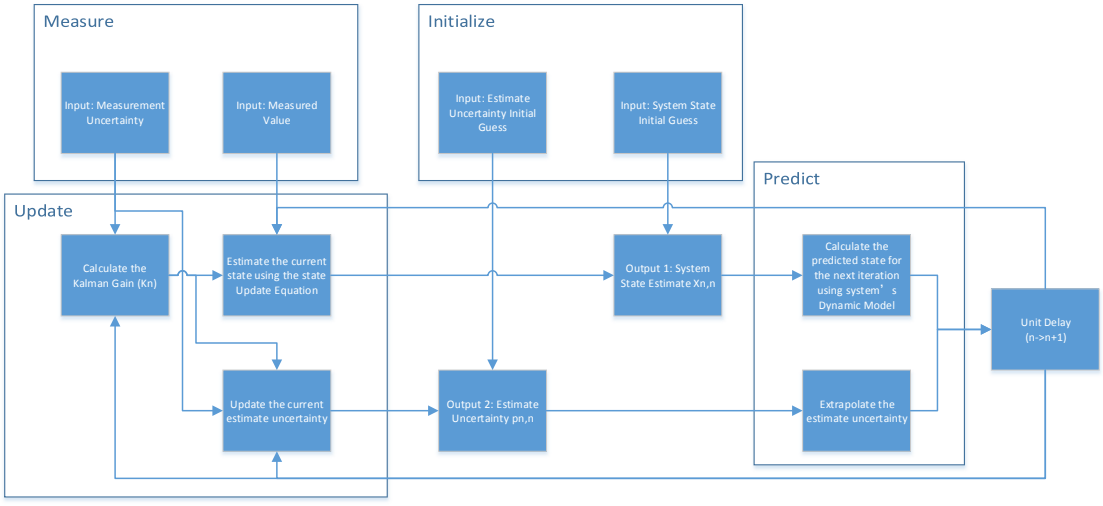

Figure 25 Kalman Filter Error Modelling

ε stands for bias error of the system

After the data is estimated by CF, it will be programmed by KF. The output will be the KF estimated value. However, this value is not the most accurate. The KF estimated value will

be calculated by CF again to generate the final value of the estimated data; this kind of data calls CFKF estimated data.

The figure 25 is the details of KF algorithm. Initially, when the data is transferred from the mobile receiver, it is calibrated and processed by the CF algorithm. This value of the data is called measurement value. It is also a system state value is guessed and estimated by the state equation, an equation is used to update the state of the object. State update equation shows below:

$$\hat{\boldsymbol{x}}_{\boldsymbol{n,n}} = \hat{\boldsymbol{x}}_{\boldsymbol{n,n-1}} + \boldsymbol{K_n}\left(\boldsymbol{y_n} - \hat{\boldsymbol{x}}_{\boldsymbol{n,n-1}}\right) = (\mathbf{1} - \boldsymbol{K_n})\,\hat{\boldsymbol{x}}_{\boldsymbol{n,n-1}} + \boldsymbol{K_n y_n} \quad (3.6)$$

The State extrapolation equation shows below:

$$\hat{\boldsymbol{x}}_{\boldsymbol{n,n-1}} = \hat{\boldsymbol{x}}_{\boldsymbol{n-1,n-1}} + \Delta \boldsymbol{t}\,\hat{\boldsymbol{x}}_{\boldsymbol{n-1,n-1}} \quad (3.7)$$

$$\hat{\boldsymbol{x}}_{\boldsymbol{n,n-1}} = \hat{\boldsymbol{x}}_{\boldsymbol{n-1,n-1}} \quad (3.8)$$

(for constant velocity dynamics)

Where $\boldsymbol{K_n}$ stands for the Kalman Gain equation:

$$\boldsymbol{K_n} = \frac{\boldsymbol{p_{n,n-1}}}{\boldsymbol{p_{n,n-1}} + \boldsymbol{r_n}} \quad (3.9)$$

In order to determine the covariance errors of two sets of the values, a covariance update equation is displayed below:

Covariance update equation:

$$\boldsymbol{p_{n,n}} = (\mathbf{1} - \boldsymbol{K_n})\boldsymbol{p_{n,n-1}} \quad (3.10)$$

Covariance extrapolation equation:

$$\boldsymbol{p_{n,n-1}} = \boldsymbol{p_{n-1,n-1}} + \boldsymbol{q_n} \quad (3.11)$$

(For constant dynamics)

where

$\boldsymbol{K_n}$ stands for Kalman Gain

$\boldsymbol{p_{n,n-1}}$ stands for Extrapolated Estimate Uncertainty

$\boldsymbol{r_n}$ stands for Measurement Uncertainty

$\boldsymbol{\hat{x}_{1,0}}$ stands for Initial System State

$\boldsymbol{p_{1,0}}$ stands for Initial State Uncertainty

$\boldsymbol{y_n}$ stands for Measured System State

$\boldsymbol{\hat{x}_{n,n}}$ stands for System State Estimate

$\boldsymbol{p_{n,n}}$ stands for Estimate Uncertainty

$\boldsymbol{\hat{x}_{n,n-1}}$ stands for Previous System State Estimate

3.7 Summary

In this chapter, we have presented many different measurement methods for indoor localisation, such as signal strength spatial mapping, time of flight, Kalman filter, trilateration, triangulation and fingerprinting. IBeacon structure and protocol have been introduced in this chapter, which include UUID, Major number, Minor number and advertising intervals. Calibration and ranging operation are also discussed as a part of the error modelling. The functional block diagram displays both the processes of system calibration and system error modelling estimation. Initially, the iBeacon transmits the raw data to the mobile receiver, which contains information of time (ms), UUID, Major ID, Minor ID, RSSI (dBm) and Device ID. Then, the mobile receiver transfers the raw data to the computer to calculate the expected RSSI at a distance of 1 meter by CF algorithm during the system calibration process. The calibration process determines the value of expected RSSI at a distance of 1 meter. According to this value, measured distance can be calculated by the distance equation (3.3). At this stage errors and noises still occur in the system, the measured distance is not accurate. KF algorithm is used to improve the accuracy of the

system. Finally, a CF algorithm is operated again on output of the KF algorithm to optimise the system results. The whole optimisation process is called A novel CFKF error modelling algorithm, which is displayed in figure 24. It generates more accurate and reliable measurement results than the results from measured distance and KF outputs. The next chapter will display the experiment and results based on the CFKF error modelling algorithm in iBeacon indoor localisation system.

Chapter 4

Research Implementation of iBeacon Localisation

In this chapter, the iBeacon localisation system experiment has been set up and operated. Calibration process is the first stage of the experiment, which has been using several different algorithms to determine the best method for the localisation accuracy. After the calibration process, the measurement experiments have been processed to demine the estimated distance. Then, the actual study in real life environment has been set up and implemented. The designed CFKF error modelling is used in all the stages and field experiment, the results have showed that CFKF error modelling provides the best accuracy for the system.

4.1 Testbed Setup for iBeacon Localisation System

Initially, the testbed of the calibration has been set up as the picture below. In order to determine that the signal strength from different angles of the transmitter may be different. 170 degree from the transmitter has been divided into 17 angles which is from 10° to 170°. Each angle is 10° different from the angle next to itself as figure 26 showed. There is 1-meter distance away from the transmitter to the receiver at each angle. The distance has been measured by tape ruler. The white labels on the ground in the figure clearly display the real positions of all the angles within 1-meter distance.

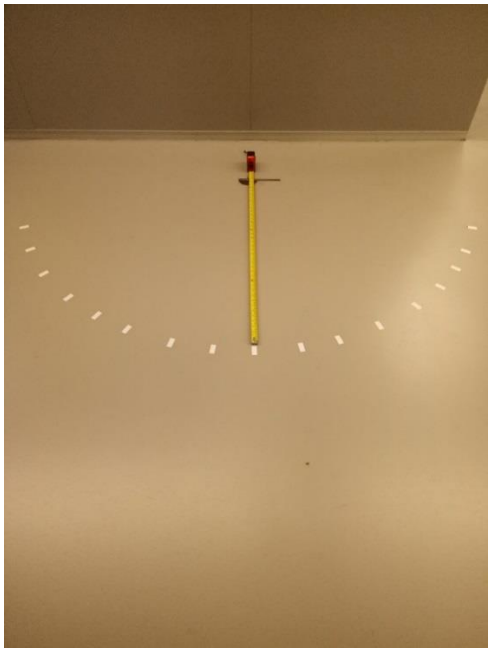

Figure 26 Testbed setup at 1-meter range for different angles from 10° to 170°

In the testbed, the iBeacon (transmitter) is set up on a stand with 50 cm high, the smart mobile phone (receiver) is also set up on another stand with the same height in one meter away from the iBeacon. 50 cm height is a reasonable height to avoid the signal reflection from the ground. The mobile phone starts to collect the data from the position of 10° as figure 27 (a) displayed. When the mobile phone finishes collecting data at the position of 10°, it will move to the next angle and continue to collect data, until it finishes collecting the data at the position of 170° as figure 27 (b) displayed. The iBeacon has been set up horizontally as displayed on figure 29. Due to the manufactory errors, different iBeacons with the same specification may have different errors. Therefore, six iBeacons have been operated in the experiments to determine the best accuracy of the system. Figure 28 displays the six iBeacons with numbers labelled.

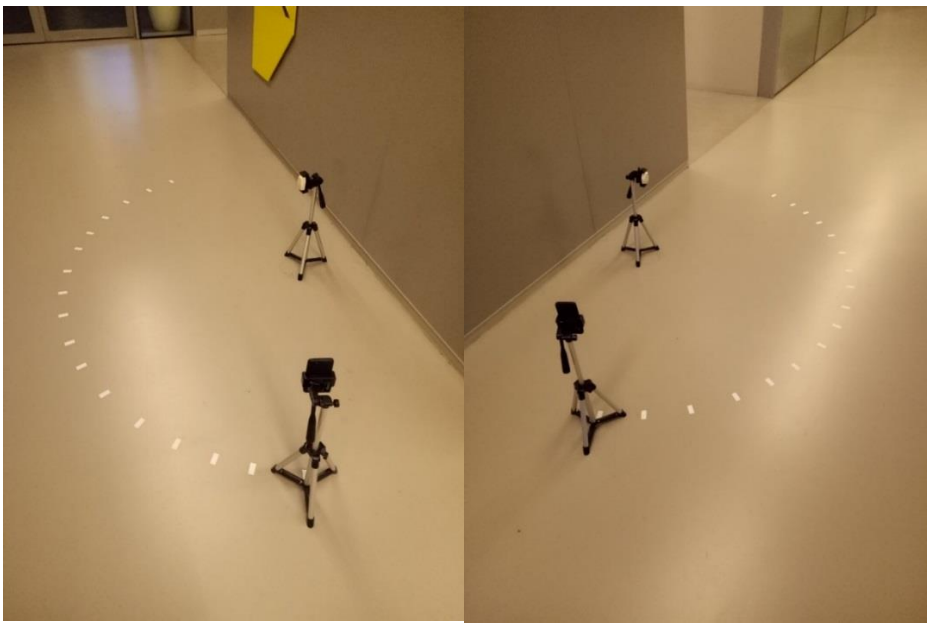

Figure 27 Testbed setup for iBeacon and mobile receiver (a) (b)

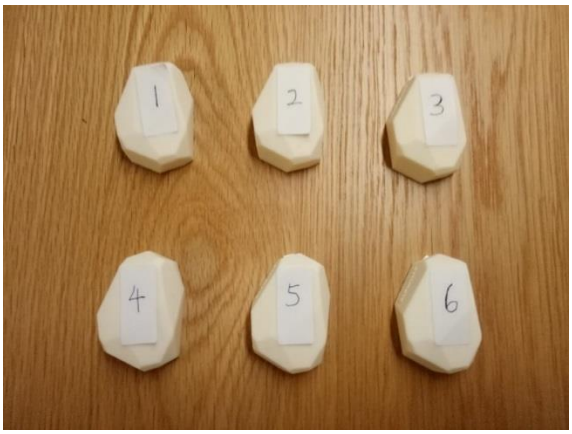

Figure 28 Six iBeacons used in the experiment

Figure 29 iBeacon set up horizontally

The iBeacon used in the experiment are from Estimote iBeacon. The specification of those IBeacons are displayed in table 2.

Table 2 Specification of iBeacon

Bluetooth® SoC
ARM® Cortex®-M4 32-bit processor with FPU
64 MHz Core speed
512 kB Flash memory
64 kB RAM memory
Radio: 2.4 GHz transceiver
Bluetooth®： 4.2 LE standard
Range: up to 200 meters (650 feet)
Output Power: -20 to +4 dBm in 4 dB steps, "Whisper mode" -40 dBm, "Long range mode" +10 dBm
Sensitivity: -96 dBm
Frequency range: 2400 MHz to 2483.5 MHz
No. of channels: 40
Adjacent channel separation: 2 MHz
Modulation: GFSK (FHSS)
Antenna: PCB Meander, Monopole
Antenna Gain: 0 dBi
Over-the-air data rate: 1 Mbps (2 Mbps supported)
Size and Weight
Length: 62.7 mm (2.47 inches)
Width: 41.2 mm (1.62 inches)
Height: 23.6 mm (0.93 inches)
Weight: 67g (2.36 ounces)

Table 3 Specification of smart phone wireless sensors

WLAN	Wi-Fi 802.11 a/b/g/n, dual-band, hotspot
Bluetooth	V4.0
GPS	A-GPS, GLONASS
Sensors	Accelerometer, gyro, proximity, compass
NETWORK	GSM / CDMA / HSPA / EVDO / LTE

4.2 Calibration Process for Different Angles

In this calibration process for angles, we measure the RSSI of iBeacon at the same distance, 1 meter, with various angles. As the positions display in the figure 27, we can find that the angle is between the wall and the line connecting the transmitter and receiver. The

frequency of the signal transmit is 10Hz. The measurement starts from 10° to 170°, each angle of measurement has 10° different from the next angle of measurement, therefore the list of angles is 10°, 20°, 30°, 40°, 50°, 60°, 70°, 80°, 90°, 100°, 110°, 120°, 130°, 140°, 150°, 160° and 170°, respectively. Six iBeacons have been measured at each different angle for the same distance. The polar diagrams for each iBeacon device are showed below:

4.2.1 System Calibration for Device 1

Figure 30 shows the variation of the RSSI of device 1 at 1-meter distance. However, the measurement of RSSI at different horizontal angles from 10° to 170° slightly changes in between -85dBm and -95dBm, as the antenna broadcasting may not cover smoothly at all angles.

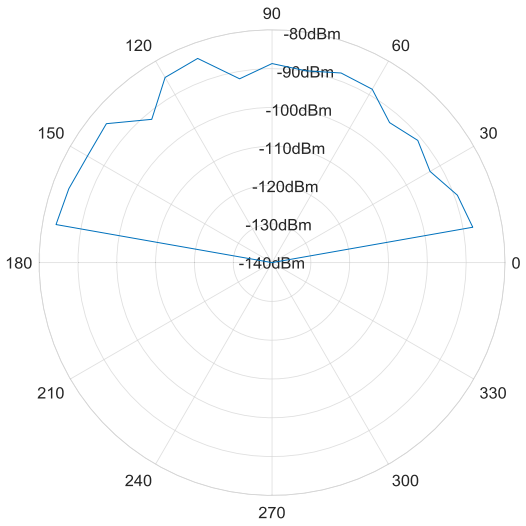

Figure 30 Polar diagram for iBeacon device 1 at different horizontal angles from 10° to 170°

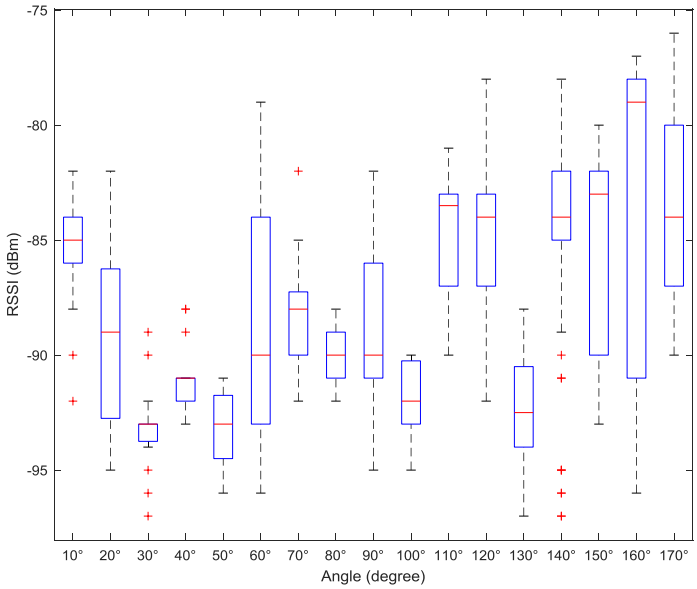

Figure 31 Box-and-whisker diagram for iBeacon device 1 at different horizontal angles from 10° to 170°

Figure 31 is the box-and-whisker diagram, which clearly shows the range and average value of RSSI from Device at different angles in the same distance. Most of the RSSI values are between -85 dBm and -95 dBm.

4.2.2 System Calibration for Device 2

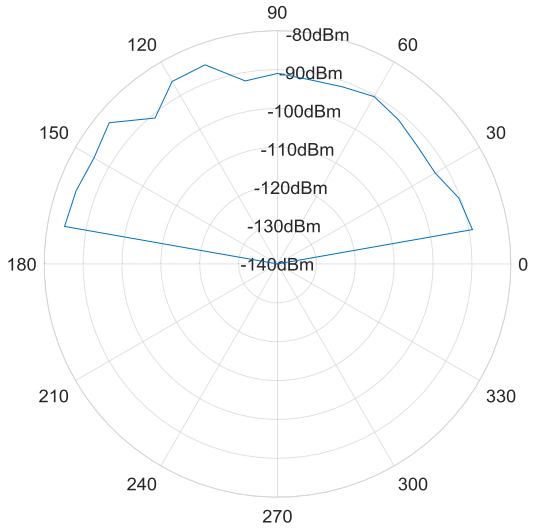

Figure 32 Polar diagram for iBeacon device 2 at different horizontal angles from 10° to 170°

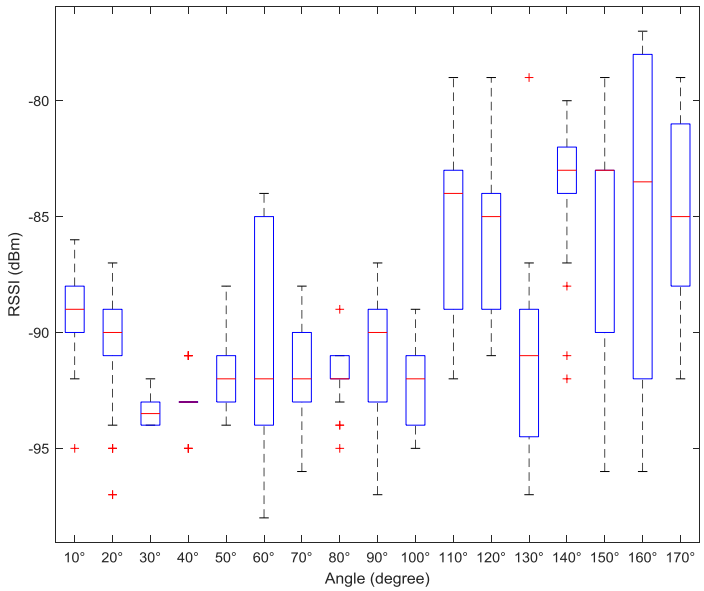

Figure 33 Box-and-whisker diagram for iBeacon device 2 at different horizontal angles from 10° to 170°

Figure 32 shows that, at 1-meter distance, RSSI of device 2 is various. However, the measurement of RSSI at different horizontal angles from 10° to 170° slightly changes in between -85dBm and -95dBm, as the antenna broadcasting may not cover smoothly at all angles.

Figure 33 is the box-and-whisker diagram, which clearly shows the range and average value of RSSI from Device at different angles in the same distance. Most of the RSSI values are between -85 dBm and -95 dBm.

4.2.3 System Calibration for Device 3

Figure 34 shows that, at 1-meter distance, RSSI of device 3 is various. However, the measurement of RSSI at different horizontal angles from 10° to 170° slightly changes in between -85dBm and -95dBm, as the antenna broadcasting may not cover smoothly at all angles.

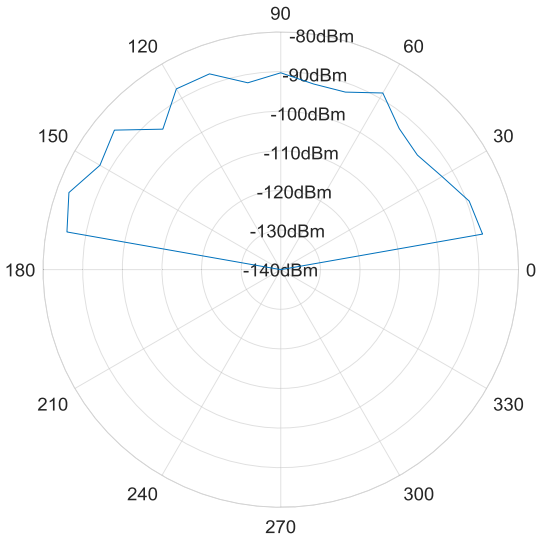

Figure 34 Polar diagram for iBeacon device 2 at different horizontal angles from 10° to 170°

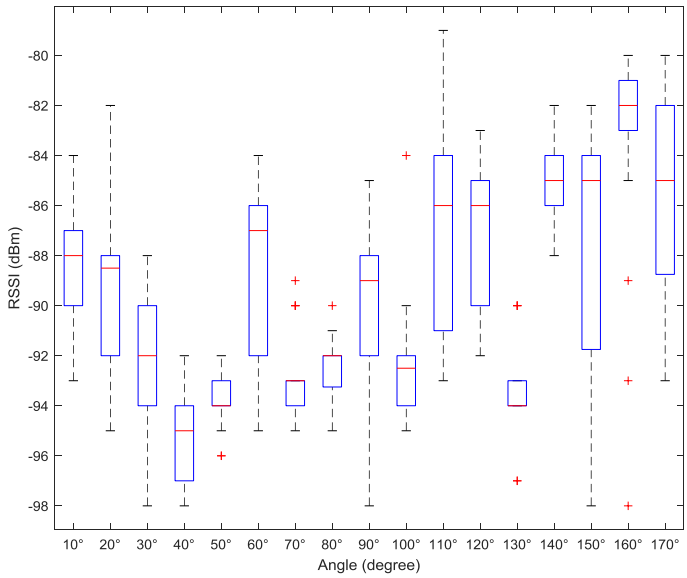

Figure 35 Box-and-whisker diagram for iBeacon device 3 at different horizontal angles from 10° to 170°

Figure 35 is the box-and-whisker diagram, which clearly shows the range and average value of RSSI from Device at different angles in the same distance. Most of the RSSI values are between -85 dBm and -95 dBm.

4.2.4 System Calibration for Device 4

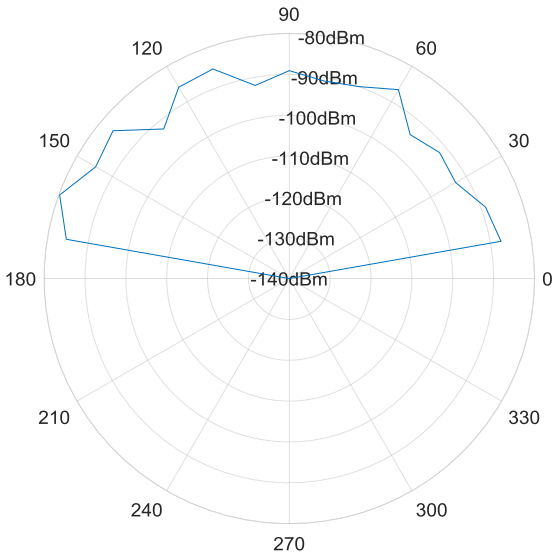

Figure 36 Polar diagram for iBeacon device 4 at different horizontal angles from 10° to 170°

Figure 36 shows that, at 1-meter distance, RSSI of device 4 is various. However, the measurement of RSSI at different horizontal angles from 10° to 170° slightly changes in between -85dBm and -95dBm, as the antenna broadcasting may not cover smoothly at all angles.

Figure 37 is the box-and-whisker diagram, which clearly shows the range and average value of RSSI from Device at different angles in the same distance. Most of the RSSI values are between -85 dBm and -95 dBm.

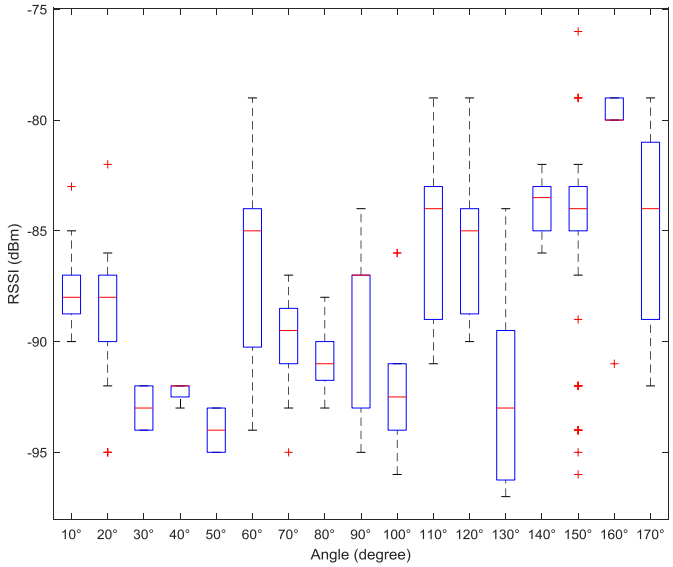

Figure 37 Box-and-whisker diagram for iBeacon device 4 at different horizontal angles from 10° to 170°

4.2.5 System Calibration for Device 5

Figure 38 shows that, at 1-meter distance, RSSI of device 5 is various. However, the measurement of RSSI at different horizontal angles from 10° to 170° slightly changes in between -85dBm and -95dBm, as the antenna broadcasting may not cover smoothly at all angles.

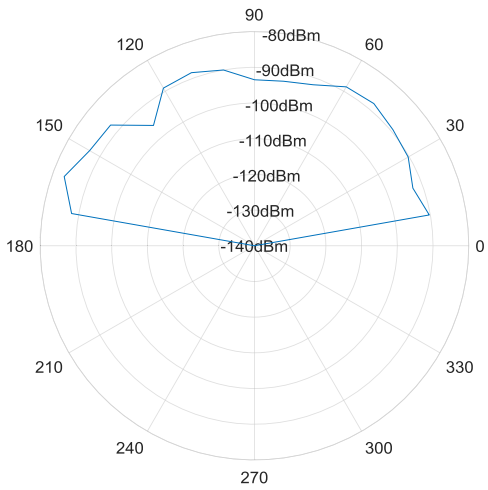

Figure 38 Polar diagram for iBeacon device 5 at different horizontal angles from 10° to 170°

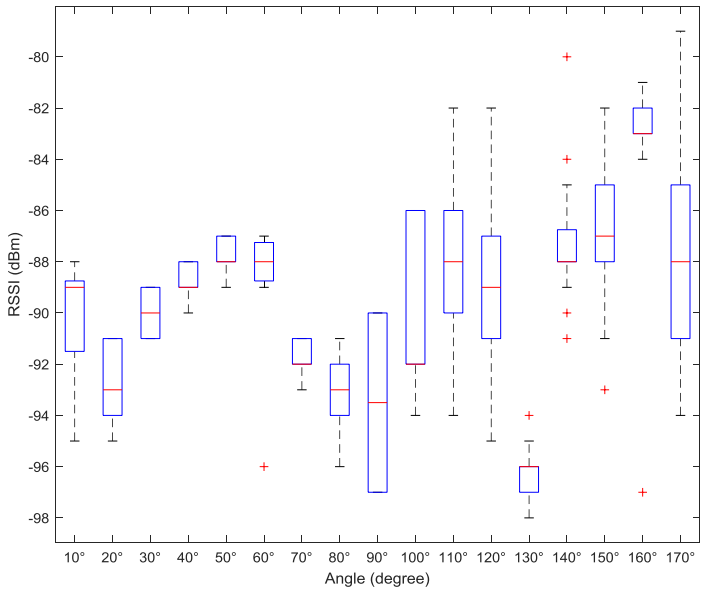

Figure 39 Box-and-whisker diagram for iBeacon device 5 at different horizontal angles from 10° to 170°

Figure 39 is the box-and-whisker diagram, which clearly shows the range and average value of RSSI from Device at different angles in the same distance. Most of the RSSI values are between -85 dBm and -95 dBm.

4.2.6 System Calibration for Device 6

Figure 40 shows that, at 1-meter distance, RSSI of device 5 is various. However, the measurement of RSSI at different horizontal angles from 10° to 170° slightly changes in between -85dBm and -95dBm, as the antenna broadcasting may not cover smoothly at all angles.

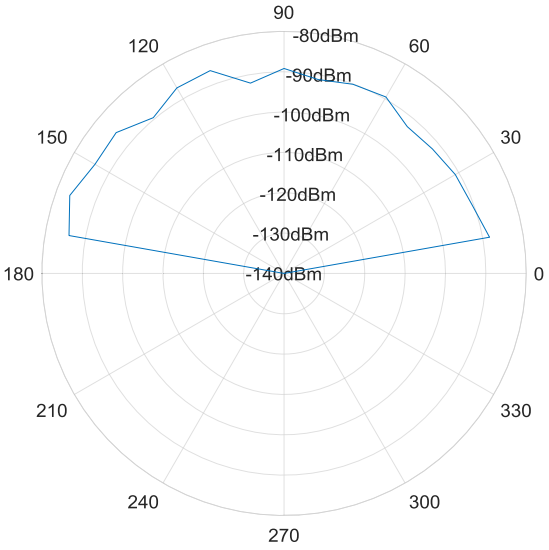

Figure 40 Polar diagram for iBeacon device 6 at different horizontal angles from 10° to 170°

Figure 41 is the box-and-whisker diagram, which clearly shows the range and average value of RSSI from Device at different angles in the same distance. Most of the RSSI values are between -80 dBm and -95 dBm.

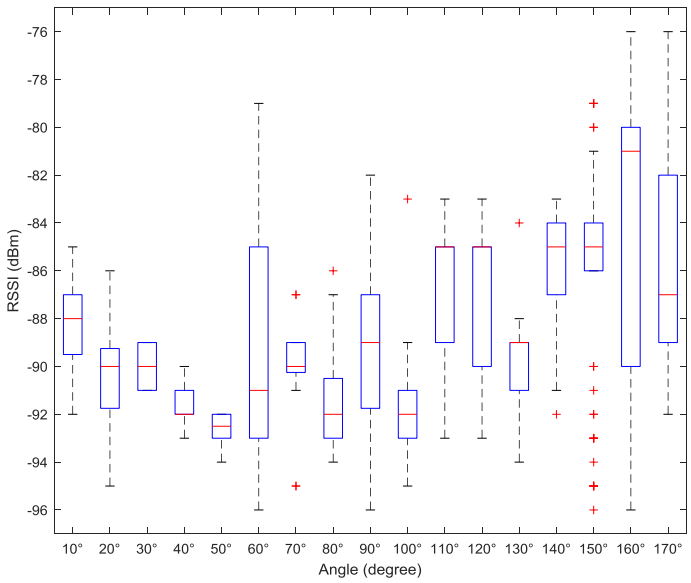

Figure 41 Box-and-whisker diagram for iBeacon device 6 at different horizontal angles from 10° to 170°

4.3 Error Modelling Calibration Process for Distance Measurement

As figure 42 and 43 displayed, both iBeacon and mobile phone are mounted on two 50 cm high stands with one-meter distance in between. Figure 42 and figure 43 displays two different views of the testbed. This testbed has been set up to calibrate the distance measurement for six different iBeacons.

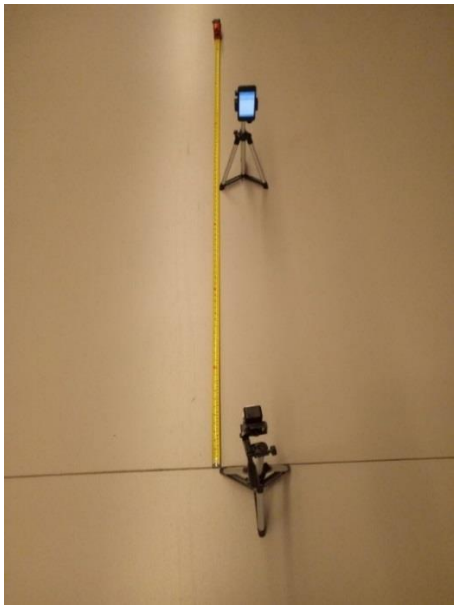

Figure 42 Testbed setup for 1-meter distance range (a)

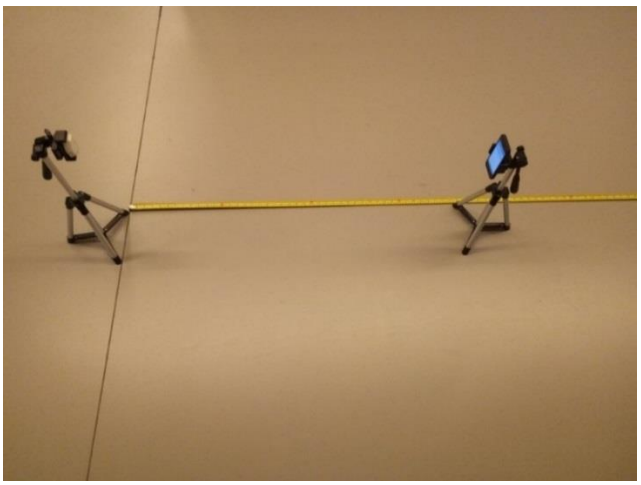

Figure 43 Testbed setup for 1-meter distance range (b)

4.3.1 Error Modelling Calibration for Device 1

The table 4 shows the iBeacon transmit data from Device 1, the data contains time (ms), UUID, Major ID, Minor ID, RSSI (dBm) and Device ID. The interval time of the signal transmit is about 300ms, the device has been setup 1 meter away from the mobile phone receiver to collect the data. 1500 sets of data have been collected. Here are some samples of them:

Table 4 Sample data table for iBeacon device 1

Time (ms)	UUID	Major	Minor	RSSI (dBm)	Device 1
1512	B9407F30-F5F8-466E-AFF9-25556B57FE6D	23772	63687	-91	Device 1
2435	B9407F30-F5F8-466E-AFF9-25556B57FE6D	23772	63687	-88	Device 1
2741	B9407F30-F5F8-466E-AFF9-25556B57FE6D	23772	63687	-89	Device 1
3366	B9407F30-F5F8-466E-AFF9-25556B57FE6D	23772	63687	-89	Device 1
3676	B9407F30-F5F8-466E-AFF9-25556B57FE6D	23772	63687	-91	Device 1
3972	B9407F30-F5F8-466E-AFF9-25556B57FE6D	23772	63687	-91	Device 1
4281	B9407F30-F5F8-466E-AFF9-25556B57FE6D	23772	63687	-90	Device 1
4586	B9407F30-F5F8-466E-AFF9-25556B57FE6D	23772	63687	-91	Device 1
5201	B9407F30-F5F8-466E-AFF9-25556B57FE6D	23772	63687	-90	Device 1
5504	B9407F30-F5F8-466E-AFF9-25556B57FE6D	23772	63687	-91	Device 1
5820	B9407F30-F5F8-466E-AFF9-25556B57FE6D	23772	63687	-92	Device 1
6131	B9407F30-F5F8-466E-AFF9-25556B57FE6D	23772	63687	-85	Device 1
7053	B9407F30-F5F8-466E-AFF9-25556B57FE6D	23772	63687	-88	Device 1
7983	B9407F30-F5F8-466E-AFF9-25556B57FE6D	23772	63687	-86	Device 1
8290	B9407F30-F5F8-466E-AFF9-25556B57FE6D	23772	63687	-88	Device 1
8898	B9407F30-F5F8-466E-AFF9-25556B57FE6D	23772	63687	-87	Device 1
9200	B9407F30-F5F8-466E-AFF9-25556B57FE6D	23772	63687	-88	Device 1
9505	B9407F30-F5F8-466E-AFF9-25556B57FE6D	23772	63687	-87	Device 1
10138	B9407F30-F5F8-466E-AFF9-25556B57FE6D	23772	63687	-87	Device 1
10436	B9407F30-F5F8-466E-AFF9-25556B57FE6D	23772	63687	-87	Device 1
10748	B9407F30-F5F8-466E-AFF9-25556B57FE6D	23772	63687	-86	Device 1
14460	B9407F30-F5F8-466E-AFF9-25556B57FE6D	23772	63687	-92	Device 1
15680	B9407F30-F5F8-466E-AFF9-25556B57FE6D	23772	63687	-93	Device 1
15993	B9407F30-F5F8-466E-AFF9-25556B57FE6D	23772	63687	-91	Device 1
16303	B9407F30-F5F8-466E-AFF9-25556B57FE6D	23772	63687	-90	Device 1
16616	B9407F30-F5F8-466E-AFF9-25556B57FE6D	23772	63687	-90	Device 1
17237	B9407F30-F5F8-466E-AFF9-25556B57FE6D	23772	63687	-90	Device 1
17555	B9407F30-F5F8-466E-AFF9-25556B57FE6D	23772	63687	-90	Device 1
17856	B9407F30-F5F8-466E-AFF9-25556B57FE6D	23772	63687	-90	Device 1
18172	B9407F30-F5F8-466E-AFF9-25556B57FE6D	23772	63687	-89	Device 1
…	…	…	…	…	…

The figure 44 displays the linear modelling of the data sets by using curve fitting algorithm, 1500 samples of RSSI have been plotted. The blue lines represent the row data of RSSI, whereas the red line represents the curve fitting data. In the modelling, a_1 represents the scale error of the curve fitting data, a_2 represents the expected RSSI at a distance of 1 meter. The curve fitting algorithm has been showed:

Error modelling (CF-RSSI):

$f(x) = a_1*x + a_2$

Coefficients (with 95% confidence bounds):

a_1 = -2.379e-05 (-0.0002463, 0.0001988)

(a_1 is -2.379e-05, which is the mean value from -0.0002463 to 0.0001988)

a_2 = -88.85 (-89.05, -88.66)

(a_2 is -88.85, which is the mean vale from -89.05 to -88.66)

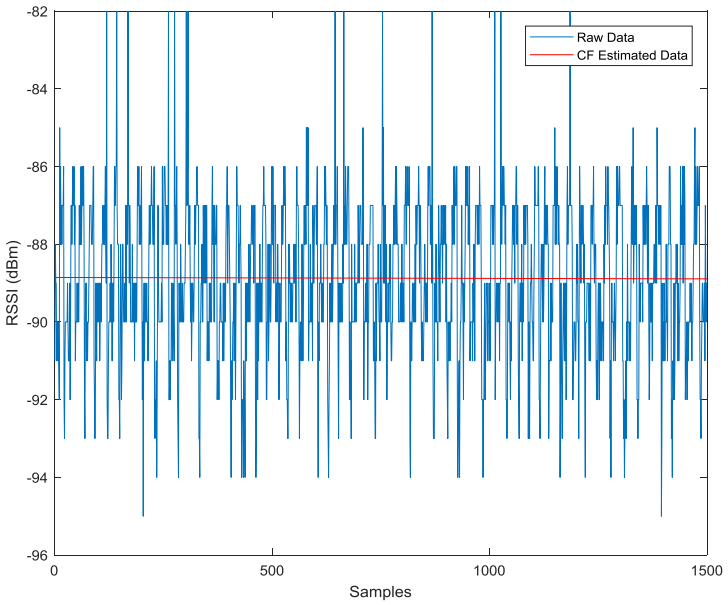

Figure 44 Diagram for Raw Data and CF Estimated Data (iBeacon device 1)

Goodness of fit:

The Sum of Squares due to Error (SSE): 6168

R-square: 2.842e-05

Adjusted R-square: -0.000618

Root Mean Squared Error (RMSE): 1.997

When we convert the RSSI into distance, the diagram 45 displays that the curve fitting is used to reduce the noise:

$A = |a_2| = 88.85$

D = 10 ^ ((abs (RSSI) - A) / (10 * n))

Distance = 1 meter

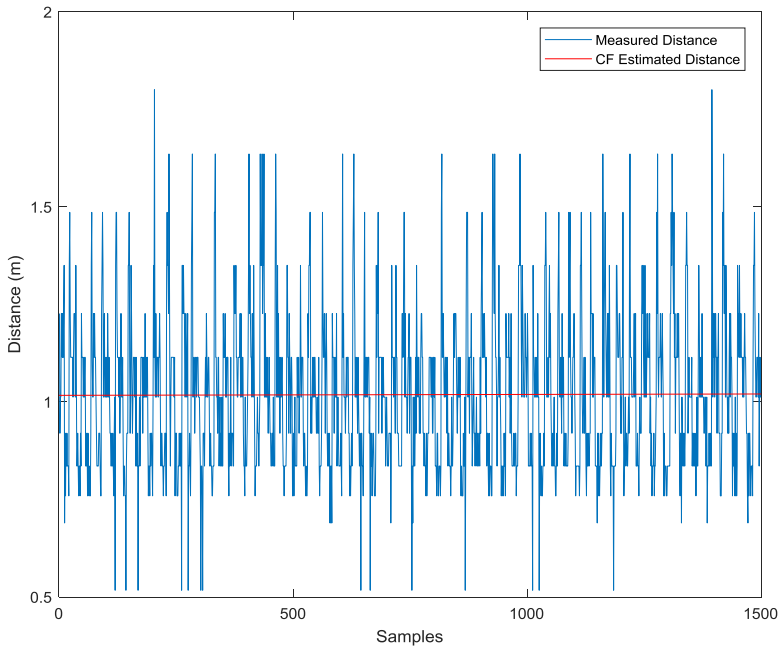

Figure 45 Diagram for Measured Distance and CF Estimated Distance (iBeacon device 1)

Error modelling (CF-Distance):

$f(x) = a_1*x + a_2$

Coefficients (with 95% confidence bounds):

$a_1 = 0.001288$ (-0.01076, 0.01333)

$a_2 = 1.027$ (1.015, 1.039)

Goodness of fit:

SSE: 90.27

R-square: 2.844e-05

Adjusted R-square: -0.000618

RMSE: 0.2416

Alternatively, when we use Kalman Filter on the data of distance to reduce the noise, the figure 46 displays below, the Kalman Filter estimated data is in red:

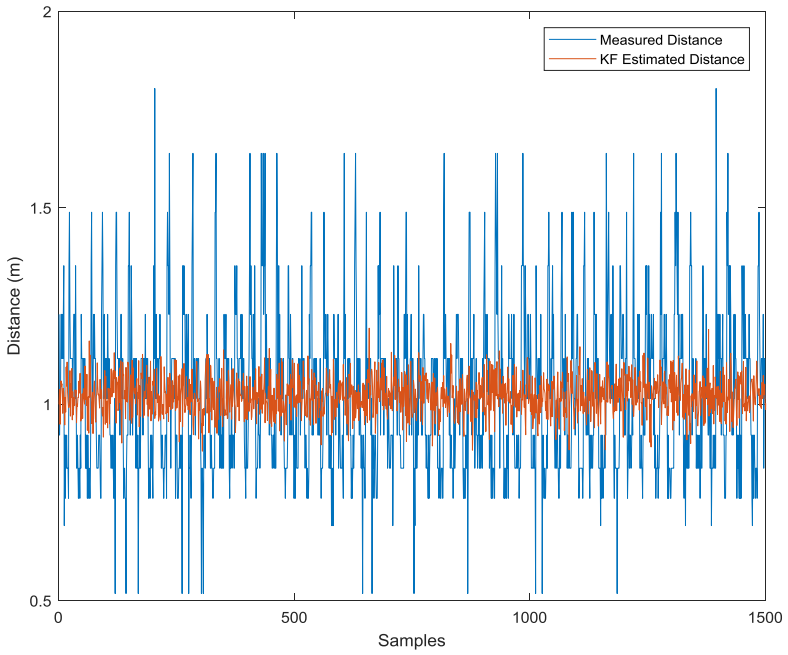

Figure 46 Diagram for Measured Distance and KF Estimated Distance (iBeacon device 1)

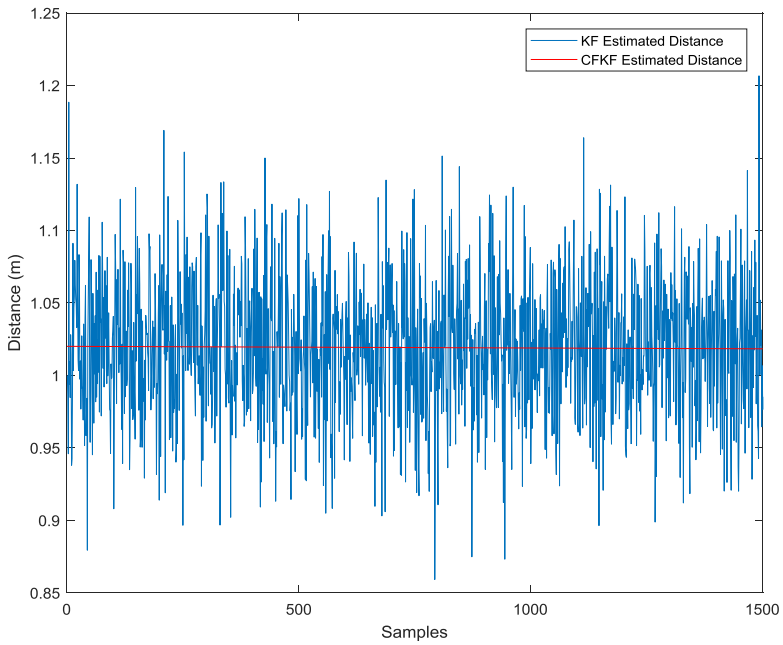

Figure 47 Diagram for KF Estimated Distance and KF Estimated Distance (iBeacon device 1)

When we use the curve fitting algorithm on the Kalman Filter estimated data, the result is more accurate than the data from curve fitting algorithm only.

Error modelling (CFKF):

$f(x) = a_1*x + a_2$

Coefficients (with 95% confidence bounds):

a_1 = -0.001535 (-0.004024, 0.0009533)

a_2 = 1.026 (1.024, 1.029)

Goodness of fit:

SSE: 3.86

R-square: 0.0009451

Adjusted R-square: 0.0002997

RMSE: 0.04994

Table 5 Algorithm error table for device 1

Positioning algorithm	Scale Factor	Error (meter)	Error Rate
Curve Fitting Error	0.001288	0.027	2.7%
Kalman Filter Error	NA	0.06-0.1	6%-10%
CFKF Error	-0.001535	0.026	2.6%
Measurement Error	NA	0.24-0.5	24%-50%

4.3.2 Error Modelling Calibration for Device 2

The table 6 shows the iBeacon transmit data from Device 2, the data contains time (ms), UUID, Major ID, Minor ID, RSSI (dBm) and Device ID. The interval time of the signal transmit is about 300ms, the device has been setup 1 meter away from the mobile phone receiver to collect the data. 1500 sets of data have been collected. Here are some samples of them:

Table 6 Sample data table for iBeacon device 2

Time (ms)	UUID	Major	Minor	RSSI (dBm)	Device 2
118	B9407F30-F5F8-466E-AFF9-25556B57FE6D	53764	59537	-89	Device 2
430	B9407F30-F5F8-466E-AFF9-25556B57FE6D	53764	59537	-88	Device 2
1358	B9407F30-F5F8-466E-AFF9-25556B57FE6D	53764	59537	-89	Device 2
2585	B9407F30-F5F8-466E-AFF9-25556B57FE6D	53764	59537	-94	Device 2
4765	B9407F30-F5F8-466E-AFF9-25556B57FE6D	53764	59537	-91	Device 2
5069	B9407F30-F5F8-466E-AFF9-25556B57FE6D	53764	59537	-90	Device 2
5375	B9407F30-F5F8-466E-AFF9-25556B57FE6D	53764	59537	-92	Device 2
5689	B9407F30-F5F8-466E-AFF9-25556B57FE6D	53764	59537	-92	Device 2
6314	B9407F30-F5F8-466E-AFF9-25556B57FE6D	53764	59537	-91	Device 2
6614	B9407F30-F5F8-466E-AFF9-25556B57FE6D	53764	59537	-90	Device 2
7530	B9407F30-F5F8-466E-AFF9-25556B57FE6D	53764	59537	-91	Device 2
8470	B9407F30-F5F8-466E-AFF9-25556B57FE6D	53764	59537	-92	Device 2
8777	B9407F30-F5F8-466E-AFF9-25556B57FE6D	53764	59537	-90	Device 2
9085	B9407F30-F5F8-466E-AFF9-25556B57FE6D	53764	59537	-90	Device 2
9393	B9407F30-F5F8-466E-AFF9-25556B57FE6D	53764	59537	-91	Device 2
9692	B9407F30-F5F8-466E-AFF9-25556B57FE6D	53764	59537	-85	Device 2
10005	B9407F30-F5F8-466E-AFF9-25556B57FE6D	53764	59537	-85	Device 2
10313	B9407F30-F5F8-466E-AFF9-25556B57FE6D	53764	59537	-86	Device 2
10612	B9407F30-F5F8-466E-AFF9-25556B57FE6D	53764	59537	-87	Device 2
11239	B9407F30-F5F8-466E-AFF9-25556B57FE6D	53764	59537	-85	Device 2
11857	B9407F30-F5F8-466E-AFF9-25556B57FE6D	53764	59537	-86	Device 2
12478	B9407F30-F5F8-466E-AFF9-25556B57FE6D	53764	59537	-86	Device 2
12794	B9407F30-F5F8-466E-AFF9-25556B57FE6D	53764	59537	-88	Device 2
13110	B9407F30-F5F8-466E-AFF9-25556B57FE6D	53764	59537	-86	Device 2
13716	B9407F30-F5F8-466E-AFF9-25556B57FE6D	53764	59537	-85	Device 2
14019	B9407F30-F5F8-466E-AFF9-25556B57FE6D	53764	59537	-87	Device 2
14321	B9407F30-F5F8-466E-AFF9-25556B57FE6D	53764	59537	-86	Device 2
16485	B9407F30-F5F8-466E-AFF9-25556B57FE6D	53764	59537	-93	Device 2
16795	B9407F30-F5F8-466E-AFF9-25556B57FE6D	53764	59537	-93	Device 2
17103	B9407F30-F5F8-466E-AFF9-25556B57FE6D	53764	59537	-94	Device 2
…	…	…	…	…	…

The figure 48 displays the linear modelling of the data sets by using curve fitting algorithm, 1500 samples of RSSI have been plotted. The blue lines represent the row data of RSSI, whereas the red line represents the curve fitting data. In the modelling, a_1 represents the scale error of the curve fitting data, a_2 represents the expected RSSI at a distance of 1 meter. The curve fitting algorithm has been showed below:

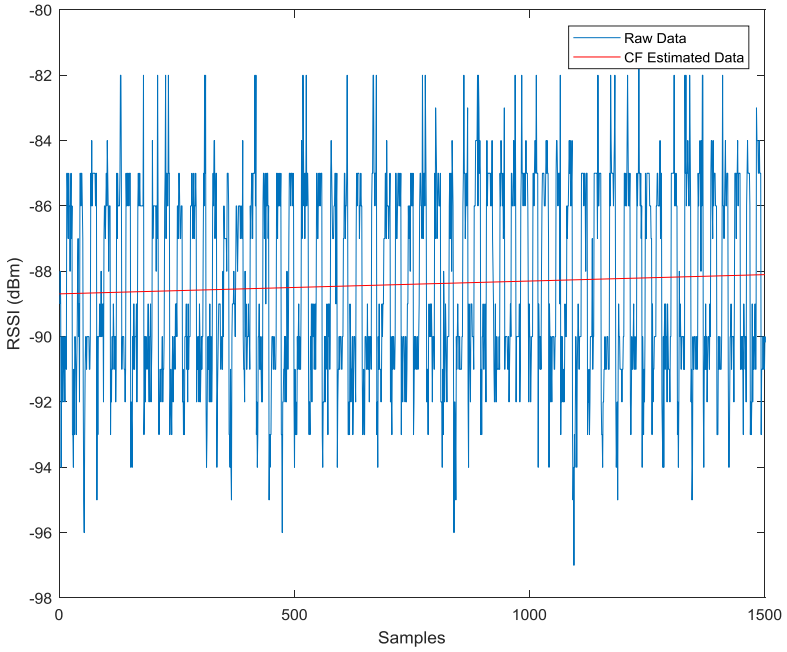

Figure 48 Diagram for Raw Data and CF Estimated Data (iBeacon device 2)

Error modelling (CF-RSSI):

$f(x) = a_1*x + a_2$

Coefficients (with 95% confidence bounds):

a_1 = 0.0003927 (5.184e-05, 0.0007335)

a_2 = -88.69 (-89, -88.39)

Goodness of fit:

SSE: 1.447e+04

R-square: 0.00329

Adjusted R-square: 0.002646

RMSE: 3.058

When we convert the RSSI into distance, the diagram 49 displays that curve fitting is used to reduce the noise:

A = $|a_2|$ = 88.69

D = 10 ^ ((abs (RSSI) - A) / (10 * n))

Distance = 1 meter

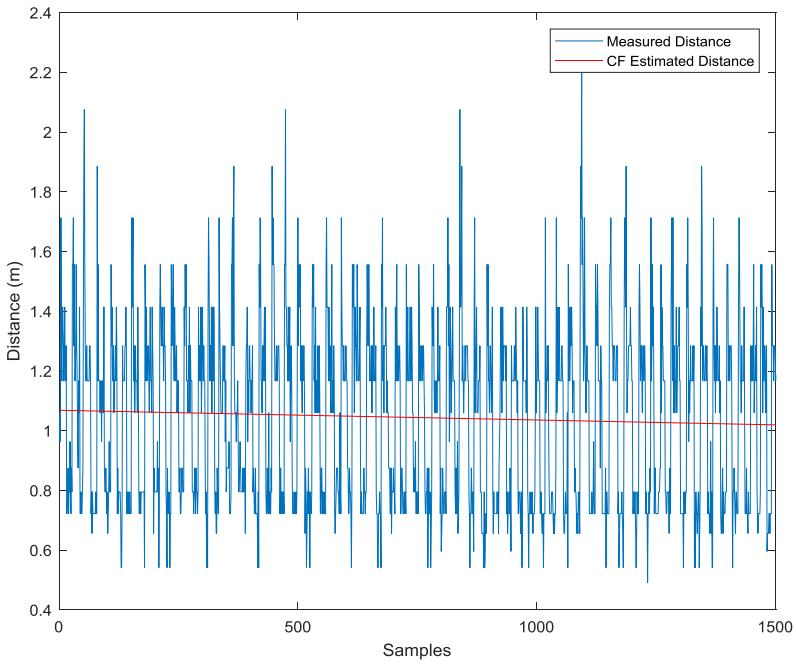

Figure 49 Diagram for Measured Distance and CF Estimated Distance (iBeacon device 2)

Error modelling (CF-Distance):

$f(x) = a_1*x + a_2$

Coefficients (with 95% confidence bounds):

a_1 = -3.265e-05 (-6.638e-05, 1.08e-06)

a_2 = 1.069 (1.038, 1.099)

Goodness of fit:

SSE: 141.7

R-square: 0.002325

Adjusted R-square: 0.00168

RMSE: 0.3026

Alternatively, when we use Kalman Filter on the data of distance to reduce the noise, the figure 50 displays, the Kalman Filter estimated data is in red:

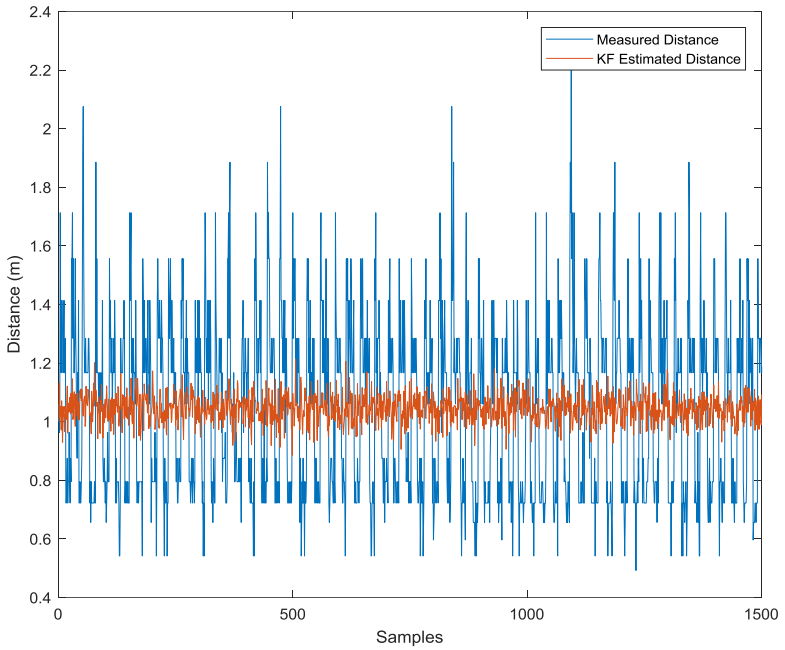

Figure 50 Diagram for Measured Distance and KF Estimated Distance (iBeacon device 2)

When we use the curve fitting algorithm on the Kalman Filter estimated data, the result is more accurate than the data from curve fitting algorithm only.

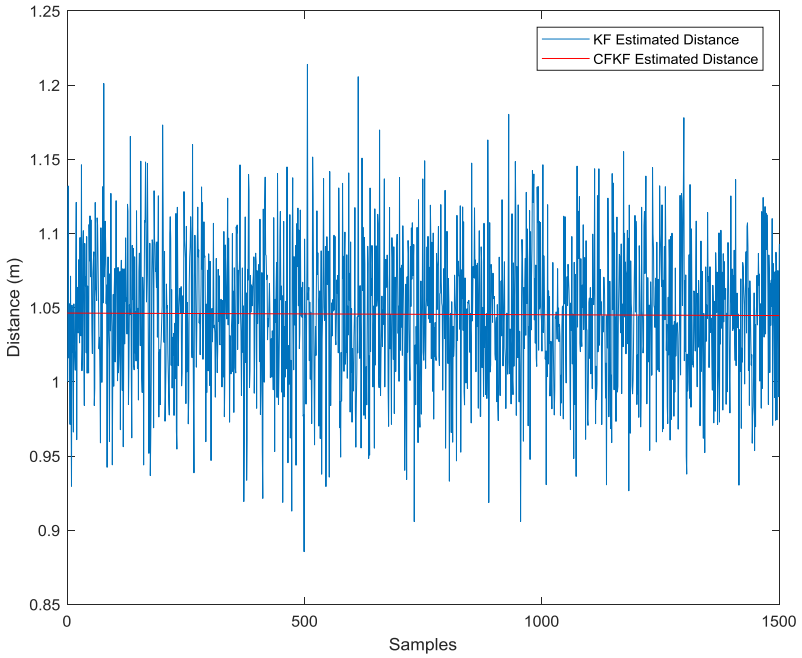

Figure 51 Diagram for KF Estimated Distance and CFKF Estimated Distance (iBeacon device 2)

Error modelling (CFKF):

$f(x) = a_1*x + a_2$

Coefficients (with 95% confidence bounds):

a_1 = -1.119e-06 (-6.421e-06, 4.182e-06)

a_2 = 1.046 (1.042, 1.051)

Goodness of fit:

SSE: 3.509

R-square: 0.0001108

Adjusted R-square: -0.0005351

RMSE: 0.04761

Table 7 Algorithm error table for device 2

Positioning algorithm	Scale Factor	Error (meter)	Error Rate
Curve Fitting Error	-3.265e-05	0.069	6.9%
Kalman Filter Error	NA	0.07-0.10	7%-10%
CFKF Error	-1.119e-06	0.046	4.6%
Measurement Error	NA	0.3-0.5	30%-50%

4.3.3 Error Modelling Calibration for Device 3

The table 8 shows the iBeacon transmit data from Device 3, the data contains time (ms), UUID, Major ID, Minor ID, RSSI (dBm) and Device ID. The interval time of the signal transmit is about 300ms, the device has been setup 1 meter away from the mobile phone receiver to collect the data. 1500 sets of data have been collected. Here are some samples of them:

Table 8 Sample data table for iBeacon device 3

Time (ms)	UUID	Major	Minor	RSSI (dBm)	Device 3
39	B9407F30-F5F8-466E-AFF9-25556B57FE6D	49245	21142	-83	Device 3
345	B9407F30-F5F8-466E-AFF9-25556B57FE6D	49245	21142	-80	Device 3
1260	B9407F30-F5F8-466E-AFF9-25556B57FE6D	49245	21142	-90	Device 3
1574	B9407F30-F5F8-466E-AFF9-25556B57FE6D	49245	21142	-90	Device 3
3112	B9407F30-F5F8-466E-AFF9-25556B57FE6D	49245	21142	-93	Device 3
3720	B9407F30-F5F8-466E-AFF9-25556B57FE6D	49245	21142	-89	Device 3
4031	B9407F30-F5F8-466E-AFF9-25556B57FE6D	49245	21142	-89	Device 3
4331	B9407F30-F5F8-466E-AFF9-25556B57FE6D	49245	21142	-89	Device 3
4643	B9407F30-F5F8-466E-AFF9-25556B57FE6D	49245	21142	-97	Device 3
4947	B9407F30-F5F8-466E-AFF9-25556B57FE6D	49245	21142	-95	Device 3
7706	B9407F30-F5F8-466E-AFF9-25556B57FE6D	49245	21142	-93	Device 3
8630	B9407F30-F5F8-466E-AFF9-25556B57FE6D	49245	21142	-95	Device 3
9251	B9407F30-F5F8-466E-AFF9-25556B57FE6D	49245	21142	-93	Device 3
9566	B9407F30-F5F8-466E-AFF9-25556B57FE6D	49245	21142	-90	Device 3
9880	B9407F30-F5F8-466E-AFF9-25556B57FE6D	49245	21142	-90	Device 3
10190	B9407F30-F5F8-466E-AFF9-25556B57FE6D	49245	21142	-91	Device 3
10499	B9407F30-F5F8-466E-AFF9-25556B57FE6D	49245	21142	-92	Device 3
11409	B9407F30-F5F8-466E-AFF9-25556B57FE6D	49245	21142	-89	Device 3
11718	B9407F30-F5F8-466E-AFF9-25556B57FE6D	49245	21142	-92	Device 3
12652	B9407F30-F5F8-466E-AFF9-25556B57FE6D	49245	21142	-91	Device 3
13267	B9407F30-F5F8-466E-AFF9-25556B57FE6D	49245	21142	-91	Device 3
13580	B9407F30-F5F8-466E-AFF9-25556B57FE6D	49245	21142	-92	Device 3
13884	B9407F30-F5F8-466E-AFF9-25556B57FE6D	49245	21142	-90	Device 3
14189	B9407F30-F5F8-466E-AFF9-25556B57FE6D	49245	21142	-91	Device 3
14492	B9407F30-F5F8-466E-AFF9-25556B57FE6D	49245	21142	-90	Device 3
15112	B9407F30-F5F8-466E-AFF9-25556B57FE6D	49245	21142	-89	Device 3
15409	B9407F30-F5F8-466E-AFF9-25556B57FE6D	49245	21142	-88	Device 3
16021	B9407F30-F5F8-466E-AFF9-25556B57FE6D	49245	21142	-90	Device 3
16337	B9407F30-F5F8-466E-AFF9-25556B57FE6D	49245	21142	-89	Device 3
17269	B9407F30-F5F8-466E-AFF9-25556B57FE6D	49245	21142	-89	Device 3
…	…	…	…	…	…

The figure 52 displays the linear modelling of the data sets by using curve fitting algorithm, 1500 samples of RSSI have been plotted. The blue lines represent the row data of RSSI, whereas the red line represents the curve fitting data. In the modelling, a_1 represents the scale error of the curve fitting data, a_2 represents the expected RSSI at a distance of 1 meter. The curve fitting algorithm has been showed below:

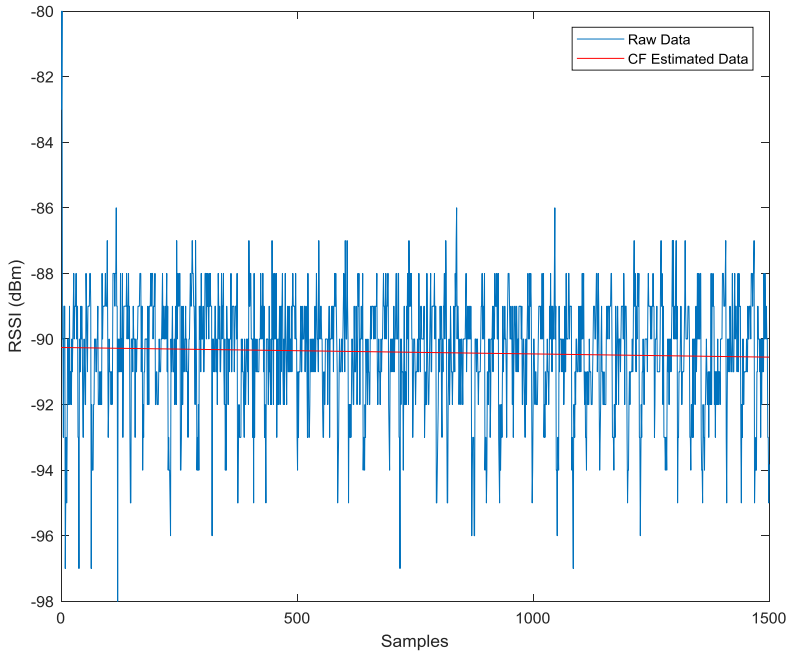

Figure 52 Diagram for Raw Data and CF Estimated Data (iBeacon device 3)

Error modelling (CF-RSSI):

$f(x) = a_1*x + a_2$

Coefficients (with 95% confidence bounds):

a_1 = -0.08598 (-0.1751, 0.003154)

a_2 = -90.41 (-90.5, -90.32)

Goodness of fit:

SSE: 4939

R-square: 0.00231

Adjusted R-square: 0.001665

RMSE: 1.787

When we convert the RSSI into distance, the diagram 53 displays that the curve fitting is used to reduce the noise:

A = $|a_2|$ = 90.41

D = 10 ^ ((abs (RSSI) - A) / (10 * n))

Distance = 1 meter

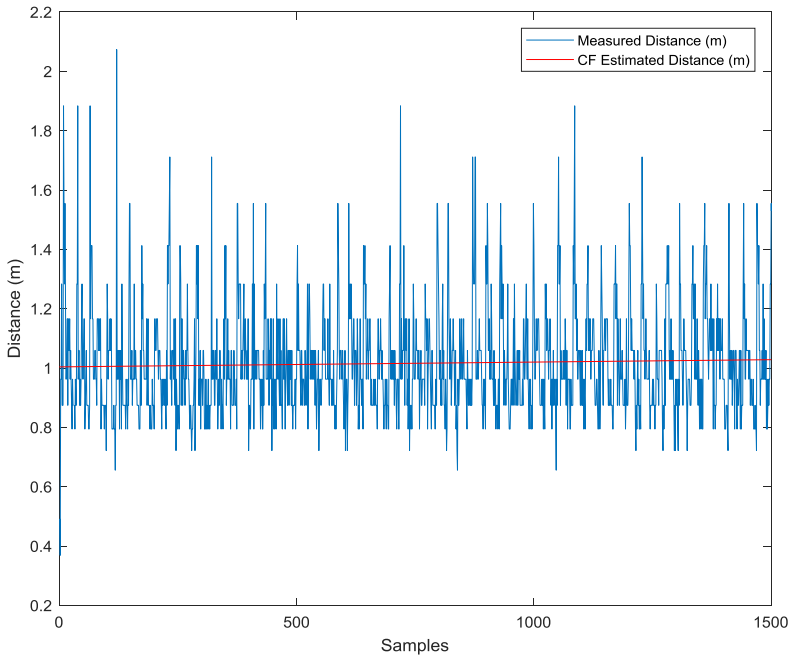

Figure 53 Diagram for Measured Distance and CF Estimated Distance (iBeacon device 3)

Error modelling (CF-Distance):

$f(x) = a_1*x + a_2$

Coefficients (with 95% confidence bounds):

a_1 = 0.007232 (-0.002023, 0.01649)

a_2 = 1.016 (1.007, 1.026)

Goodness of fit:

SSE: 53.24

R-square: 0.001517

Adjusted R-square: 0.0008713

RMSE: 0.1856

Alternatively, when we use Kalman Filter on the data of distance to reduce the noise, the figure 54 displays below, the Kalman Filter estimated data is in red:

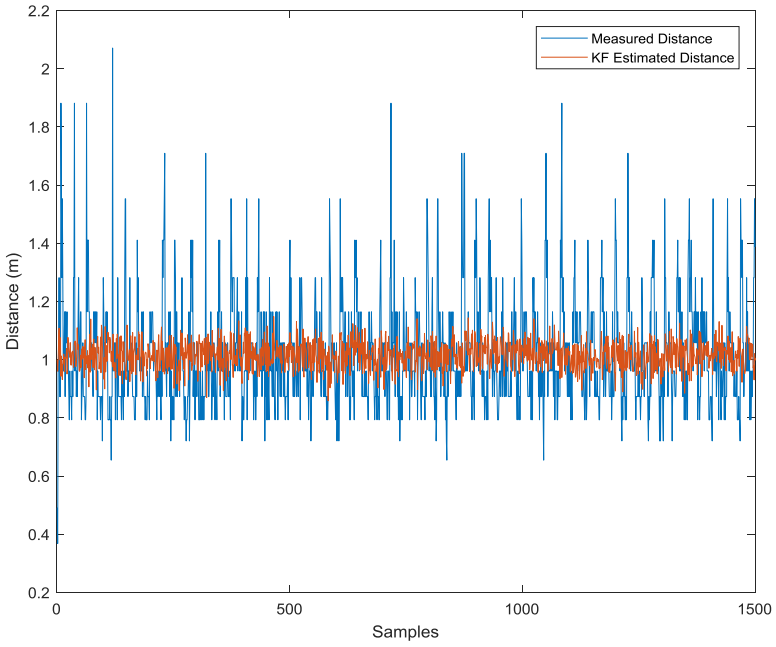

Figure 54 Diagram for Measured Distance and KF Estimated Distance (iBeacon device 3)

When we use the curve fitting algorithm on the Kalman Filter estimated data, the result is more accurate than the data from curve fitting algorithm only.

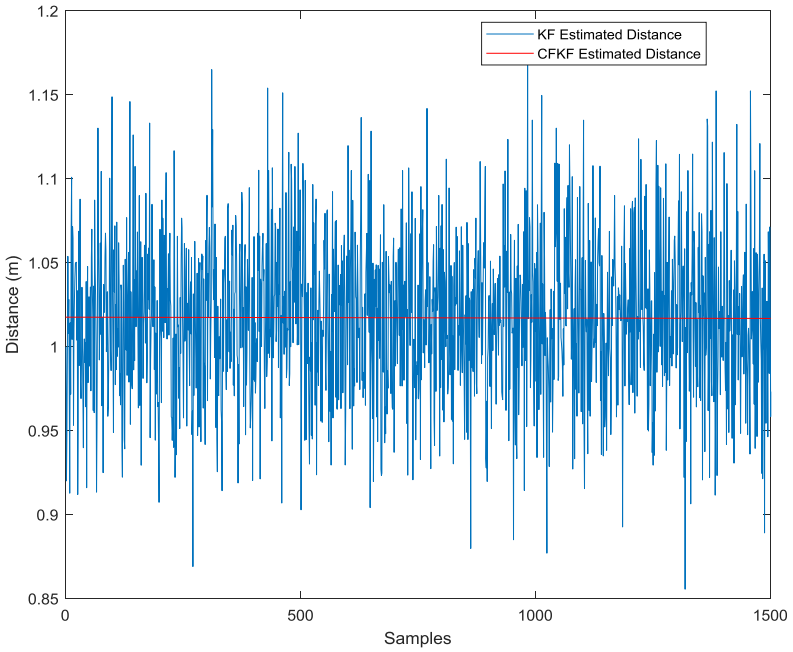

Figure 55 Diagram for KF Estimated Distance and CFKF Estimated Distance (iBeacon device 3)

Error modelling (CFKF):

$f(x) = a_1*x + a_2$

Coefficients (with 95% confidence bounds):

a_1 = -0.0002229 (-0.002574, 0.002128)

a_2 = 1.015 (1.01, 1.02)

Goodness of fit:

SSE: 3.445

R-square: 2.235e-05

Adjusted R-square: -0.0006236

RMSE: 0.04717

Table 9 Algorithm error table for device 3

Positioning algorithm	Scale Factor	Error (meter)	Error Rate
Curve Fitting Error	0.007232	0.016	1.6%
Kalman Filter Error	NA	0.05-0.10	5%-10%
CFKF Error	-0.0002229	0.015	1.5%
Measurement Error	NA	0.2-0.4	20%-40%

4.3.4 Error Modelling Calibration for Device 4

The table 10 shows the iBeacon transmit data from Device 4, the data contains time (ms), UUID, Major ID, Minor ID, RSSI (dBm) and Device ID. The interval time of the signal transmit

is about 300ms, the device has been setup 1 meter away from the mobile phone receiver to collect the data. 1500 sets of data have been collected. Here are some samples of them:

Table 10 Sample data table for iBeacon device 4

Time (ms)	UUID	Major	Minor	RSSI (dBm)	Device 4
359	B9407F30-F5F8-466E-AFF9-25556B57FE6D	23060	60056	-92	Device 4
673	B9407F30-F5F8-466E-AFF9-25556B57FE6D	23060	60056	-92	Device 4
1287	B9407F30-F5F8-466E-AFF9-25556B57FE6D	23060	60056	-89	Device 4
1589	B9407F30-F5F8-466E-AFF9-25556B57FE6D	23060	60056	-92	Device 4
1891	B9407F30-F5F8-466E-AFF9-25556B57FE6D	23060	60056	-92	Device 4
2195	B9407F30-F5F8-466E-AFF9-25556B57FE6D	23060	60056	-92	Device 4
2508	B9407F30-F5F8-466E-AFF9-25556B57FE6D	23060	60056	-92	Device 4
2820	B9407F30-F5F8-466E-AFF9-25556B57FE6D	23060	60056	-90	Device 4
3126	B9407F30-F5F8-466E-AFF9-25556B57FE6D	23060	60056	-88	Device 4
3750	B9407F30-F5F8-466E-AFF9-25556B57FE6D	23060	60056	-91	Device 4
4059	B9407F30-F5F8-466E-AFF9-25556B57FE6D	23060	60056	-91	Device 4
4373	B9407F30-F5F8-466E-AFF9-25556B57FE6D	23060	60056	-90	Device 4
4989	B9407F30-F5F8-466E-AFF9-25556B57FE6D	23060	60056	-91	Device 4
5290	B9407F30-F5F8-466E-AFF9-25556B57FE6D	23060	60056	-90	Device 4
5910	B9407F30-F5F8-466E-AFF9-25556B57FE6D	23060	60056	-85	Device 4
6227	B9407F30-F5F8-466E-AFF9-25556B57FE6D	23060	60056	-85	Device 4
6547	B9407F30-F5F8-466E-AFF9-25556B57FE6D	23060	60056	-84	Device 4
7150	B9407F30-F5F8-466E-AFF9-25556B57FE6D	23060	60056	-85	Device 4
7450	B9407F30-F5F8-466E-AFF9-25556B57FE6D	23060	60056	-85	Device 4
7772	B9407F30-F5F8-466E-AFF9-25556B57FE6D	23060	60056	-86	Device 4
8062	B9407F30-F5F8-466E-AFF9-25556B57FE6D	23060	60056	-85	Device 4
8369	B9407F30-F5F8-466E-AFF9-25556B57FE6D	23060	60056	-85	Device 4
8682	B9407F30-F5F8-466E-AFF9-25556B57FE6D	23060	60056	-85	Device 4
9305	B9407F30-F5F8-466E-AFF9-25556B57FE6D	23060	60056	-84	Device 4
9621	B9407F30-F5F8-466E-AFF9-25556B57FE6D	23060	60056	-85	Device 4
9927	B9407F30-F5F8-466E-AFF9-25556B57FE6D	23060	60056	-84	Device 4
10241	B9407F30-F5F8-466E-AFF9-25556B57FE6D	23060	60056	-85	Device 4
10546	B9407F30-F5F8-466E-AFF9-25556B57FE6D	23060	60056	-85	Device 4
10861	B9407F30-F5F8-466E-AFF9-25556B57FE6D	23060	60056	-93	Device 4
11787	B9407F30-F5F8-466E-AFF9-25556B57FE6D	23060	60056	-93	Device 4
...	...	...	...	...	...

The figure 56 displays the linear modelling of the data sets by using curve fitting algorithm, 1500 samples of RSSI have been plotted. The blue lines represent the row data of RSSI, whereas the red line represents the curve fitting data. In the modelling, a_1 represents the

scale error of the curve fitting data, a_2 represents the expected RSSI at a distance of 1 meter.

The curve fitting algorithm has been showed below:

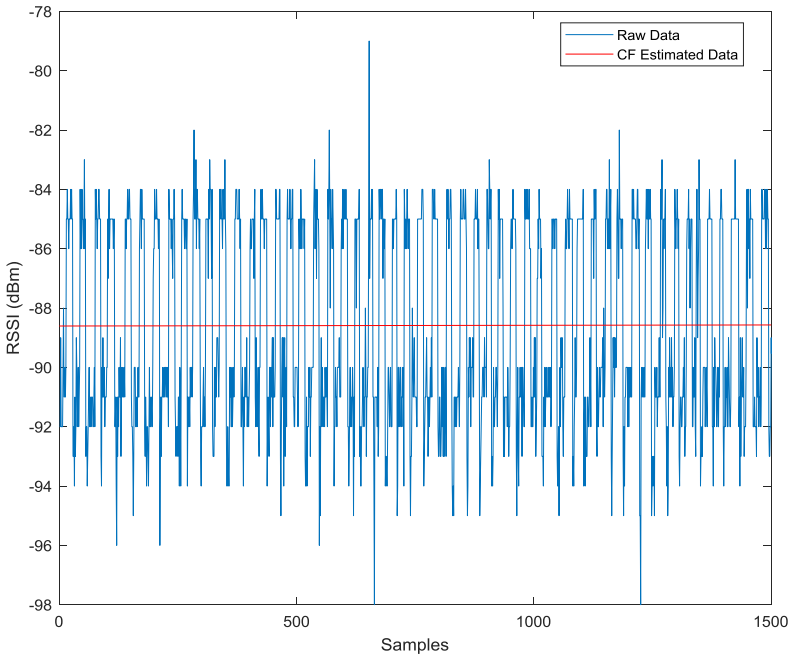

Figure 56 Diagram for Raw Data and CF Estimated Data (iBeacon device 4)

Error modelling (CF-RSSI):

$f(x) = a_1*x + a_2$

Coefficients (with 95% confidence bounds):

a_1 = 0.01069 (-0.1593, 0.1807)

a_2 = -88.59 (-88.76, -88.42)

Goodness of fit:

SSE: 1.8e+04

R-square: 9.822e-06

Adjusted R-square: -0.0006366

RMSE: 3.411

When we convert the RSSI into distance, the diagram 57 displays that the curve fitting is used to reduce the noise:

$A = |a_2| = 88.59$

D = 10 ^ ((abs (RSSI) - A) / (10 * n))

Distance = 1 meter

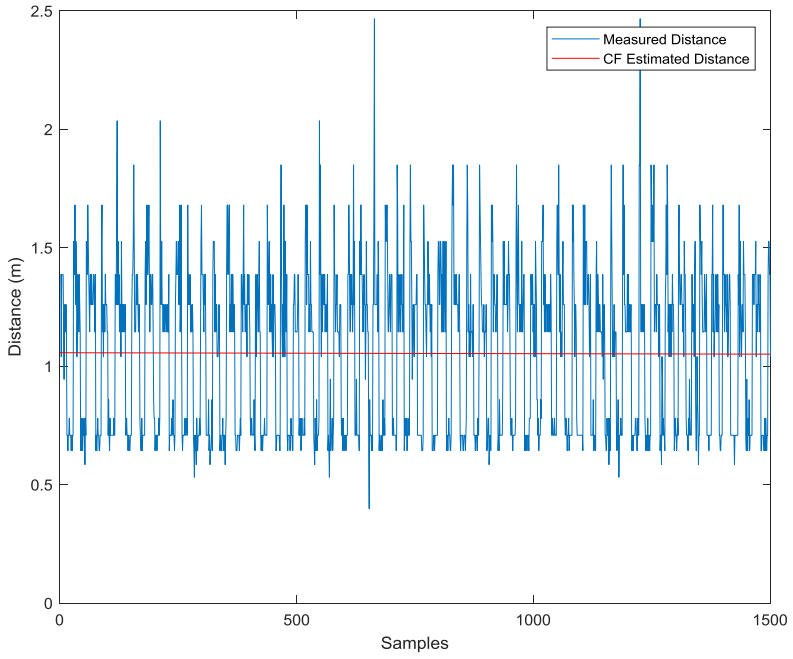

Figure 57 Diagram for Measured Distance and CF Estimated Distance (iBeacon device 4)

Error modelling (CF-Distance):

$f(x) = a_1*x + a_2$

Coefficients (with 95% confidence bounds):

a_1 = -3.984e-06 (-4.171e-05, 3.374e-05)

a_2 = 1.057 (1.023, 1.091)

Goodness of fit:

SSE: 177.2

R-square: 2.774e-05

Adjusted R-square: -0.0006187

RMSE: 0.3385

Alternatively, when we use Kalman Filter on the data of distance to reduce the noise, the figure 58 displays below, the Kalman Filter estimated data is in red:

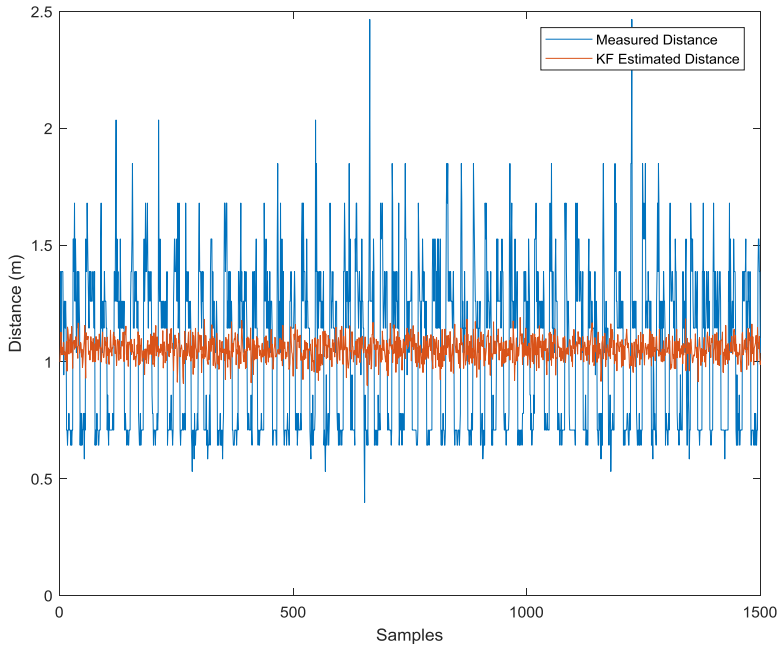

Figure 58 Diagram for Measured Distance and KF Estimated Distance (iBeacon device 4)

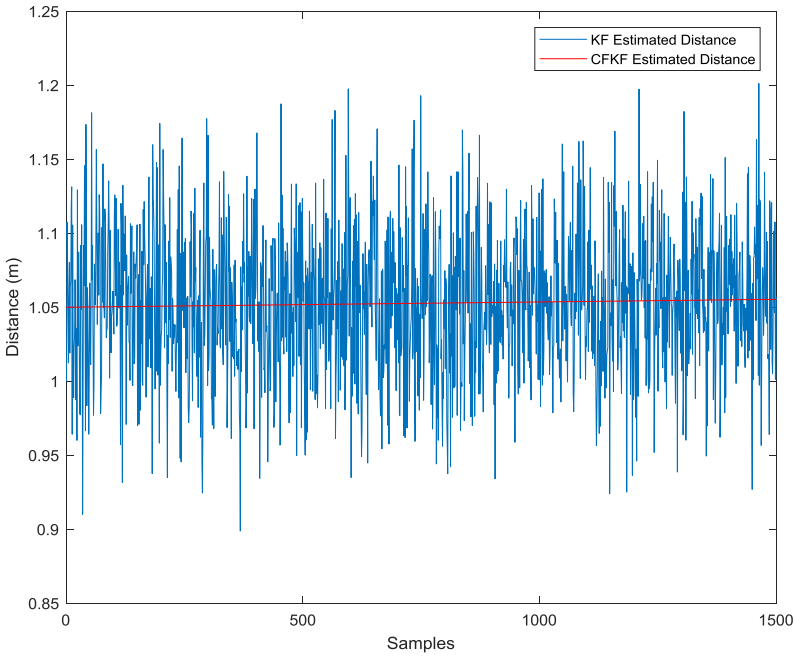

Figure 59 Diagram for CF Estimated Distance and CFKF Estimated Distance (iBeacon device 4)

When we use the curve fitting algorithm on the Kalman Filter estimated data, the result is more accurate than the data from curve fitting algorithm only.

Error modelling (CFKF):

$f(x) = a_1*x + a_2$

Coefficients (with 95% confidence bounds):

a_1 = -8.68e-07 (-6.208e-06, 4.472e-06)

a_2 = 1.055 (1.05, 1.06)

Goodness of fit:

SSE: 3.561

R-square: 6.566e-05

Adjusted R-square: -0.0005803

RMSE: 0.04796

Table 11 Algorithm error table for device 4

Positioning algorithm	Scale Factor	Error (meter)	Error Rate
Curve Fitting Error	-3.984e-06	0.057	5.7%
KF Error	NA	0.05-0.1	6%-15%
CFKF Error	-8.68e-07	0.055	5.5%
Measurement Error	NA	0.4-0.5	40%-50%

4.3.5 Error Modelling Calibration for Device 5

The table 12 shows the iBeacon transmit data from Device 5, the data contains time (ms), UUID, Major ID, Minor ID, RSSI (dBm) and Device ID. The interval time of the signal transmit is about 300ms, the device has been setup 1 meter away from the mobile phone receiver to collect the data. 1500 sets of data have been collected. Here are some samples of them:

Table 12 Sample data table for iBeacon device 5

Time (ms)	UUID	Major	Minor	RSSI (dBm)	Device 5
568	B9407F30-F5F8-466E-AFF9-25556B57FE6D	18691	17592	-90	Device 5
869	B9407F30-F5F8-466E-AFF9-25556B57FE6D	18691	17592	-92	Device 5
1176	B9407F30-F5F8-466E-AFF9-25556B57FE6D	18691	17592	-92	Device 5
1476	B9407F30-F5F8-466E-AFF9-25556B57FE6D	18691	17592	-93	Device 5
1779	B9407F30-F5F8-466E-AFF9-25556B57FE6D	18691	17592	-91	Device 5
2704	B9407F30-F5F8-466E-AFF9-25556B57FE6D	18691	17592	-91	Device 5
3014	B9407F30-F5F8-466E-AFF9-25556B57FE6D	18691	17592	-95	Device 5
3329	B9407F30-F5F8-466E-AFF9-25556B57FE6D	18691	17592	-90	Device 5
3635	B9407F30-F5F8-466E-AFF9-25556B57FE6D	18691	17592	-85	Device 5
3934	B9407F30-F5F8-466E-AFF9-25556B57FE6D	18691	17592	-84	Device 5
4240	B9407F30-F5F8-466E-AFF9-25556B57FE6D	18691	17592	-84	Device 5
4552	B9407F30-F5F8-466E-AFF9-25556B57FE6D	18691	17592	-86	Device 5
4859	B9407F30-F5F8-466E-AFF9-25556B57FE6D	18691	17592	-84	Device 5
5492	B9407F30-F5F8-466E-AFF9-25556B57FE6D	18691	17592	-84	Device 5
6404	B9407F30-F5F8-466E-AFF9-25556B57FE6D	18691	17592	-85	Device 5
7025	B9407F30-F5F8-466E-AFF9-25556B57FE6D	18691	17592	-85	Device 5
7332	B9407F30-F5F8-466E-AFF9-25556B57FE6D	18691	17592	-84	Device 5
7651	B9407F30-F5F8-466E-AFF9-25556B57FE6D	18691	17592	-85	Device 5
9200	B9407F30-F5F8-466E-AFF9-25556B57FE6D	18691	17592	-88	Device 5
10736	B9407F30-F5F8-466E-AFF9-25556B57FE6D	18691	17592	-88	Device 5
11353	B9407F30-F5F8-466E-AFF9-25556B57FE6D	18691	17592	-89	Device 5
12606	B9407F30-F5F8-466E-AFF9-25556B57FE6D	18691	17592	-89	Device 5
13214	B9407F30-F5F8-466E-AFF9-25556B57FE6D	18691	17592	-91	Device 5
13519	B9407F30-F5F8-466E-AFF9-25556B57FE6D	18691	17592	-91	Device 5
14134	B9407F30-F5F8-466E-AFF9-25556B57FE6D	18691	17592	-91	Device 5
14451	B9407F30-F5F8-466E-AFF9-25556B57FE6D	18691	17592	-92	Device 5
14765	B9407F30-F5F8-466E-AFF9-25556B57FE6D	18691	17592	-92	Device 5
15377	B9407F30-F5F8-466E-AFF9-25556B57FE6D	18691	17592	-92	Device 5
15691	B9407F30-F5F8-466E-AFF9-25556B57FE6D	18691	17592	-90	Device 5
15992	B9407F30-F5F8-466E-AFF9-25556B57FE6D	18691	17592	-89	Device 5
...	...	...	...	...	...

The figure 60 displays the linear modelling of the data sets by using curve fitting algorithm, 1500 samples of RSSI have been plotted. The blue lines represent the row data of RSSI, whereas the red line represents the curve fitting data. In the modelling, a_1 represents the scale error of the curve fitting data, a_2 represents the expected RSSI at a distance of 1 meter. The curve fitting algorithm has been showed below:

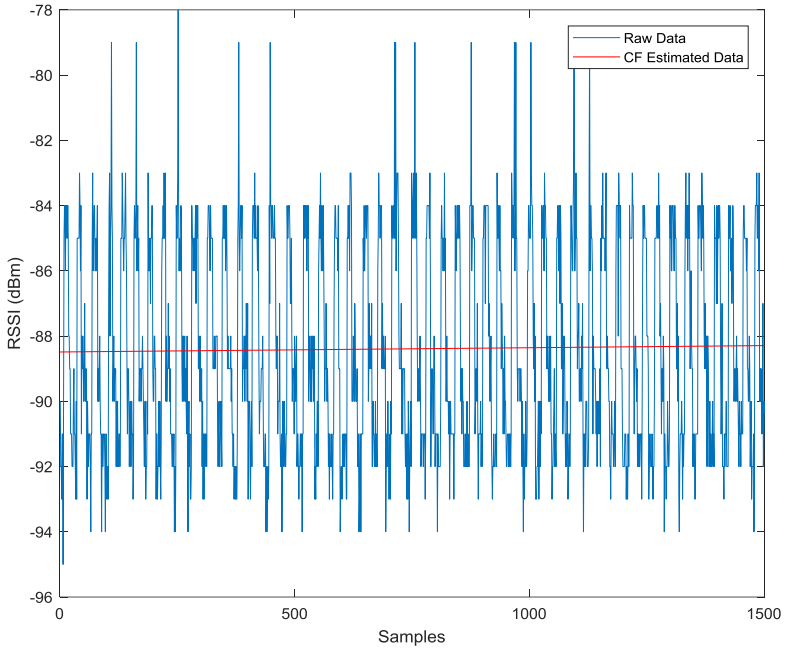

Figure 60 Diagram for Raw Data and CF Estimated Data (iBeacon device 5)

Error modelling (CF-RSSI):

$f(x) = a_1*x + a_2$

Coefficients (with 95% confidence bounds):

a_1 = 0.05836 (-0.1039, 0.2206)

a_2 = -88.39 (-88.55, -88.22)

Goodness of fit:

SSE: 1.638e+04

R-square: 0.0003218

Adjusted R-square: -0.0003244

RMSE: 3.254

When we convert the RSSI into distance, the diagram 61 displays that the curve fitting is used to reduce the noise:

$A = |a_2| = 88.39$

D = 10 ^ ((abs (RSSI) - A) / (10 * n))

Distance = 1 meter

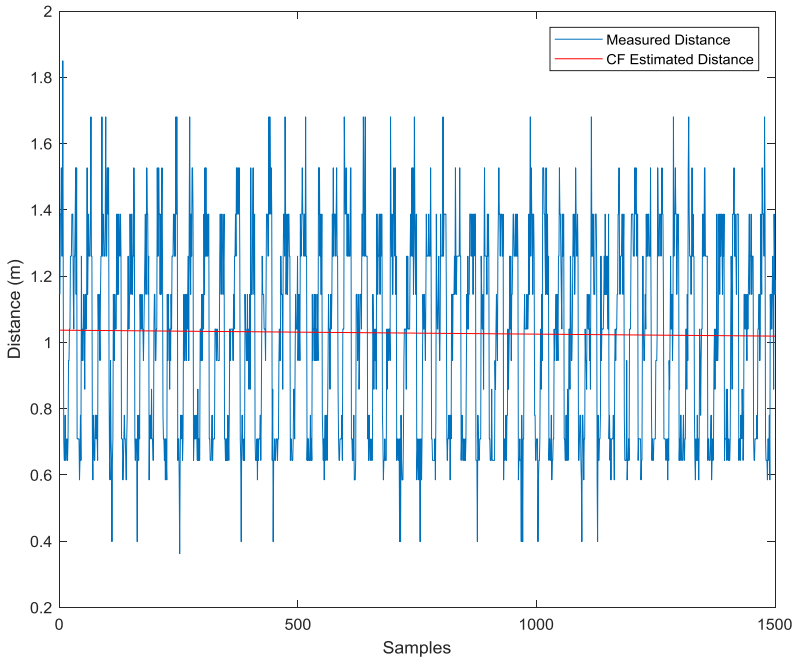

Figure 61 Diagram for Measured Distance and CF Estimated Distance (iBeacon device 5)

Error modelling (CF-Distance):

$f(x) = a_1*x + a_2$

Coefficients (with 95% confidence bounds):

a_1 = -1.223e-05 (-4.656e-05, 2.21e-05)

a_2 = 1.057 (1.026, 1.088)

Goodness of fit:

SSE: 146.8

R-square: 0.0003156

Adjusted R-square: -0.0003306

RMSE: 0.308

Alternatively, when we use Kalman Filter on the data of distance to reduce the noise, the figure 62 displays below, the Kalman Filter estimated data is in red:

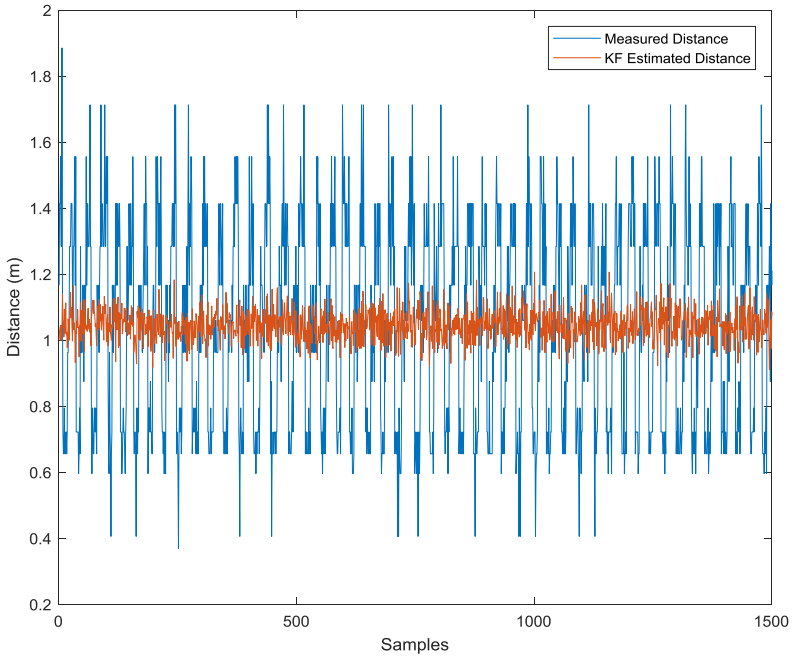

Figure 62 Diagram for Measured Distance and KF Estimated Distance (iBeacon device 5)

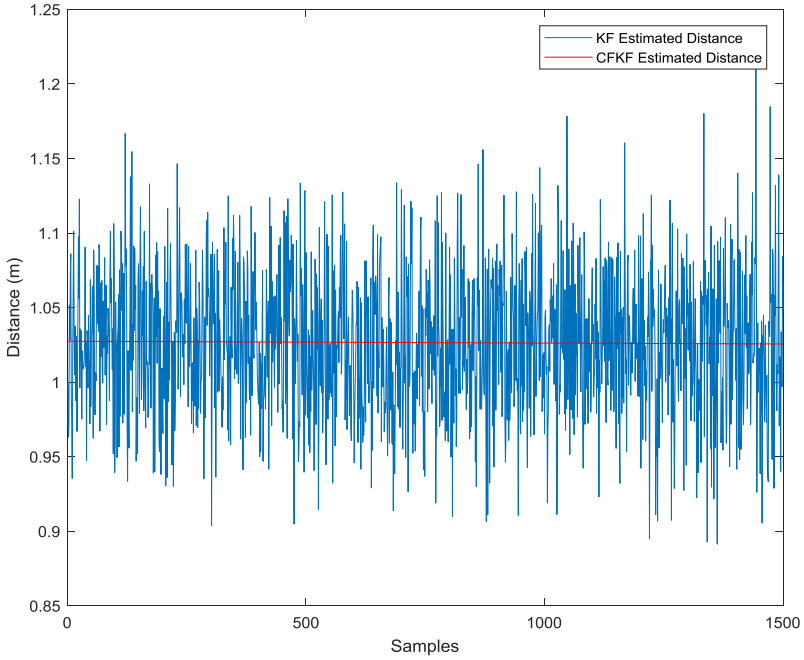

Figure 63 Diagram for KF Estimated Distance and CFKF Estimated Distance (iBeacon device 5)

When we use the curve fitting algorithm on the Kalman Filter estimated data, the result is more accurate than the data from curve fitting algorithm only.

Error modelling (CFKF):

$f(x) = a_1*x + a_2$

Coefficients (with 95% confidence bounds):

a_1 = 2.595e-06 (-2.594e-06, 7.784e-06)

a_2 = 1.045 (1.04, 1.049)

Goodness of fit:

SSE: 3.362

R-square: 0.0006212

Adjusted R-square: -2.443e-05

RMSE: 0.04661

Table 13 Algorithm error table for device 5

Positioning algorithm	Scale Factor	Error (meter)	Error Rate
Curve Fitting Error	-1.223e-05	0.057	5.7%
KF Error	NA	0.07-0.13	7%-13%
CFKF Error	2.595e-06	0.045	4.5%
Measurement Error	NA	0.25-0.56	25%-56%

4.3.6 Error Modelling Calibration for Device 6

The table 14 shows the iBeacon transmit data from Device 6, the data contains time (ms), UUID, Major ID, Minor ID, RSSI (dBm) and Device ID. The interval time of the signal transmit is about 300ms, the device has been setup 1 meter away from the mobile phone receiver to collect the data. 1500 sets of data have been collected. Here are some samples of them:

Table 14 Sample data table for iBeacon device 6

Time (ms)	UUID	Major	Minor	RSSI (dBm)	Device 6
348	B9407F30-F5F8-466E-AFF9-25556B57FE6D	15487	17347	-91	Device 6
976	B9407F30-F5F8-466E-AFF9-25556B57FE6D	15487	17347	-92	Device 6
1288	B9407F30-F5F8-466E-AFF9-25556B57FE6D	15487	17347	-92	Device 6
1586	B9407F30-F5F8-466E-AFF9-25556B57FE6D	15487	17347	-86	Device 6
1888	B9407F30-F5F8-466E-AFF9-25556B57FE6D	15487	17347	-88	Device 6
2197	B9407F30-F5F8-466E-AFF9-25556B57FE6D	15487	17347	-93	Device 6
2502	B9407F30-F5F8-466E-AFF9-25556B57FE6D	15487	17347	-92	Device 6
2820	B9407F30-F5F8-466E-AFF9-25556B57FE6D	15487	17347	-90	Device 6
3435	B9407F30-F5F8-466E-AFF9-25556B57FE6D	15487	17347	-90	Device 6
3744	B9407F30-F5F8-466E-AFF9-25556B57FE6D	15487	17347	-89	Device 6
4363	B9407F30-F5F8-466E-AFF9-25556B57FE6D	15487	17347	-91	Device 6
4664	B9407F30-F5F8-466E-AFF9-25556B57FE6D	15487	17347	-92	Device 6
4983	B9407F30-F5F8-466E-AFF9-25556B57FE6D	15487	17347	-92	Device 6
5288	B9407F30-F5F8-466E-AFF9-25556B57FE6D	15487	17347	-91	Device 6
5599	B9407F30-F5F8-466E-AFF9-25556B57FE6D	15487	17347	-91	Device 6
5906	B9407F30-F5F8-466E-AFF9-25556B57FE6D	15487	17347	-92	Device 6
6212	B9407F30-F5F8-466E-AFF9-25556B57FE6D	15487	17347	-92	Device 6
6522	B9407F30-F5F8-466E-AFF9-25556B57FE6D	15487	17347	-91	Device 6
6831	B9407F30-F5F8-466E-AFF9-25556B57FE6D	15487	17347	-94	Device 6
7144	B9407F30-F5F8-466E-AFF9-25556B57FE6D	15487	17347	-87	Device 6
7447	B9407F30-F5F8-466E-AFF9-25556B57FE6D	15487	17347	-87	Device 6
7760	B9407F30-F5F8-466E-AFF9-25556B57FE6D	15487	17347	-86	Device 6
8069	B9407F30-F5F8-466E-AFF9-25556B57FE6D	15487	17347	-82	Device 6
9001	B9407F30-F5F8-466E-AFF9-25556B57FE6D	15487	17347	-88	Device 6
10218	B9407F30-F5F8-466E-AFF9-25556B57FE6D	15487	17347	-86	Device 6
10524	B9407F30-F5F8-466E-AFF9-25556B57FE6D	15487	17347	-87	Device 6
14208	B9407F30-F5F8-466E-AFF9-25556B57FE6D	15487	17347	-92	Device 6
16053	B9407F30-F5F8-466E-AFF9-25556B57FE6D	15487	17347	-92	Device 6
16967	B9407F30-F5F8-466E-AFF9-25556B57FE6D	15487	17347	-91	Device 6
17280	B9407F30-F5F8-466E-AFF9-25556B57FE6D	15487	17347	-90	Device 6
…	…	…	…	…	…

The figure 64 below displays the linear modelling of the data sets by using curve fitting algorithm, 1500 samples of RSSI have been plotted. The blue lines represent the row data of RSSI, whereas the red line represents the curve fitting data. In the modelling, a_1 represents the scale error of the curve fitting data, a_2 represents the expected RSSI at a distance of 1 meter. The curve fitting algorithm has been showed below:

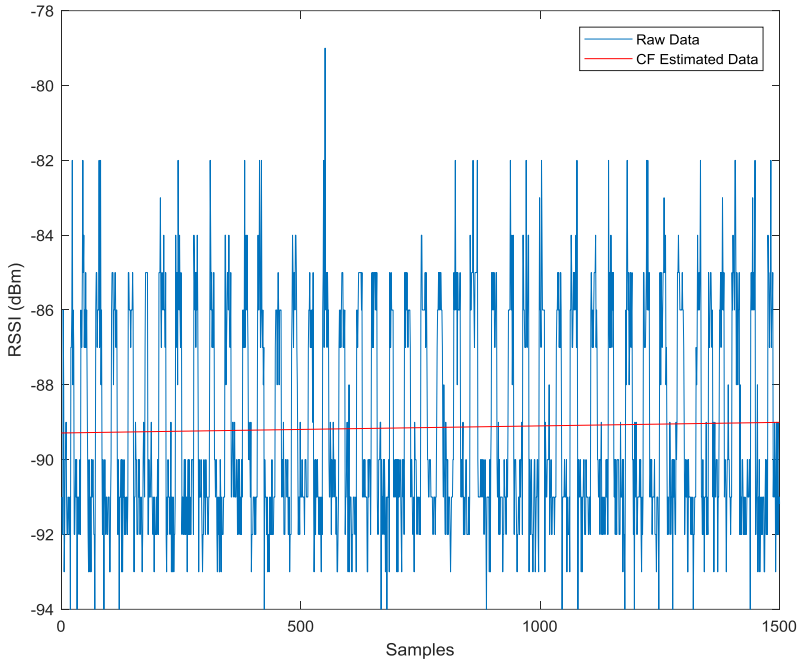

Figure 64 Diagram for Raw Data and CF Estimated Data (iBeacon device 6)

Error modelling (CF-RSSI):

$f(x) = a_1*x + a_2$

Coefficients (with 95% confidence bounds):

$a_1 = 0.08474$ (-0.05854, 0.228)

$a_2 = -89.14$ (-89.28, -89)

Goodness of fit:

SSE: 1.278e+04

R-square: 0.0008692

Adjusted R-square: 0.0002233

RMSE: 2.874

When we convert the RSSI into distance, the diagram 65 displays that the curve fitting is used to reduce the noise:

A = $|a_2|$ = 89.14

D = 10 ^ ((abs (RSSI) - A) / (10 * n))

Distance = 1 meter

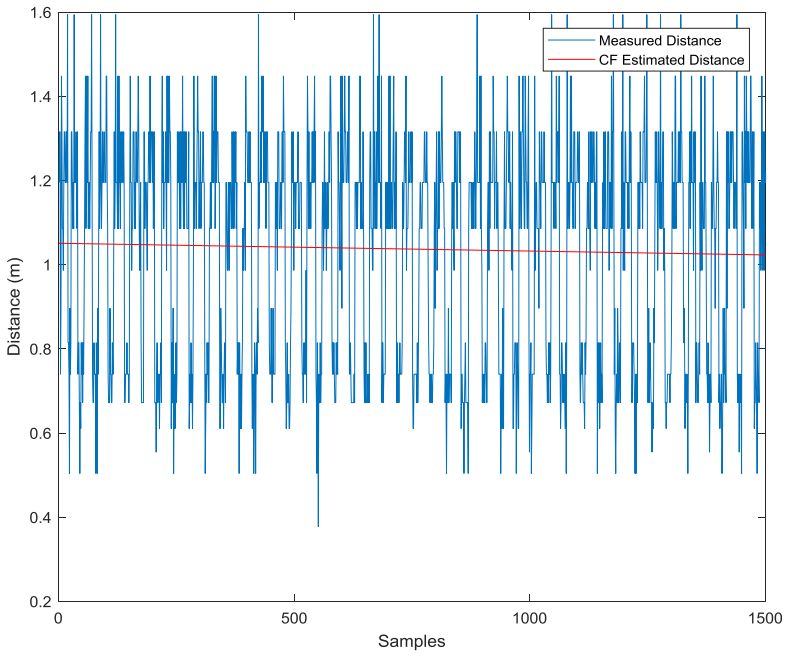

Figure 65 Diagram for Measured Distance and CF Estimated Distance (iBeacon device 6)

Error modelling (CF-Distance):

$f(x) = a_1*x + a_2$

Coefficients (with 95% confidence bounds):

a_1 = -1.844e-05 (-4.773e-05, 1.084e-05)

a_2 = 1.051 (1.025, 1.077)

Goodness of fit:

SSE: 106.8

R-square: 0.0009856

Adjusted R-square: 0.0003398

RMSE: 0.2627

Alternatively, when we use Kalman Filter on the data of distance to reduce the noise, the figure 66 displays below, the Kalman Filter estimated data is in red:

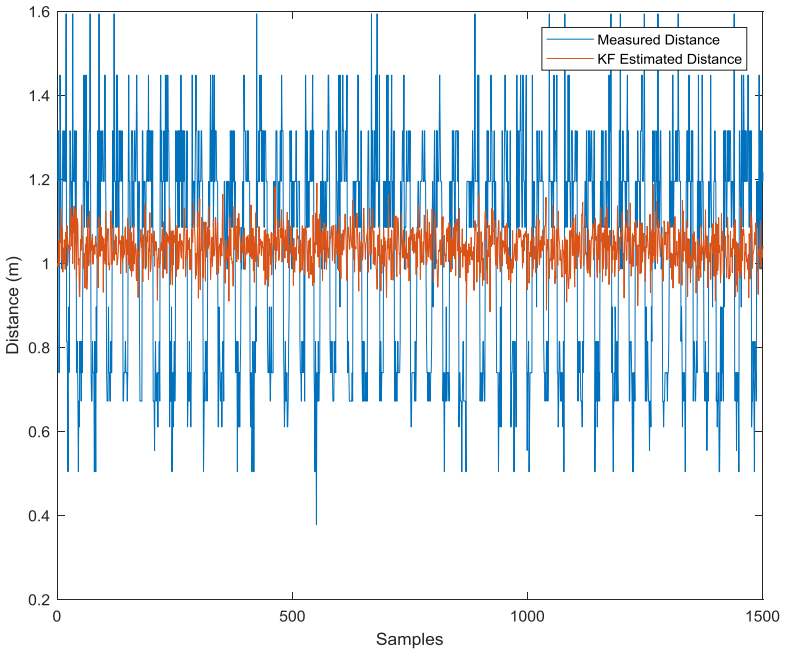

Figure 66 Diagram for Measured Distance and KF Estimated Distance (iBeacon device 6)

When we use the curve fitting algorithm on the Kalman Filter estimated data, the result is more accurate than the data from curve fitting algorithm only.

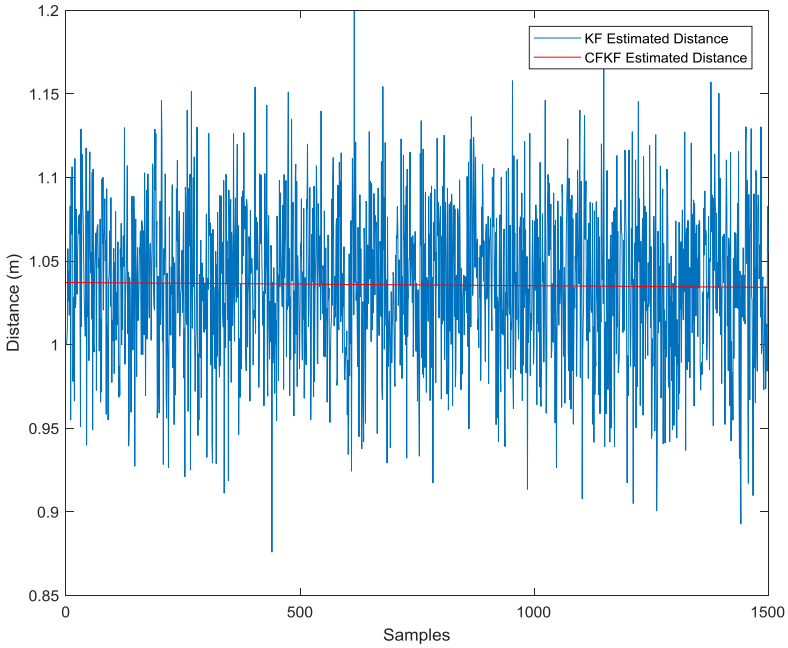

Figure 67 Diagram for KF Estimated Distance and CFKF Estimated Distance (iBeacon device 6)

Error modelling (CFKF):

$f(x) = a_1*x + a_2$

Coefficients (with 95% confidence bounds):

a_1 = -7.191e-06 (-1.23e-05, -2.083e-06)

a_2 = 1.043 (1.038, 1.047)

Goodness of fit:

SSE: 3.259

R-square: 0.004901

Adjusted R-square: 0.004258

RMSE: 0.04588

Table 15 Algorithm error table for device 6

Positioning algorithm	Scale Factor	Error (meter)	Error Rate
Curve Fitting Error	-1.844e-05	0.051	5.1%
Kalman Filter Error	NA	0.05-0.09	5%-9%
CFKF Error	-7.191e-06	0.043	4.3%
Measurement Error	NA	0.3-0.42	30%-42%

4.4 Error Modelling Optimised Calibration Results

According to the results from chapter 4.3, CFKF estimated distance is more accurate than other algorithms. Gathering all the results for device 1 into the same diagram. As Figure 68 showed, the CFKF estimated distance reduced noise and errors; It is much closer to the ground true distance than other methods.

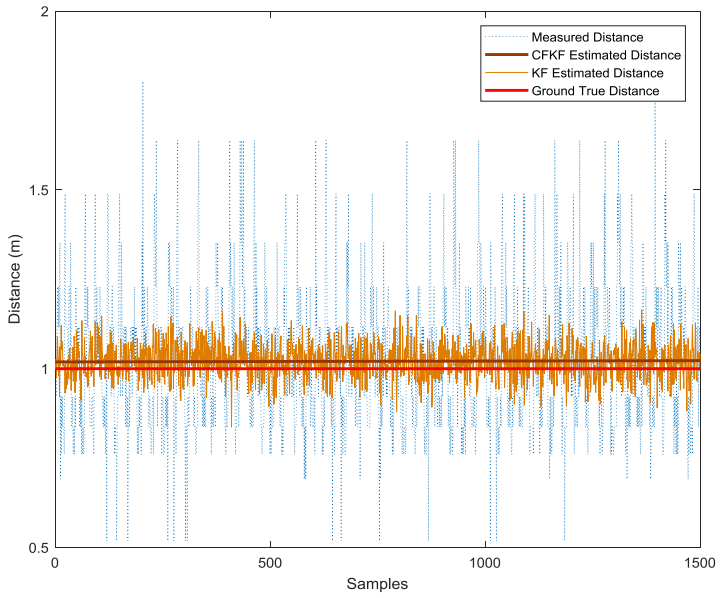

Figure 68 Diagram of Error Modelling Calibration Result (iBeacon device 1)

According to the results from chapter 4.3, CFKF estimated distance is more accurate than other algorithms. Gathering all the results for device 2 into the same diagram. As Figure 69 showed, the CFKF estimated distance reduced noise and errors; It is much closer to the ground true distance than other methods.

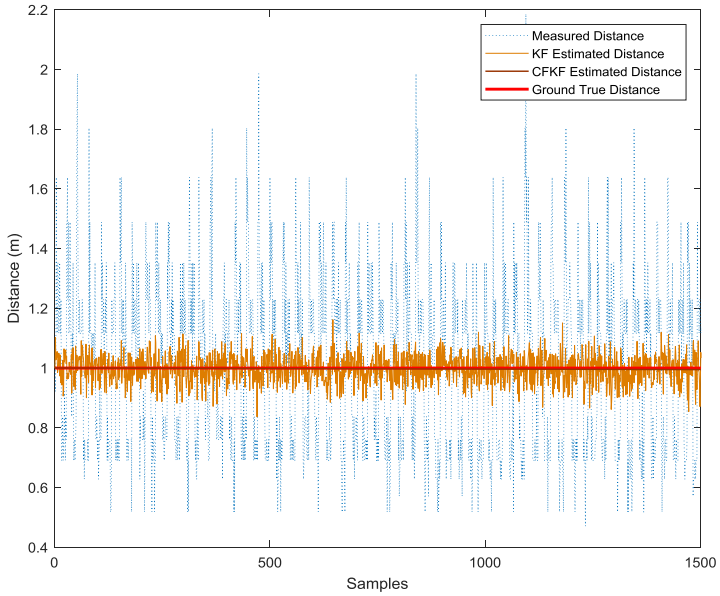

Figure 69 Diagram of Error Modelling Calibration Result (iBeacon device 2)

According to the results from chapter 4.3, CFKF estimated distance is more accurate than other algorithms. Gathering all the results for device 3 into the same diagram. As Figure 70 showed, the CFKF estimated distance reduced noise and errors; It is much closer to the ground true distance than other methods.

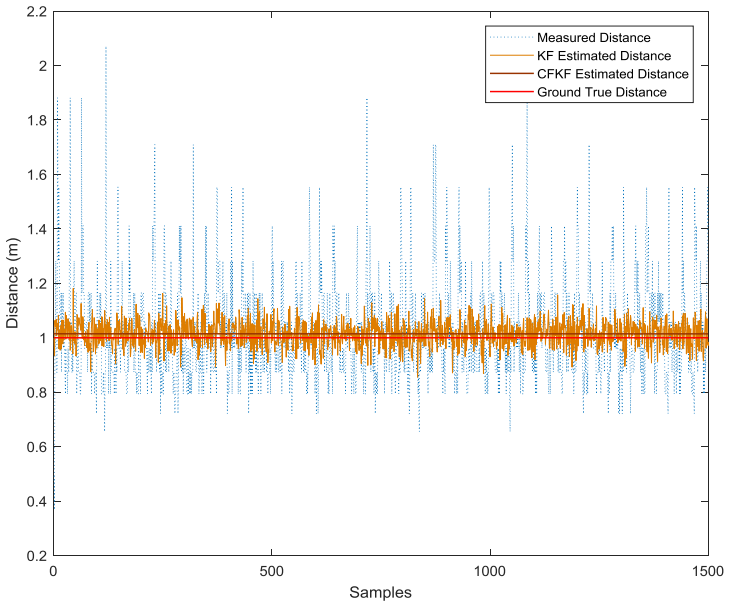

Figure 70 Diagram of Error Modelling Calibration Result (iBeacon device 3)

According to the results from chapter 4.3, CFKF estimated distance is more accurate than other algorithms. Gathering all the results for device 4 into the same diagram. As Figure 71 showed, the CFKF estimated distance reduced noise and errors; It is much closer to the ground true distance than other methods.

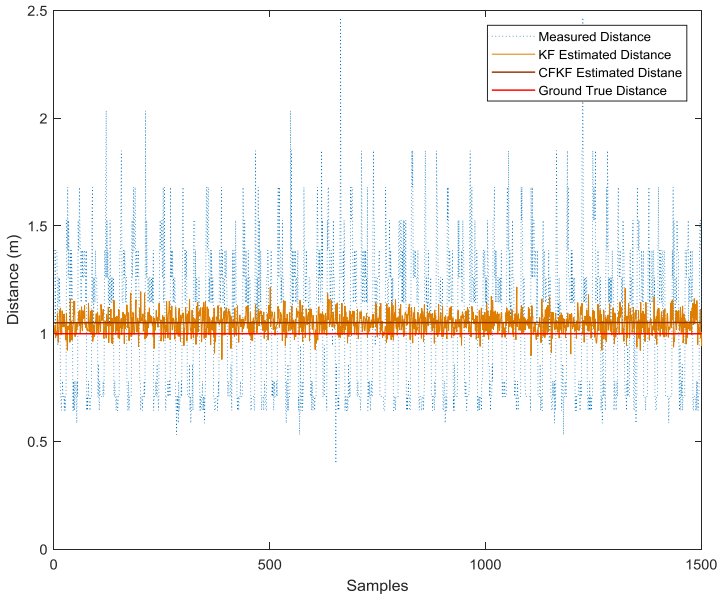

Figure 71 Diagram of Error Modelling Calibration Result (iBeacon device 4)

According to the results from chapter 4.3, CFKF estimated distance is more accurate than other algorithms. Gathering all the results for device 5 into the same diagram. As Figure 72 showed, the CFKF estimated distance reduced noise and errors; It is much closer to the ground true distance than other methods.

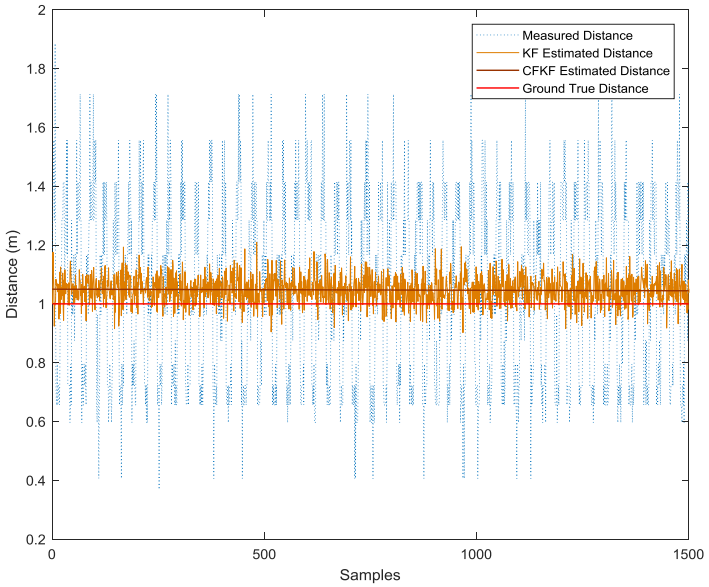

Figure 72 Diagram of Error Modelling Calibration Result (iBeacon device 5)

According to the results from chapter 4.3, CFKF estimated distance is more accurate than other algorithms. Gathering all the results for device 6 into the same diagram. As Figure 73 showed, the CFKF estimated distance reduced noise and errors; It is much closer to the ground true distance than other methods.

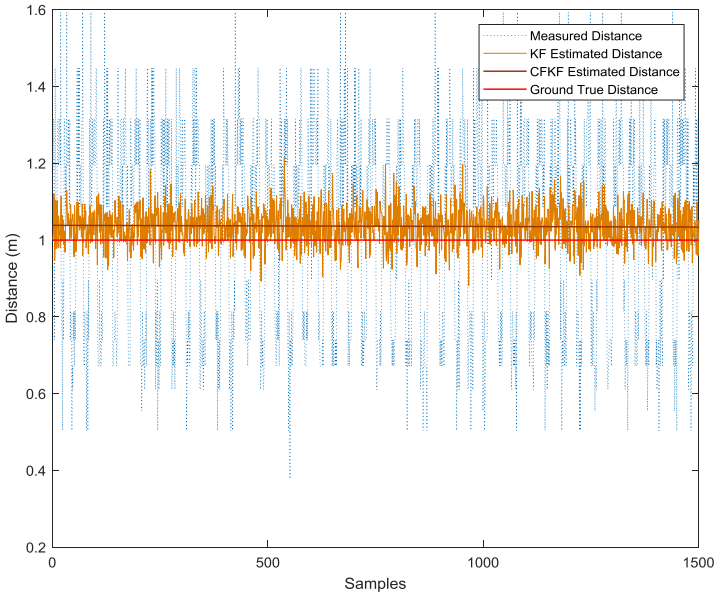

Figure 73 Diagram of Error Modelling Calibration Result (iBeacon device 6)

4.5 Field Experiment of iBeacon Localisation

At the first stage, the calibration of device 1 for vertical angles from 10° to 170° is set up and operated. Figure 74 displays that iBeacon is set up vertically.

Figure 74 iBeacon set up vertically

Figure 75 shows that, at 1-meter distance, RSSI of device 1 is various. However, the measurement of RSSI at different vertical angles from 10° to 170° slightly changes in between -85dBm and -95dBm, as the antenna broadcasting may not cover smoothly at all angles.

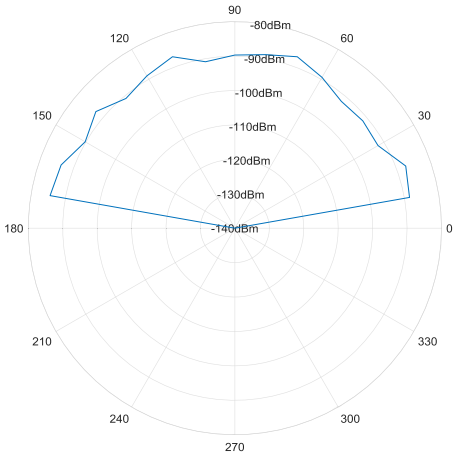

Figure 75 Polar diagram for iBeacon device 1 at different vertical angles from 10° to 170°

As figure 77 (b) displayed that the iBeacon has been set up 2.53 meters high on the wall of the office. It is about 0.2 meters away from the celling to avoid the signal reflection when the signals transmit towards to the celling and reflect back to interfere the other signals transmitting from different angles. A stand with the mobile phone is set up on the top is located a meter away from the wall. The stand is about 0.8 meters high, as the figure showed, it is about 30 degree between the wall and the line connecting iBeacon and Mobile phone. The distance between iBeacon and mobile phone is about 2 meters. This is a field experiment in a real-life environment. The calculation will be processed to validate the result of our CFKF error modelling process.

Figure 76 Testbed for iBeacon localisation field experiment (a)

Figure 77 Testbed for iBeacon localisation field experiment (b) and (c)

In this case, iBeacon device 1 has been selected. According to the figure 75, we can find that the expected RSSI at a distance of 1 meter for device 1 at 30° (from the top it is vertical 150°) is -90 dBm, and 1000 of RSSI samples received from the mobile phone is showed below:

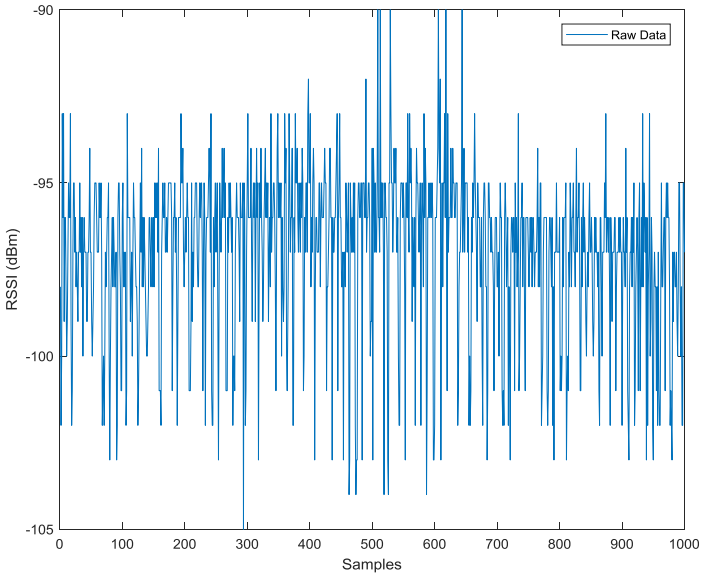

Figure 78 Raw data of RSSI in the field experiment

To calculate the distance in this case, we use the equation (4.1) below:

$$D = 10^{\left(\frac{|RSSI|-A}{10\times n}\right)} \quad (4.1)$$

Error modelling (CF-Distance)

$f(x) = a_1 * x + a_2$

Coefficients (with 95% confidence bounds):

$a_1 = 0.06706$ (0.03709, 0.09702)

$a_2 = 2.098$ (2.058, 2.138)

Goodness of fit:

SSE: 332.9

R-square: 0.01588

Adjusted R-square: 0.01506

RMSE: 0.528

In the distance diagram, figure 79, we compare the result with the KF algorithm and CFKF algorithm, the diagram displays below:

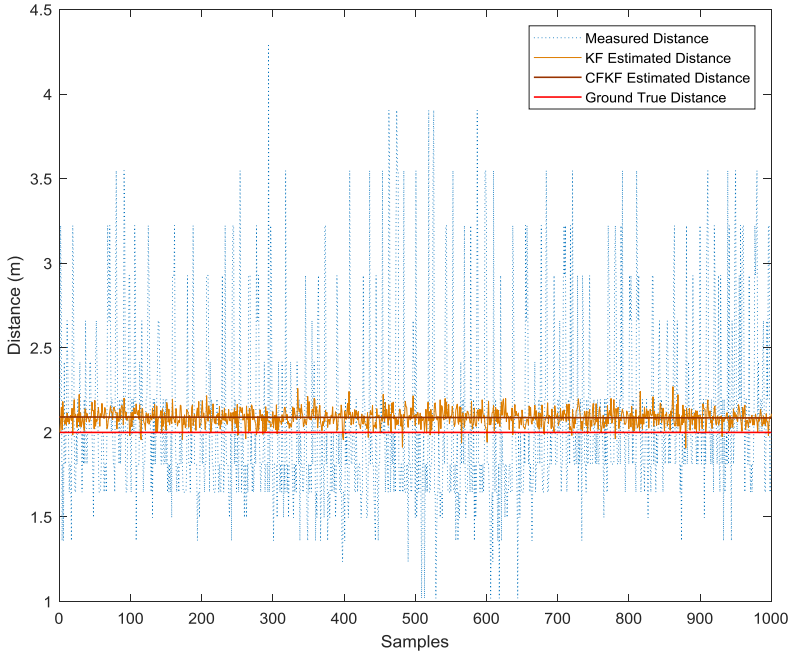

Figure 79 Diagram of error modelling calibration result for field experiment

Error modelling (CFKF):

$f(x) = a_1*x + a_2$

Coefficients (with 95% confidence bounds):

a_1 = -3.354e-06 (-8.739e-06, 2.032e-06)

a_2 = 2.09 (2.085, 2.094)

Goodness of fit:

SSE: 3.621

R-square: 0.0009629

Adjusted R-square: 0.0003176

RMSE: 0.04837

From the diagram of the distance, we notice that the result of CFKF estimated distance is very close to the ground true which is 2.09 meters, it is more accurate than the result of KF estimated distance which is from 1.89 to 2.31. It is also much more accurate than the measure distance which is from 1.019 to 3.55. Therefore, this field experiment validates that the CFKF error modelling is effective and reliable in the iBeacon localisation system.

Table 16 Algorithm error table for field experiment

Positioning algorithm	Scale Factor	Error (meter)	Error Rate
Curve Fitting Error	0.0001941	0.049	4.9%
Kalman Filter Error	NA	0.06-0.15	6%-15%
CFKF Error	-3.354e-06	0.045	4.5%
Measurement Error	NA	0.35-0.67	35%-67%

According to the algorithm error table 16 for field experiment, the measurement error rate in 1 meter is around 35% - 67%. The Kalman filter estimated error rate is about 6%-15%. The curve fitting error rate is about 4.9%. And the CFKF error modelling error rate is 4.5%.

Therefore, the results from CFKF algorithm increase the accuracy about 30%-60% more than the measured results. They are about 1%-10% more accurate than the results from KF estimated distance. And they improve 0.4% accuracy from the CF estimated distance. CFKF error modelling provides the best accuracy in the field experiment.

4.6 Summary

Table 17 Algorithm error table for device 1-6

Positioning Algorithm	Scale Factor	Error (meter)	Error Rate
Device 1			
Curve Fitting Error	0.001288	0.027	2.7%
Kalman Filter Error	NA	0.06-0.1	6%-10%
CFKF Error	-0.001535	0.026	2.6%
Measurement Error	NA	0.24-0.5	24%-50%
Device 2			
Curve Fitting Error	-3.265e-05	0.069	6.9%
Kalman Filter Error	NA	0.07-0.10	7%-10%
CFKF Error	-1.119e-06	0.046	4.6%
Measurement Error	NA	0.3-0.5	30%-50%
Device 3			
Curve Fitting Error	0.007232	0.016	1.6%
Kalman Filter Error	NA	0.05-0.10	5%-10%
CFKF Error	-0.0002229	0.015	1.5%
Measurement Error	NA	0.2-0.4	20%-40%
Device 4			
Curve Fitting Error	-3.984e-06	0.057	5.7%
KF Error	NA	0.05-0.1	6%-15%
CFKF Error	-8.68e-07	0.055	5.5%
Measurement Error	NA	0.4-0.5	40%-50%
Device 5			
Curve Fitting Error	-1.223e-05	0.057	5.7%
KF Error	NA	0.07-0.13	7%-13%
CFKF Error	2.595e-06	0.045	4.5%
Measurement Error	NA	0.25-0.56	25%-56%
Device 6			
Curve Fitting Error	-1.844e-05	0.051	5.1%
Kalman Filter Error	NA	0.05-0.09	5%-9%
CFKF Error	-7.191e-06	0.043	4.3%
Measurement Error	NA	0.3-0.42	30%-42%
Field Experiment			
Curve Fitting Error	0.0001941	-0.049	4.9%
Kalman Filter Error	NA	0.06-0.15	6%-15%
CFKF Error	-3.354e-06	0.045	4.5%
Measurement Error	NA	0.35-0.77	35%-77%

In this chapter, the research of iBeacon localisation has been experimented. At the first stage, the testbed has been set up for the experiment. There are six iBeacons have been used in the experiment. During the angel calibration process, different angles of the iBeacon transmit different signal strength. The value of the received RSSI is slightly different from different angles. During the process of error modelling calibration for distance measurement, iBeacon is set up a meter away from the mobile receiver. Initially, CF algorithm is applied to calibrate the raw date and determine the expected RSSI at a distance of 1 meter. Then the distance equation is used to calculate the measured distance by using the received RSSI. Then, we use KF algorithm and CFKF error modelling algorithm to optimise the accuracy of the system. According to the table 17, at 1-meter range, the measurement of device 1 has 24%-50% errors rate, the KF algorithm can reduce the error rate to 6%-10%, the CF algorithm can improve the error rate to 2.7%. The CFKF error modelling algorithm has the most accuracy results with the error rate at only 2.6%. For device 2, the error rate of the measurement is 30%-50%, the error rate from the result of KF algorithm is 7%-10%, the error rate from the result of CF algorithm is 6.9%, The result of CFKF error modelling algorithm is 4.6%. For device 3, the results of the error rate are: Measurement (20%-40%), KF algorithm (5%-10%), CF algorithm (1.6%) and CFKF error modelling algorithm (1.5%). For device 4, the results of the error rate are: Measurement (40%-50%), KF algorithm (6%-15%), CF algorithm (5.7%) and CFKF error modelling algorithm (5.5%). For device 5, the results of the error rate are: Measurement (25%-56%), KF algorithm (7%-13%), CF algorithm (5.7%) and CFKF error modelling algorithm (4.5%). For device 6, the results of the error rate are: Measurement (30%-42%), KF algorithm (5%-9%), CF algorithm (5.1%) and CFKF error modelling algorithm (4.3%). And in the field experiment, the results of the error rate are: Measurement (35%-77%), KF algorithm (6%-15%), CF algorithm (4.9%)

and CFKF error modelling algorithm (4.5%). All the results display that the result from CFKF error modelling algorithm provide the best accuracy and robust for the system.

Chapter 5

Research Implementation of UWB Localisation

In this chapter, the UWB localisation system experiment has been set up and calibrated. Several different algorithms have been used to determine the best method for calibration at the first stage. After the calibration process, the measurement experiments have been processed to demine the estimated distance. Then, the actual study of moving object in real life environment has been set up and implemented. The results have showed that the CFKF error modelling generates the best accuracy of the system.

5.1 Testbed Setup for UWB Localisation System

At the first stage, the testbed of the calibration has been set up as figure 81 displayed. In order to determine that the ToF from different angles of the UWB tag may be different. Same as the testbed setup in chapter 4.1. 170 degree from the UWB tag has been divided into 17 angles which is from 10° to 170°. Each angle is 10° different from the angle next to itself. There is 1-meter distance away from the UWB tag to the anchor at each angle. The distance has been measured by tape ruler. The white labels on the ground in the figure clearly display the real positions of all the angles within 1-meter distance. Figure 78 and figure 79 display the testbed when the anchor moves to different position of the angles.

In the testbed, the UWB tag is set up on a stand with 50 cm high. A USB data cable from the UWB tag is connected to the laptop to collect the data from UWB anchor synchronously. The UWB anchor is also set up on another stand with the same height in one meter away from the iBeacon. 50 cm height is a reasonable height to avoid the signal reflection from the ground. The anchor starts to send the data from the position of 10°. Then, it will move to the next angle and continue to send data, until it finishes sending the data at the position of 170° as figure 81 (a) displayed. The tag has been set up horizontally as displayed on figure 81 (a) and (b). Due to the manufactory errors, different anchor with the same specification may have different errors. Therefore, three anchors have been operated in the experiments to determine the best accuracy of the system. Figure 81 (a)(b)(c) and 82 display the different view of the testbed when the anchor is at different position of the angles.

Figure 80 Three UWB Anchors and one UWB tag

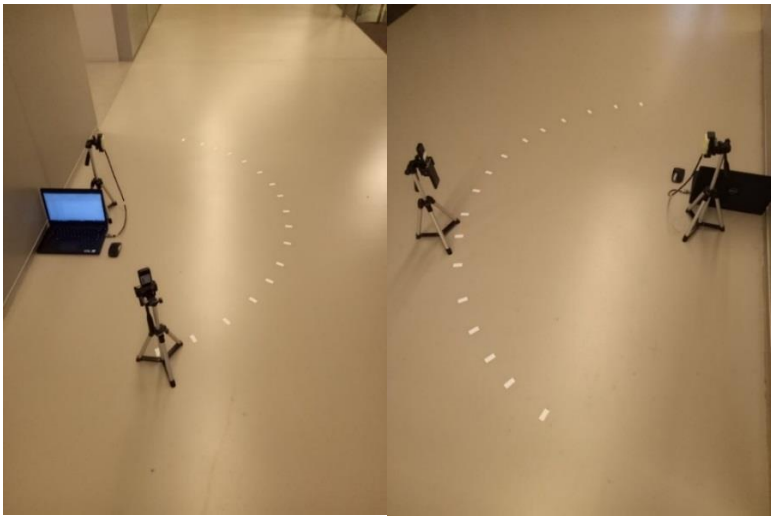

Figure 81 Testbed setup for UWB anchor and tag (a) and (b)

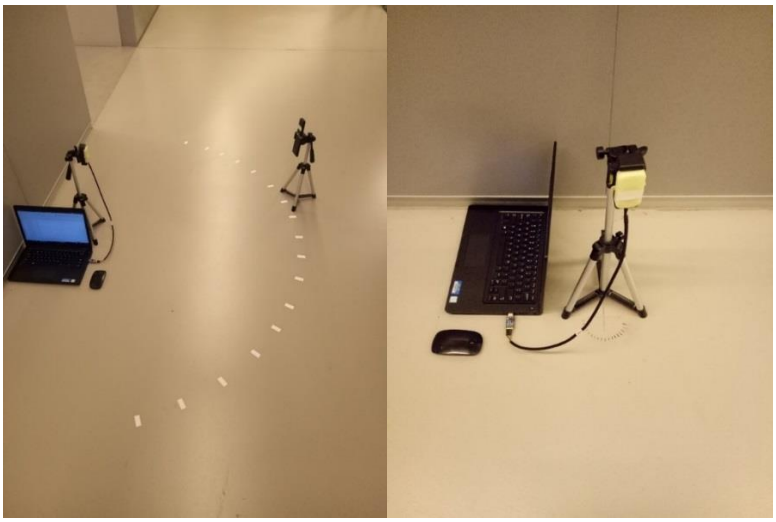

Figure 82 Testbed setup for UWB anchor and tag (c) and testbed setup for UWB tag (d)

The UWB anchors and tag used in the experiment are manufactured by Boostar. Unlike iBeacon, UWB system uses ToF method to calculate the distance, it does not need value of RSSI to determine the distance, the value of distance is readable from the data logger. The specification of those UWB is displayed in table 18.

Table 18 UWB Anchor and Tag specification

Measurement Method: ToF
Factory Error: Line of Sight<15 cm, None Line of Sight<30cm
Anchor range: 100 m
Tag Number: Max 7 in the system
Data refresh rate: Single tag 5Hz
Power: average 0.5W
Temperature: -40℃ to 85℃
Operating frequency: 6.2GHz to 6.7GHz
Size: Anchor: 82.5mm×38mm×11.5mm, Tag: 69mm×38mm×11.9mm
Power supply: DC5V, 1A

5.2 UWB Calibration Process for Angles

In this calibration process for angles, we measure the same distance, 1 meter, with various angles. As the positions display in the figure, we can find that the angle is between the wall and the line between tag and anchor. The frequency of the signal transmit is 5Hz. The measurement starts from 10° to 170°, each angle of measurement has 10° different from the next angle of measurement, therefore the list of angles is 10°, 20°, 30°, 40°, 50°, 60°, 70°, 80°, 90°, 100°, 110°, 120°, 130°, 140°, 150°, 160° and 170°. Three anchors have been measured at each different angle for the same distance. The polar diagrams for each iBeacon device are showed in figure 83.

5.2.1 System Calibration for UWB Anchor 1

Figure 83 shows that, at 1-meter distance, RSSI of device 1 is various. However, the measurement of the distance at different horizontal angles from 10° to 170° slightly changes in between -67 dBm and -69 dBm, as the antenna broadcasting may not cover smoothly at all angles.

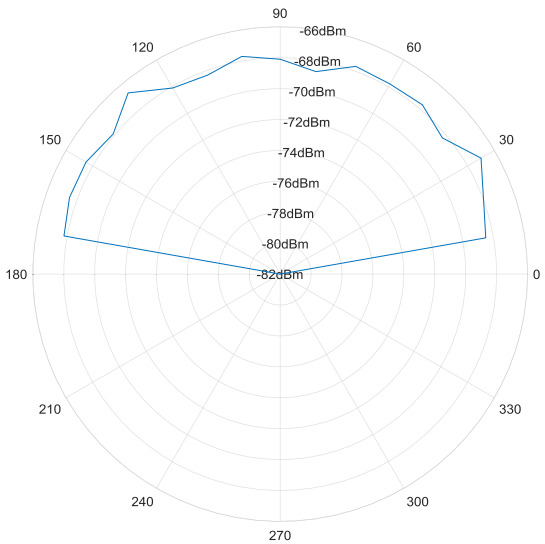

Figure 83 Polar diagram for UWB Anchor 1 at different horizontal angles from 10° to 170°

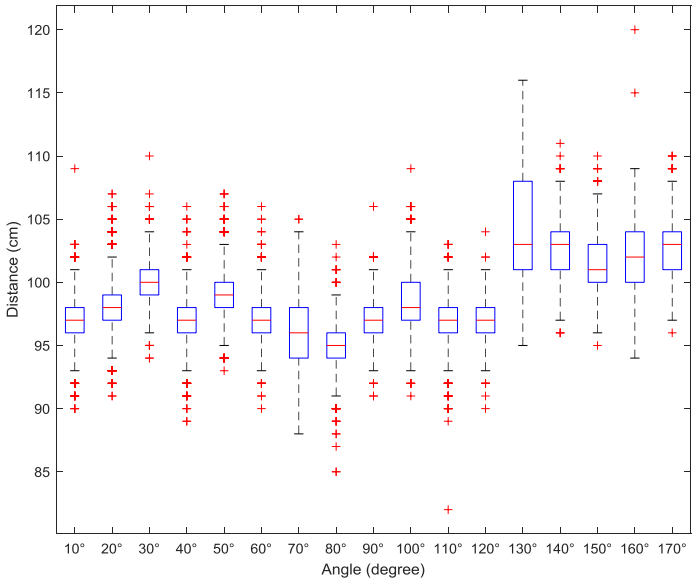

Figure 84 Box-and-whisker diagram for UWB Anchor 1 at different horizontal angles from 10° to 170°

The figure 84 is the box-and-whisker diagram, which clearly shows the range and average value of distance from Device at different angles. Most of the values of distance are between 95 cm and 105 cm.

5.2.2 System Calibration for UWB Anchor 2

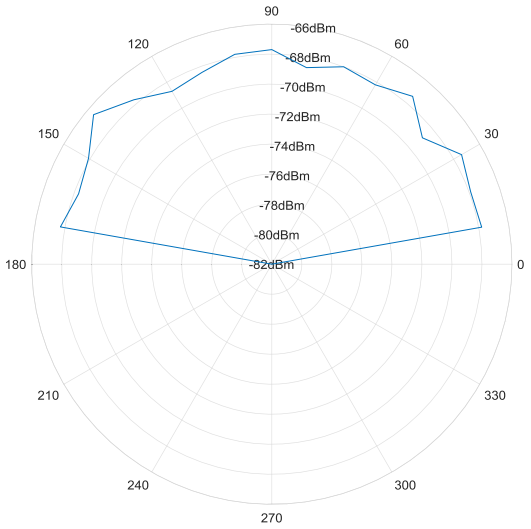

Figure 85 Polar diagram for UWB Anchor 2 at different horizontal angles from 10° to 170°

Figure 85 shows that, at 1-meter distance, RSSI of device 1 is various. However, the measurement of the distance at different horizontal angles from 10° to 170° slightly changes in between -67 dBm and -69 dBm, as the antenna broadcasting may not cover smoothly at all angles.

Figure 86 is the box-and-whisker diagram, which clearly shows the range and average value of distance from Device at different angles. Most of the values of distance are between 100 cm and 115 cm.

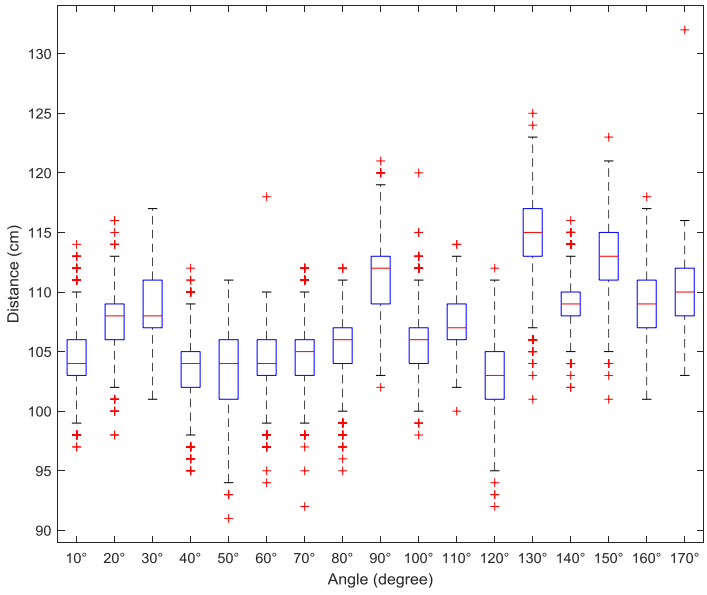

Figure 86 Box-and-whisker diagram for UWB Anchor 2 at different horizontal angles from 10° to 170°

5.2.3 System Calibration for UWB Anchor 3

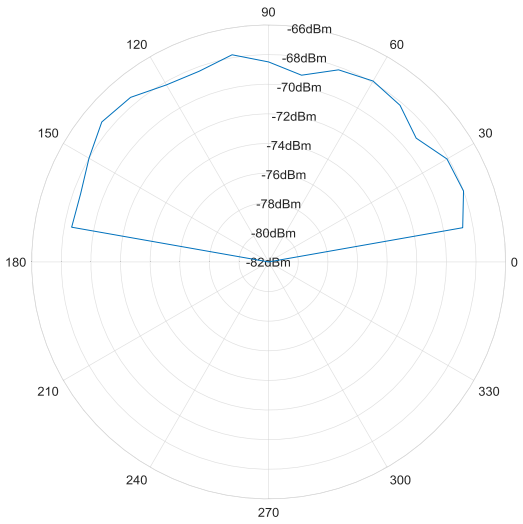

Figure 87 Polar diagram for UWB Anchor 3 at different horizontal angles from 10° to 170°

Figure 87 shows that, at 1-meter distance, RSSI of device 1 is various. However, the measurement of the distance at different horizontal angles from 10° to 170° slightly changes in between -67 dBm and -69 dBm, as the antenna broadcasting may not cover smoothly at all angles.

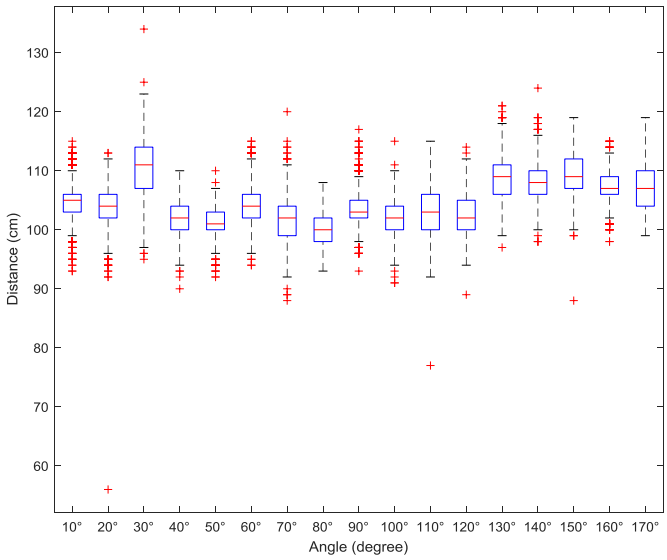

Figure 88 Box-and-whisker diagram for UWB Anchor 3 at different horizontal angles from 10° to 170°

Figure 88 is the box-and-whisker diagram, which clearly shows the range and average value of distance from Device at different angles. Most of the values of distance are between 100 cm and 115 cm.

5.3 UWB Calibration Process for Distance

As figure 89 displayed, both tag and anchor are mounted on two 50 cm high stands with one-meter distance in between. Figure 90(b), 90(c) and figure 91 displays three different views of the testbed. This testbed has been set up to calibrate the distance measurement for three different anchors.

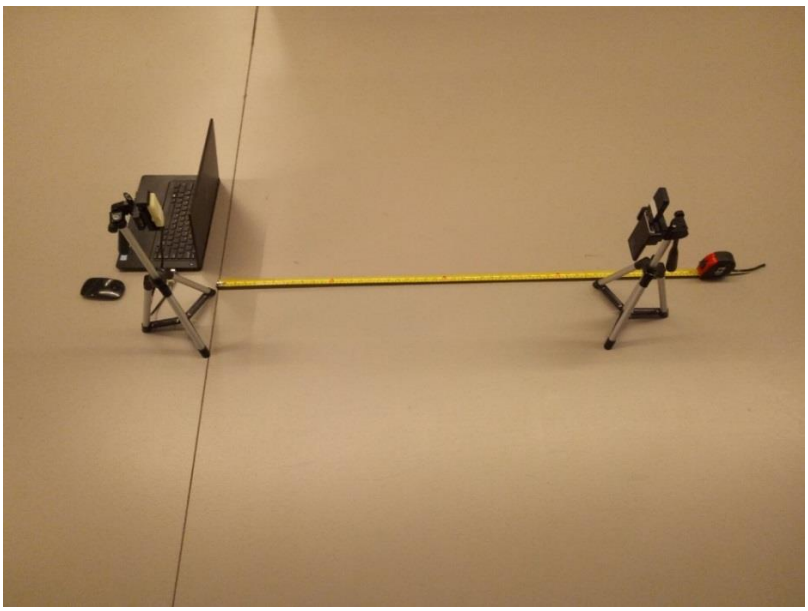

Figure 89 Testbed setup for 1-meter distance range for UWB localisation (a)

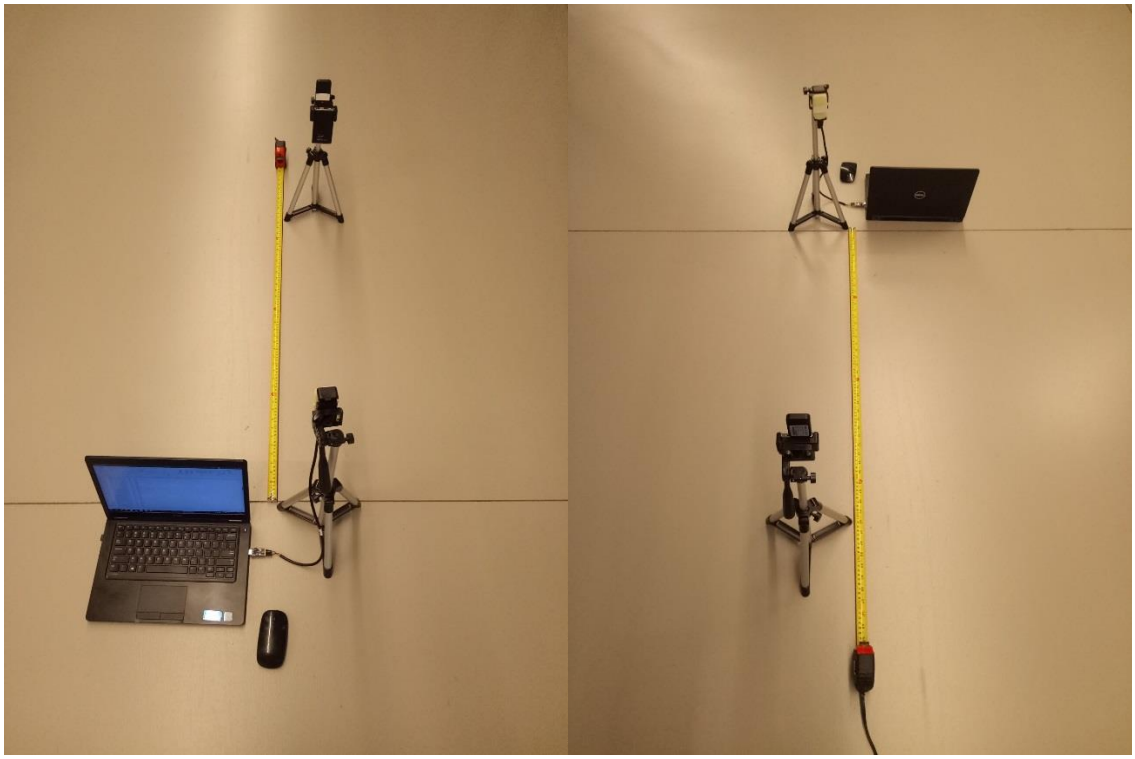

Figure 90 Testbed setup for 1-meter distance range for UWB localisation (b) (c)

Figure 91 Testbed setup for 1-meter distance range for UWB localisation (d)

5.3.1 Error Modelling Calibration for UWB Anchor 1

The table 19 shows the iBeacon transmit data from UWB anchor 1, the data contains Tag No, Time (ms), Anchor ID, and Distance(cm). The sample rate is about 100ms, the tag has been setup 1 meter away from the anchor to collect the data. 1500 sets of data have been collected. Here are some samples of them:

Table 19 Sample data table for anchor 1

Tag No	Time (ms)	Anchor ID	Distance (cm)
TagNo:1	26151	Anchor 1	100
TagNo:1	26207	Anchor 1	103
TagNo:1	26263	Anchor 1	104
TagNo:1	26319	Anchor 1	100
TagNo:1	26375	Anchor 1	100
TagNo:1	26431	Anchor 1	106
TagNo:1	26488	Anchor 1	105
TagNo:1	26544	Anchor 1	101
TagNo:1	26600	Anchor 1	100
TagNo:1	26688	Anchor 1	102
TagNo:1	26744	Anchor 1	100
TagNo:1	26800	Anchor 1	94
TagNo:1	26857	Anchor 1	108
TagNo:1	26913	Anchor 1	102
TagNo:1	26969	Anchor 1	96
TagNo:1	27025	Anchor 1	102
TagNo:1	27081	Anchor 1	105
TagNo:1	27137	Anchor 1	103
TagNo:1	27225	Anchor 1	104
TagNo:1	27282	Anchor 1	105
TagNo:1	27338	Anchor 1	102
TagNo:1	27394	Anchor 1	99
TagNo:1	27450	Anchor 1	107
TagNo:1	27506	Anchor 1	105
TagNo:1	27562	Anchor 1	102
TagNo:1	27619	Anchor 1	100
TagNo:1	27675	Anchor 1	105
TagNo:1	27763	Anchor 1	100
TagNo:1	27819	Anchor 1	99
TagNo:1	27875	Anchor 1	105
TagNo:1	27931	Anchor 1	100

The figure 92 displays the linear modelling of the data sets by using curve fitting algorithm, 1500 samples of distance have been plotted. The blue lines represent the row data of distance, whereas the red line represents the curve fitting data. In the modelling, a_1

represents the scale error of the curve fitting data, a_2 represents the expected distance at a distance of 1 meter. The KF algorithm has been showed in the figure 92.

When we use the CFKF algorithm to estimate the data, the result is more accurate than the data from KF algorithm only.

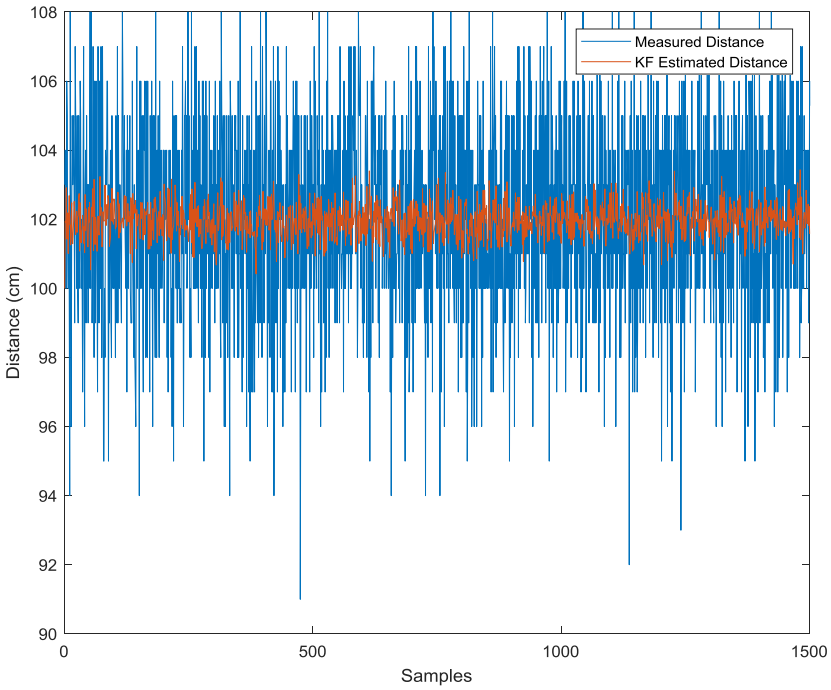

Figure 92 Diagram for Measured Distance and KF Estimated Distance (UWB anchor 1)

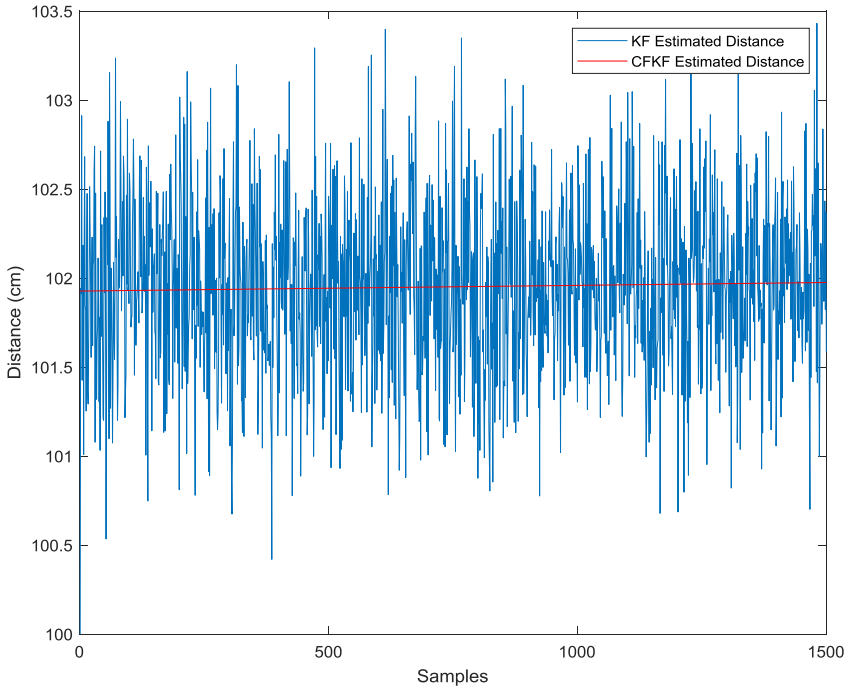

Figure 93 Diagram for KF Estimated Distance and CFKF Estimated Distance (UWB anchor 1)

Error modelling (CFKF):

$f(x) = a_1*x + a_2$

Coefficients (with 95% confidence bounds):

a_1 = 3.215e-05 (-2.178e-05, 8.608e-05)

a_2 = 101.9 (101.9, 102)

Goodness of fit:

SSE: 363.1

R-square: 0.0008825

Adjusted R-square: 0.0002371

RMSE: 0.4843

5.3.2 Error Modelling Calibration for UWB Anchor 2

The table 20 shows the iBeacon transmit data from UWB anchor 2, the data contains Tag No, Time (ms), Anchor ID and Distance(cm). The sample rate is about 100ms, the tag has been setup 1 meter away from the anchor to collect the data. 1500 sets of data have been collected. Here are some samples of them:

Table 20 Sample data table for anchor 2

Tag No	Time (ms)	Anchor ID	Distance (cm)
TagNo:1	1211714	Anchor 2	95
TagNo:1	1211770	Anchor 2	95
TagNo:1	1211826	Anchor 2	95
TagNo:1	1211882	Anchor 2	92
TagNo:1	1211938	Anchor 2	102
TagNo:1	1211994	Anchor 2	95
TagNo:1	1212050	Anchor 2	97
TagNo:1	1212107	Anchor 2	97
TagNo:1	1212195	Anchor 2	98
TagNo:1	1212251	Anchor 2	92
TagNo:1	1212307	Anchor 2	96
TagNo:1	1212363	Anchor 2	98
TagNo:1	1212419	Anchor 2	101
TagNo:1	1212476	Anchor 2	97
TagNo:1	1212532	Anchor 2	97
TagNo:1	1212588	Anchor 2	100
TagNo:1	1212644	Anchor 2	102
TagNo:1	1212732	Anchor 2	101
TagNo:1	1212788	Anchor 2	102
TagNo:1	1212845	Anchor 2	103
TagNo:1	1212901	Anchor 2	103
TagNo:1	1212957	Anchor 2	105
TagNo:1	1213013	Anchor 2	105
TagNo:1	1213069	Anchor 2	102
TagNo:1	1213125	Anchor 2	106
TagNo:1	1213181	Anchor 2	102
TagNo:1	1213270	Anchor 2	98
TagNo:1	1213326	Anchor 2	97
TagNo:1	1213382	Anchor 2	101
TagNo:1	1213438	Anchor 2	102
TagNo:1	1213494	Anchor 2	105

The figure 94 displays the linear modelling of the data sets by using curve fitting algorithm, 1500 samples of distance have been plotted. The blue lines represent the row data of distance, whereas the red line represents the curve fitting data. In the modelling, a_1 represents the scale error of the curve fitting data, a_2 represents the expected distance at a distance of 1 meter. The curve fitting algorithm has been showed in figure 94.

When we use the CFKF algorithm to estimate the data, the result is more accurate than the data from KF algorithm only.

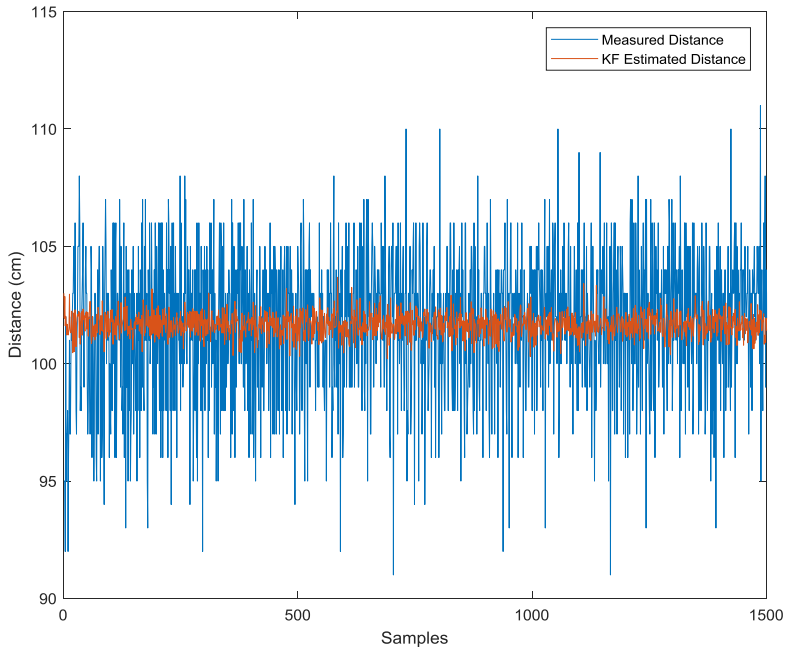

Figure 94 Diagram for Measured Distance and KF Estimated Distance (UWB anchor 2)

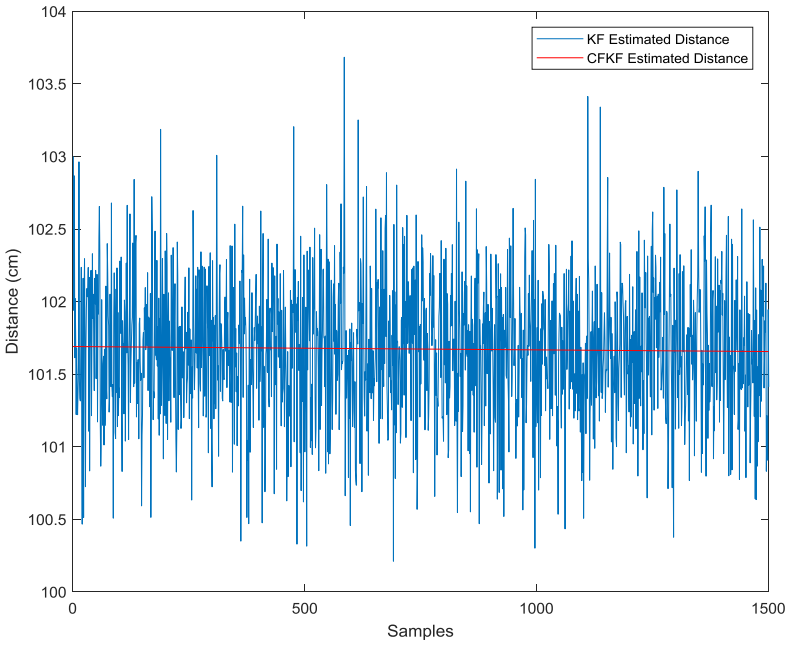

Figure 95 Diagram for KF Estimated Distance and CFKF Estimated Distance (UWB anchor 2)

Error model:

$f(x) = a_1*x + a_2$

Coefficients (with 95% confidence bounds):

a_1 = -2.297e-05 (-7.705e-05, 3.111e-05)

a_2 = 101.7 (101.6, 101.7)

Goodness of fit:

SSE: 365.2

R-square: 0.0004481

Adjusted R-square: -0.0001976

RMSE: 0.4857

5.3.3 Error Modelling Calibration for UWB Anchor 3

The table 21 shows the iBeacon transmit data from UWB anchor 3, the data contains Tag No, Time (ms), Anchor ID and Distance(cm). The sample rate is about 100ms, the tag has been setup 1 meter away from the anchor to collect the data. 1500 sets of data have been collected. Here are some samples of them:

Table 21 Sample data table for anchor 3

Tag No	Time (ms)	Anchor ID	Distance (cm)
TagNo:1	2291288	Anchor 3	95
TagNo:1	2291345	Anchor 3	105
TagNo:1	2291401	Anchor 3	90
TagNo:1	2291457	Anchor 3	98
TagNo:1	2291513	Anchor 3	103
TagNo:1	2291601	Anchor 3	104
TagNo:1	2291657	Anchor 3	97
TagNo:1	2291714	Anchor 3	98
TagNo:1	2291770	Anchor 3	101
TagNo:1	2291826	Anchor 3	98
TagNo:1	2291882	Anchor 3	101
TagNo:1	2291938	Anchor 3	100
TagNo:1	2291994	Anchor 3	102
TagNo:1	2292050	Anchor 3	100
TagNo:1	2292139	Anchor 3	104
TagNo:1	2292195	Anchor 3	100
TagNo:1	2292251	Anchor 3	90
TagNo:1	2292307	Anchor 3	96
TagNo:1	2292363	Anchor 3	96
TagNo:1	2292419	Anchor 3	103
TagNo:1	2292475	Anchor 3	102
TagNo:1	2292532	Anchor 3	102
TagNo:1	2292588	Anchor 3	103
TagNo:1	2292676	Anchor 3	98
TagNo:1	2292732	Anchor 3	101
TagNo:1	2292788	Anchor 3	102
TagNo:1	2292844	Anchor 3	106
TagNo:1	2292901	Anchor 3	103
TagNo:1	2292957	Anchor 3	100
TagNo:1	2293013	Anchor 3	102
TagNo:1	2293069	Anchor 3	102

Figure 96 displays the linear modelling of the data sets by using curve fitting algorithm, 1500 samples of distance have been plotted. The blue lines represent the row data of distance, whereas the red line represents the curve fitting data. In the modelling, a_1 represents the scale error of the curve fitting data, a_2 represents the expected distance at a distance of 1 meter. The curve fitting algorithm has been showed in figure 96.

When we use the CFKF algorithm to estimate the data, the result is more accurate than the data from KF algorithm only.

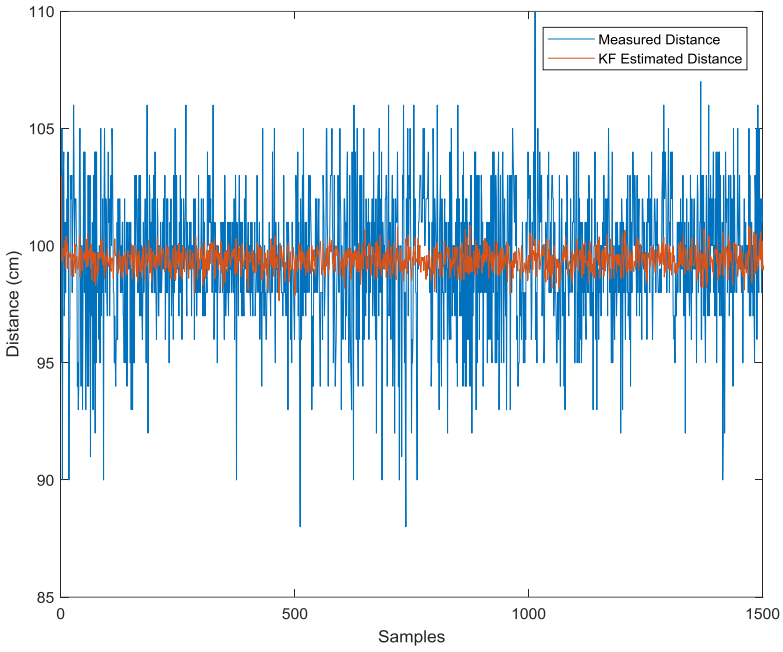

Figure 96 Diagram for Measured Distance and KF Estimated Distance (UWB anchor 3)

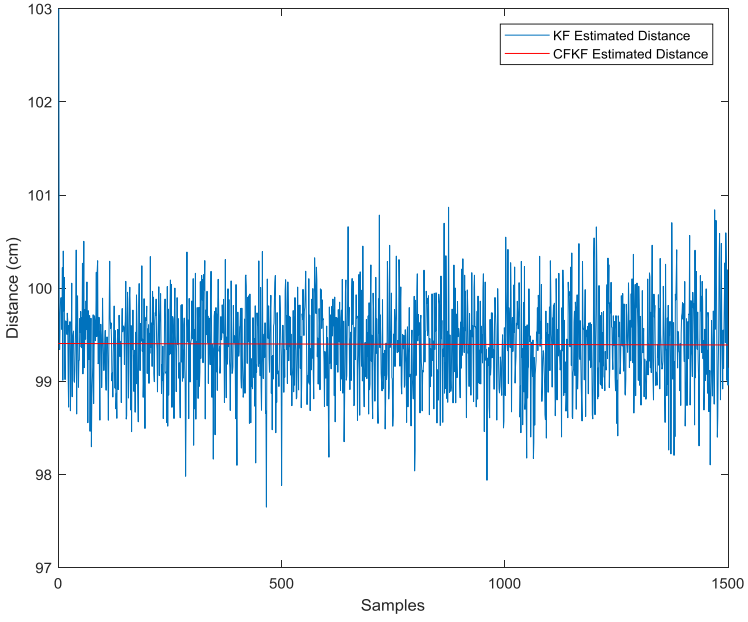

Figure 97 Diagram for KF Estimated Distance and CFKF Estimated Distance (UWB anchor 3)

Error model:

$f(x) = a_1*x + a_2$

Coefficients (with 95% confidence bounds):

a_1 = -1.025e-05 (-6.469e-05, 4.42e-05)

a_2 = 99.41 (99.36, 99.45)

Goodness of fit:

SSE: 370

R-square: 8.802e-05

Adjusted R-square: -0.0005579

RMSE: 0.4889

5.4 Error Modelling Optimised Calibration Results

According to the results from chapter 5.3, CFKF estimated distance is more accurate than other algorithms. Gathering all the results for Anchor 1 into the same diagram. As Figure 98 showed, the CFKF estimated distance reduced noise and errors; It is much closer to the ground true distance than other methods.

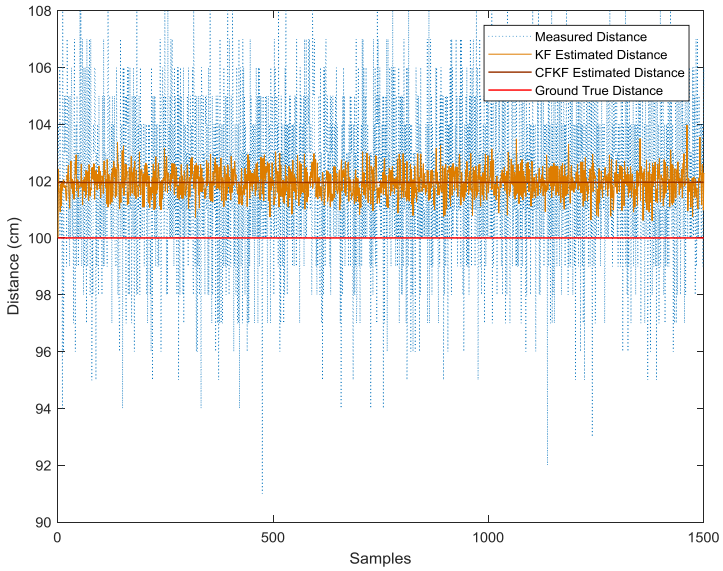

Figure 98 Diagram of Error Modelling Calibration Result (UWB anchor 1)

Table 22 Algorithm error table for UWB Anchor 1

Positioning algorithm	Scale Factor	Error (meter)	Error Rate
Kalman Filter Error	NA	0.017-0.03	1.7%-3%
CFKF Error	3.215e-05	0.019	1.9%
Measurement Error	NA	0.05-0.10	5%-10%

According to the results from chapter 5.3, CFKF estimated distance is more accurate than other algorithms. Gathering all the results for Anchor 2 into the same diagram. As Figure 99 showed, the CFKF estimated distance reduced noise and errors; It is much closer to the ground true distance than other methods.

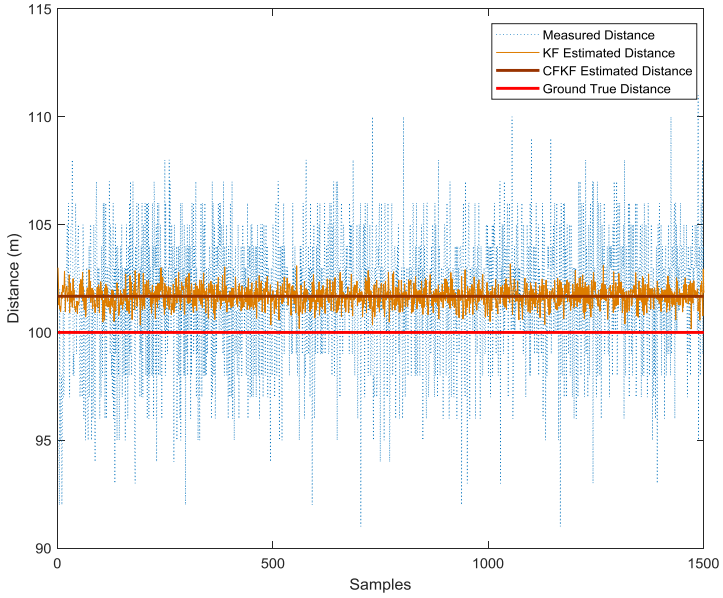

Figure 99 Diagram of Error Modelling Calibration Result (UWB anchor 2)

Table 23 Algorithm error table for UWB Anchor 2

Positioning algorithm	Scale Factor	Error (meter)	Error Rate
Kalman Filter Error	NA	0.015-0.026	1.5%-2.6%
CFKF Error	-2.297e-05	0.017	1.7%
Measurement Error	NA	0.05-0.10	5%-10%

According to the results from chapter 5.3, CFKF estimated distance is more accurate than other algorithms. Gathering all the results for Anchor 3 into the same diagram. As Figure 100 showed, the CFKF estimated distance reduced noise and errors; It is much closer to the ground true distance than other methods.

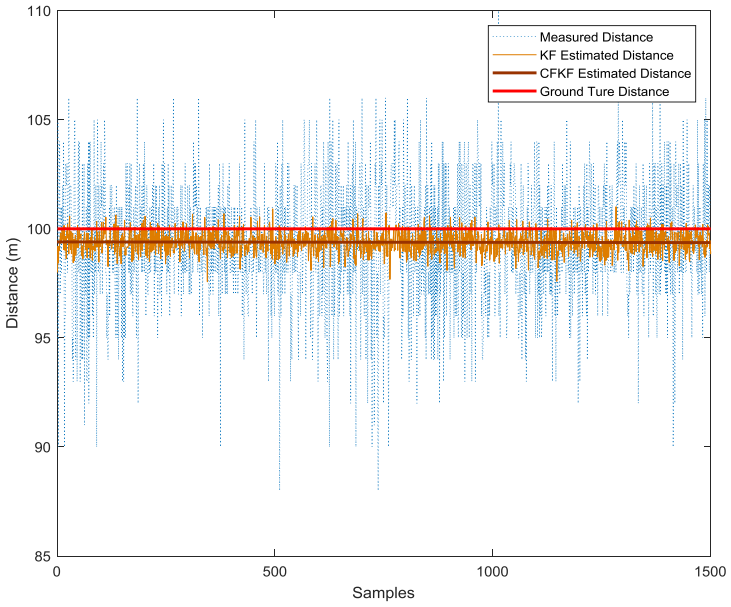

Figure 100 Diagram of Error Modelling Calibration Result (UWB anchor 3)

Table 24 Algorithm error table for UWB Anchor 3

Positioning algorithm	Scale Factor	Error (meter)	Error Rate
Kalman Filter Error	NA	-0.02-0.01	1%-2%
CFKF Error	-1.025e-05	-0.006	0.6%
Measurement Error	NA	0.05-0.10	5%-12%

5.5 Field Experiment of UWB Localisation

In this field experiment of UWB localisation, the testbed is set up for a real-time moving object. The purpose of this field experiment is to validate the accuracy of the CFKF error modelling in a dynamic scenario. As showed on figure 102 and 103, there is a white rectangle on the ground. The length and width of the rectangle are 400 cm and 200 cm. Anchor 1 has been mounted on the stand with 50 cm high. It is set up in the same line as

side A but 50 cm away from corner 2. Anchor 2 has been mounted on the stand with 50 high. It is set up in the same line as side B but 50 cm away from corner 3. Anchor 3 has been also mounted on the stand with 50 high. It is set up in the same line as side C but 50 cm away from corner 3. Anchors are set up 50 cm away from the rectangle, this setup is to avoid the moving platform touching the anchors when it moves to the corner. The tag mounted on the stand has been set up on the moving platform with the same height, 50 cm in total, including the height of the platform. A laptop is connected to the tag to log the real-time data from the tag.

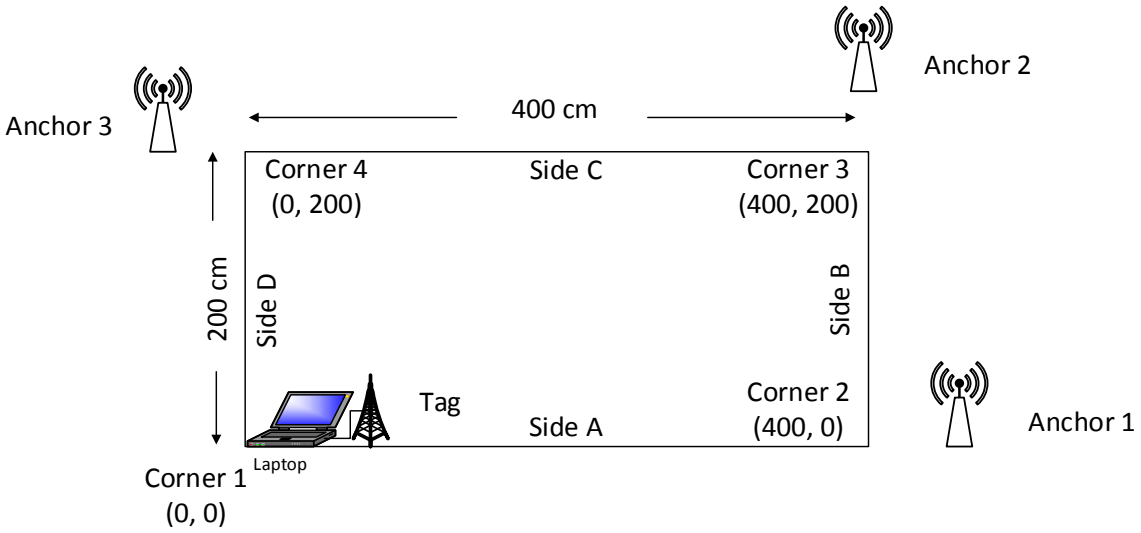

Figure 101 Floor plan for the testbed of UWB field experiment

Figure 101 displays the floor plan for the testbed. Corner 1 has been set up as the coordinate origin (0, 0) where x = 0 and y = 0. Side A is set up on the x axis, side D is set up on the y axis. Therefore, the coordinate of corner 2 should be (400, 0), where x = 400 cm, y = 0. The coordinate of corner 3 should be (400, 200), where x = 400 cm, y = 200 cm. The coordinate of corner 4 should be (0, 200), where x = 0 cm, y = 200 cm. The testbed has been set up as figure 102 and figure 103 displayed.

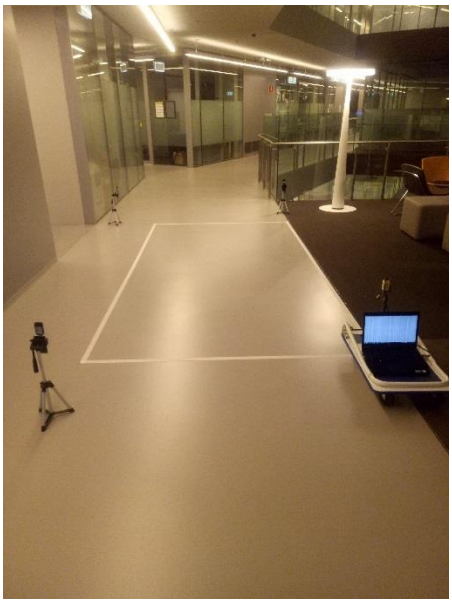

Figure 102 Testbed for UWB field experiment (a)

Figure 103 Testbed for UWB field experiment (b)

Table 25 shows the data from three anchors are received and logged by UWB tag when the platform moves. The data contains Tag No, Time (ms), Anchor 1 distance, Anchor 2 distance and Anchor 3 distance, and RSSI (dBm) from each anchor. As each anchor is set up 50 cm away from the rectangle, the coordinates of anchor 1 is (450, 0), where x = 450 cm, y = 0. The coordinates of anchor 2 is (400, 250), where x = 400 cm, y = 250. The coordinates of anchor 3 is (0, 200), where x = 0 cm, y = 250. When the platform moves, here are the part of data samples:

Table 25 Sample data table for UWB field experiment

TagNo:1	372500	Anchor 1	455	-69.1	Anchor 2	482	-70.8	Anchor 3	216	-68.4
TagNo:1	372676	Anchor 1	458	-69.6	Anchor 2	484	-71.1	Anchor 3	215	-69.9
TagNo:1	372829	Anchor 1	458	-71.1	Anchor 2	482	-70.4	Anchor 3	215	-68.8
TagNo:1	372981	Anchor 1	456	-70	Anchor 2	483	-70.2	Anchor 3	215	-69.8
TagNo:1	373134	Anchor 1	455	-69.6	Anchor 2	485	-70.2	Anchor 3	215	-69.3
TagNo:1	373286	Anchor 1	453	-70.2	Anchor 2	482	-71.5	Anchor 3	214	-69.7
TagNo:1	373438	Anchor 1	456	-69.5	Anchor 2	483	-71.7	Anchor 3	211	-69.9
TagNo:1	373591	Anchor 1	456	-69.8	Anchor 2	484	-71.4	Anchor 3	213	-68.1
TagNo:1	373743	Anchor 1	456	-69.1	Anchor 2	485	-70.4	Anchor 3	214	-68.8
TagNo:1	373896	Anchor 1	457	-70.7	Anchor 2	484	-70.7	Anchor 3	212	-69.2
TagNo:1	374072	Anchor 1	456	-69.2	Anchor 2	487	-69.8	Anchor 3	210	-68.4
TagNo:1	374224	Anchor 1	455	-69.3	Anchor 2	485	-70.6	Anchor 3	212	-70.2
TagNo:1	374377	Anchor 1	457	-69.5	Anchor 2	482	-70.9	Anchor 3	215	-70.1
TagNo:1	374529	Anchor 1	459	-69.4	Anchor 2	485	-70.8	Anchor 3	214	-69.9
TagNo:1	374714	Anchor 1	457	-70	Anchor 2	484	-71.8	Anchor 3	216	-68.3
TagNo:1	374866	Anchor 1	458	-69.6	Anchor 2	485	-70.4	Anchor 3	210	-69.8
TagNo:1	375018	Anchor 1	458	-70.7	Anchor 2	486	-70.5	Anchor 3	211	-69.2
TagNo:1	375171	Anchor 1	459	-69.9	Anchor 2	486	-71.3	Anchor 3	216	-68.6
TagNo:1	375323	Anchor 1	459	-70.4	Anchor 2	486	-72	Anchor 3	213	-69.6
TagNo:1	375500	Anchor 1	456	-69.1	Anchor 2	483	-71	Anchor 3	212	-69.3
TagNo:1	375652	Anchor 1	456	-70.6	Anchor 2	484	-71.6	Anchor 3	214	-70
TagNo:1	375805	Anchor 1	455	-69.8	Anchor 2	484	-70.1	Anchor 3	214	-69.9
TagNo:1	375957	Anchor 1	457	-70.1	Anchor 2	486	-70.3	Anchor 3	210	-68.7
TagNo:1	376109	Anchor 1	455	-70.1	Anchor 2	488	-69.9	Anchor 3	213	-68.3
TagNo:1	376262	Anchor 1	457	-69.5	Anchor 2	485	-71.1	Anchor 3	210	-69.9
TagNo:1	376414	Anchor 1	459	-69.1	Anchor 2	483	-70	Anchor 3	214	-68.9
TagNo:1	376566	Anchor 1	454	-69.6	Anchor 2	484	-70.8	Anchor 3	212	-69.6
TagNo:1	376719	Anchor 1	455	-69.1	Anchor 2	486	-69.8	Anchor 3	214	-69.4
TagNo:1	376895	Anchor 1	457	-70.2	Anchor 2	488	-70.1	Anchor 3	213	-70.3
TagNo:1	377048	Anchor 1	457	-69.9	Anchor 2	486	-70.7	Anchor 3	214	-69.9
TagNo:1	377200	Anchor 1	453	-70.1	Anchor 2	485	-71.9	Anchor 3	214	-69.2
TagNo:1	377353	Anchor 1	453	-69.2	Anchor 2	483	-70.8	Anchor 3	215	-68.9

In this field experiment, a programmed robotic moving platform is moving at a constant speed with 0.2m/s, which equals to 20cm/s following the sides of the rectangle. The moving platform starts from corner A. When it arrives the corner of the rectangle, it turns 90° left to continue to move along with the next side of the rectangle. The platform keeps moving until it arrives to the original start point corner A. During the time, anchor 1, anchor 2 and anchor 3 keeps sending data to the tag. The tag on the platform is receiving the data from all anchors and is logging the data into the laptop synchronously. To calculate distance and coordinate of the moving object, the trilateration method is used for the 3 anchors and 1 tag UWB localisation system.

Firstly, from the Pythagorean theorem:

$$\begin{cases} (x_1 - x)^2 + (y_1 - y)^2 = d_1^2 \\ \vdots \\ (x_n - x)^2 + (y_n - y)^2 = d_n^2 \end{cases} \tag{5.1}$$

$$\begin{cases}(x_1 - x)^2 + (y_1 - y)^2 = d_1^2 \\ (x_2 - x)^2 + (y_2 - y)^2 = d_2^2 \\ (x_3 - x)^2 + (y_3 - y)^2 = d_3^2 \end{cases} \quad (5.2)$$

Secondly, using the $(n-1)_{th}$ function minus the n_{th} function to generate the linear equation (5.3), n is the number of the anchors.

$$AX = b \quad (5.3)$$

when

$$A = \begin{bmatrix} 2(x_1 - x_3) & 2(y_1 - y_3) \\ 2(x_2 - x_3) & 2(y_2 - y_3) \end{bmatrix} \quad (5.4)$$

$$b = \begin{bmatrix} x_1^2 - x_3^2 + y_1^2 - y_3^2 + d_3^2 - d_1^2 \\ x_2^2 - x_3^2 + y_2^2 - y_3^2 + d_3^2 - d_2^2 \end{bmatrix} \quad (5.5)$$

After using the Least Squares algorithm,

$$X = (A^T A)^{-1} A^T b \quad (5.6)$$

$$X = \begin{bmatrix} x \\ y \end{bmatrix} \quad (5.7)$$

X (x,y) is the coordinate of the moving tag from the device measurement.

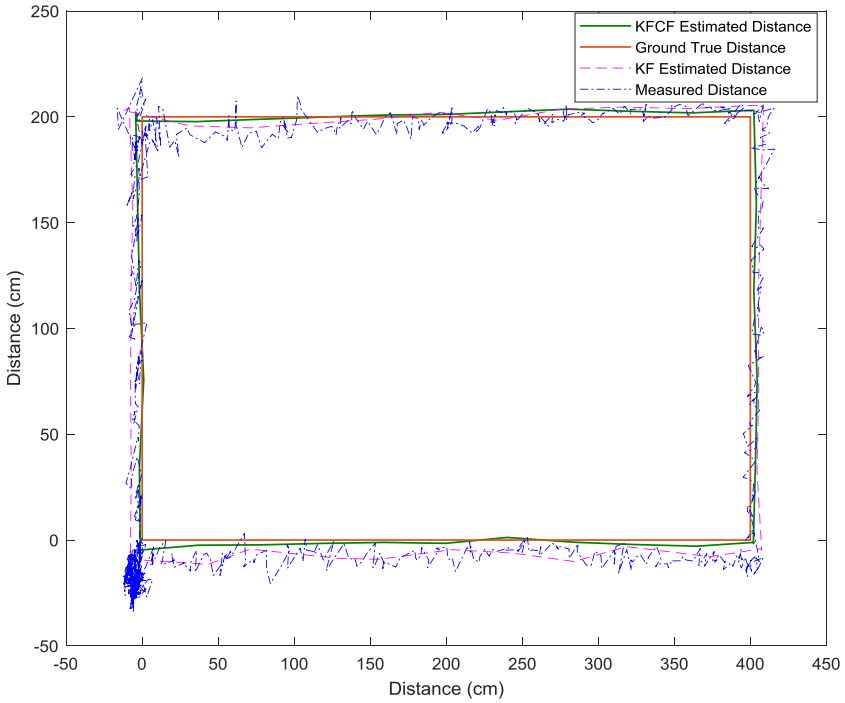

Figure 104 Diagram of UWB field experiment results

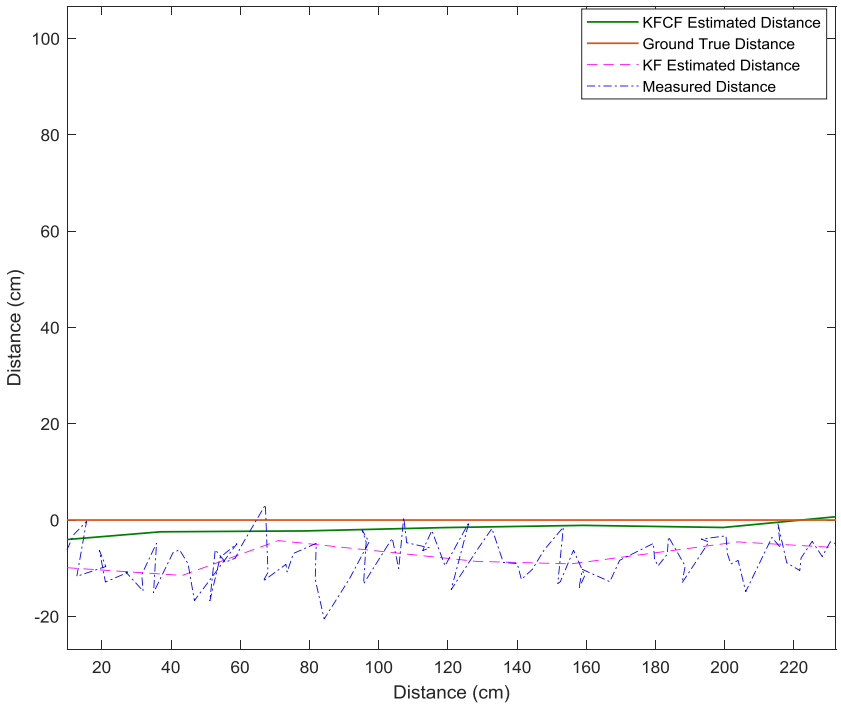

Figure 105 Diagram of UWB field experiment zoomed results

Table 26 Algorithm error table for field experiment

Positioning algorithm	Error (meter)	Error Rate
Kalman Filter Error	0.02-0.10	2%-10%
CFKF Error	0.01-0.02	1%-2%
Measurement Error	0.02-0.20	2%-20%

As figure 104 displayed, the blue dotted line is the measured distance from the UWB tag. The manufactory error of the UWB system is 10-30 cm. On corner 1, there is a big blue area near the coordinate origin, this is the time when the platform gets ready for a few seconds and start to move. Due to the manufactory error, the measured distance is about 2-20 cm away from the coordinate (0, 0). The pink dotted line is the data for KF estimated distance, as showed on figure 104. The pink line reduced the noise, it is smoother than the blue line. However, comparing with the red line (ground true distance), it still contains errors from the ground true data. Figure 105 is the zoomed diagram of the part of the figure 104. It displays that the KF estimated distance contains about 2-10 cm error from the ground true distance. The green line is the estimated distance data from the CFKF error modelling. From both figure 104 and figure 105, it is clearly showed the green line is much closer to the ground true red line. It has 1-2 cm errors, whereas the KF estimated distance has 2-10 cm errors. The accuracy has been improved for about 1% to 8%. Comparing with the raw measured distance, the accuracy has been optimised for about 1%-18%.

5.6 Summary

Table 27 Algorithm error table for UWB Anchor 1-3 and field experiment

Positioning Algorithm	Scale Factor	Error (meter)	Error Rate
UWB Anchor 1			
Kalman Filter Error	NA	0.017-0.03	1.7%-3%
CFKF Error	3.215e-05	0.019	1.9%
Measurement Error	NA	0.05-0.10	5%-10%
UWB Anchor 2			
Kalman Filter Error	NA	0.015-0.026	1.5%-2.6%
CFKF Error	-2.297e-05	0.017	1.7%
Measurement Error	NA	0.05-0.10	5%-10%
UWB Anchor 3			
Kalman Filter Error	NA	-0.02-0.01	1%-2%
CFKF Error	-1.025e-05	-0.006	0.6%
Measurement Error	NA	0.05-0.10	5%-12%
Field Experiment			
Kalman Filter Error	NA	0.02-0.10	2%-10%
CFKF Error	NA	0.01-0.02	1%-2%
Measurement Error	NA	0.02-0.20	2%-20%

In this chapter, the UWB localisation system has been experimented. Angles calibration has been processed to determine that the distance measurements are various from different angles. As using ToF method in UWB system, the RSSI value doesn't affect the value of the distance. Three anchors and one tag have been set up in the testbed. Different anchor may have different manufactory error. Individually calibration process has been applied. The field experiment is a dynamic research, a developed Least Squares algorithm based CFKF

error modelling is used to determine the distance and coordinate of the moving object. According to the results displayed in table 27, when the experiment is using anchor 1, the error rate from the measurement results are 5%-10%, the error rate from the Kalman filter results are 1.7%-3%, and the error rate from CFKF error modelling algorithm results are 1.9%. If we average the error rate from the Kalman filter results, the value is 2.35%, which is higher than the results from CFKF error modelling algorithm. Therefore, the results from CFKF error modelling algorithm are about 3%-8% more accurate than the results from the measurement, and it is 0.45% more accurate than the results from the Kalman filter. For anchor 2, the error rates are: measurement (5%-10%), Kalman filter (1.5%-2.6%), CFKF error modelling algorithm (1.7%). For anchor 3, measurement (5%-12%), Kalman filter (1%-2%), CFKF error modelling algorithm (0.6%). For the field experiment, measurement (2%-20%), Kalman filter (2%-10%), CFKF error modelling algorithm (1%-2%). According all the records, it is validated that the results from CFKF error modelling algorithm is the most accurate and robust method for UWB system.

Chapter 6

Conclusions and Future Work

This chapter presents a summary of all preceding chapters and addresses the potential for future research. Section 6.1 summary of each chapter, Section 6.2 contains the thesis contribution, Section 6.3 Discussion and Limitation of the research work. Section 6.4 presents the future research.

6.1 Summary

Chapter 1 presents the background information and the introduction to an indoor localisation system for this thesis. In particular, various indoor localisation methodologies have been reviewed. Research problem, research hypothesis, research contributions and thesis structure are also stated and explained.

Chapter 2 starts by getting familiar with the research topic and discovering the problems in the area. Literature related of indoor localisation techniques and their background is reviewed. Various indoor localisation technologies have also been reviewed such as ultrasonic sensors, iBeacon system, and the UWB system.

Chapter 3 has presented many different measurement methods for indoor localisation, such as signal strength spatial mapping, time of flight, Kalman filter, trilateration, triangulation and fingerprinting. IBeacon structure and protocol have been introduced in the chapter,

which includes UUID, major number, minor number and advertising interval. Calibration and ranging operation are also discussed as a part of the error modelling. The functional block diagram displays both the processes of system calibration and system error modelling estimation. A novel CFKF error modelling algorithm is introduced in this chapter to generate more accurate and reliable measurement results for the indoor localisation system.

Chapter 4 starts from a testbed set up and system calibration for iBeacon localisation system. The experiments involve a set-up of six iBeacons. During the angel calibration process, different angles of the iBeacon transmit different signal strengths. The value of the received RSSI is slightly different from different angles. The standard RSSI for 1 meter has been calculated with the developed CFKF error modelling to reduce the outliers of the raw data and measured distances. The developed RSSI distance algorithm calculates the values of the distances for transmission. Diagrams are plotted to analyse the accuracy of the localisation method. The field experiment is operated to validate improvement of the accuracy of the CFKF error modelling method in real life. After comparing with other localisation algorithm, the result from CFKF error modelling algorithm with the error rate about 4.5% provides the best accuracy and reliability for the iBeacon localisation system.

Chapter 5 provides the experiment with 3 UWB anchors and 1 tag. The UWB localisation system testbed has been set up and calibrated. Angles calibration has been processed to determine that the distance measurements are various from different angles. Several different algorithms have been used to determine the best method for calibration at the first stage. After the calibration process, the measurement experiments have been processed to determine the estimated distance. The field experiment is a dynamic research,

a developed Least Squares algorithm based CFKF error modelling is used to determine the distance and coordinate of the moving object. Finally, according all the records, it is validated that the results with error rate (1%-2%) from CFKF error modelling algorithm are the most accurate and robust method for UWB system.

Chapter 6 provides the conclusion to this thesis. It starts to with summarise of each chapter. Then the chapter contains thesis contribution, discussion and imitation of the research work and the future work.

Chapter 7 presents reference list.

6.2 Thesis Contribution

In this research work, localisation methods are used to estimate the distance, such as RSSI method for iBeacon localisation system and the Time of Flight (ToF) method for UWB localisation system. Most of WSN devices can obtain the value of RSSI; however, the estimated distance from RSSI is not accurate and robust. Unlike iBeacon, UWB anchor provides higher accuracy, but various errors still occur in the received sensor data. In order to solve these issues, a novel CFKF error modelling is proposed for an indoor localisation system. In our publications, we have developed an error modelling for Micro-Electro-Mechanical-Systems (MEMS) accelerometers (Yu et al, 2019), Inertial Measurement Unit (IMU) (Yu et al, 2018), and RFID (Chaczko & Yu et al, 2019) for the indoor localisation.

The main contributions of the research are:

• Improved estimation of the distance using orientation awareness calibration

• The calibration and experimental measurements from RSSI method in iBeacon system using the mean fitted and curve-fitting algorithm

• A novel error modelling with CFKF method has been proposed to improve the estimation accuracy in the experiment and field experiment for both iBeacon and UWB indoor localisation systems.

• A developed Least Squares algorithm based CFKF error modelling is introduced to improve the accuracy of the distance and coordinates for the UWB moving tag.

The followings are the publications of my research work:

Book Chapters (Published):

1. Yu Z., Chaczko Z., Shi J. (2020) Low Cost Wireless Micro-Electro-Mechanical-Systems Accelerometers Linear Sensor Model. In: Klempous R., Nikodem J. (eds) Smart Innovations in Engineering and Technology. ICACON 2017, APCASE 2017. Topics in Intelligent Engineering and Informatics, vol 15. Springer, Cham
2. Chaczko Z., Chiu C., Yu Z. (2020) Assessment of a Multi-agent RFID Platform for Industrial Logistic Operations. In: Klempous R., Nikodem J. (eds) Smart Innovations in Engineering and Technology. ICACON 2017, APCASE 2017. Topics in Intelligent Engineering and Informatics, vol 15. Springer, Cham

Papers (Published)

3. Yu Z, Chaczko Z, Optimization of IMU Indoor Localization with Wireless Sensors, 2018 4th IEEE International Conference on Computer and Communications, December 7-10, 2018.
4. Yu Z, Chaczko Z, Jiang J. Development and Optimization of Wireless Indoor Localization Error Modelling, International Conference on Systems Engineering. IEEE Computer Society, 2017:475-479.

6.3 Discussion and Limitation

The research work presented in this thesis made a significant contribution to the indoor localisation field by the proposed novel CFKF error modelling algorithm used in iBeacon and UWB systems.

The novel error modelling has been implemented in both calibration process and field experiment. In the iBeacon systems, six iBeacons have been tested due to different manufactory errors. The CFKF error modelling generated the most accurate distance than the distance estimated by other traditional algorithms. The field experiment validated the result of the CFKF error modelling. In the UWB systems, three UWB anchors and one UWB tag have been implemented in the research. The CFKF error modelling optimised the calibration results. It is more accurate than other used methods. The field experiment is a dynamic validation of the error modelling. The results prove that the CFKF error modelling produced a significant improvement of accuracy for the system.

However, here are the limitations of the research work:

1. The research work will cover other condition environments.

CFKF error modelling is experimented in an indoor environment in the research work. It has not been tested under water or some outdoor environments, such as winding, raining, and snowing. In the future, the algorithm should be experimented in the other environments.

2. The research work should consider optimising other localisation sensors

In the research work, two kind of systems, iBeacon and UWB have been implemented by CFKF error modelling. In the future work, more sensors, such as Radar, Ultrasonic, and infrared system can be validated by CFKF error modelling.

3. The novel CFKF error modelling should consider other fields of the implementation.

The thesis focuses on the accuracy of the indoor localisation environment, as an error modelling, CFKF is possible to be implemented in some other fields to reduce errors and noises, such as optimisation of sound quality, accuracy of face recognition and improvement of photo quality

6.4 Future work

As discussed in the chapter, both iBeacon and UWB system have been used in the experiment. In future research, more localisation sensors will be added into the system, data fusion will be developed to improve the error modelling. Also, an indoor and outdoor localisation system should be developed, so the device can switch to receive different sensor in different environments. All the data could be fused in the same system and optimised by the same error modelling. As mentioned in chapter 6.3, further

implementation of sensors should be develop in the future, such as Radar, ultrasonic, and infrared system.

Chapter 7

Reference

Adams, J.C., Gregorwich, W., Capots, L. & Liccardo, D. 2001, 'Ultra-wideband for navigation and communications', *2001 IEEE Aerospace Conference Proceedings (Cat. No. 01TH8542)*, vol. 2, IEEE, pp. 2/785-2/92 vol. 2.

Aiello, R. & Batra, A. 2006, *Ultra wideband systems: technologies and applications*, Elsevier.

Akyildiz, I.F., Su, W., Sankarasubramaniam, Y. & Cayirci, E. 2002, 'A survey on sensor networks', *IEEE Communications magazine*, vol. 40, no. 8, pp. 102-14.

Alarifi, A., Al-Salman, A., Alsaleh, M., Alnafessah, A., Al-Hadhrami, S., Al-Ammar, M.A. & Al-Khalifa, H.S. 2016, 'Ultra wideband indoor positioning technologies: Analysis and recent advances', *Sensors*, vol. 16, no. 5, p. 707.

Alomainy, A., Hao, Y., Yuan, Y. & Liu, Y. 2006, 'Modelling and characterisation of radio propagation from wireless implants at different frequencies', *2006 European Conference on Wireless Technology*, IEEE, pp. 119-22.

Arnitz, D., Muehlmann, U. & Witrisal, K. 2012, 'Characterization and modeling of UHF RFID channels for ranging and localisation', *IEEE transactions on antennas and propagation*, vol. 60, no. 5, pp. 2491-501.

Ashton, K. 2009, 'That 'internet of things' thing', *RFID journal*, vol. 22, no. 7, pp. 97-114.

Bahl, P., Padmanabhan, V.N., Bahl, V. & Padmanabhan, V. 2000, 'RADAR: An in-building RF-based user location and tracking system'.

Bassbouss, L., Güçlü, G. & Steglich, S. 2014, 'Towards a remote launch mechanism of TV companion applications using iBeacon', *2014 IEEE 3rd Global Conference on Consumer Electronics (GCCE)*, pp. 538-9.

Bellavista, P., Küpper, A. & Helal, S. 2008, 'Location-based services: Back to the future', *IEEE Pervasive Computing*, vol. 7, no. 2, pp. 85-9.

Beuchat, P.N., Hesse, H., Domahidi, A. & Lygeros, J. 2019, 'Enabling Optimization-Based Localisation for IoT Devices', *IEEE Internet of Things Journal*, vol. 6, no. 3, pp. 5639-50.

Borah, D.K., Boucouvalas, A.C., Davis, C.C., Hranilovic, S. & Yiannopoulos, K. 2012, 'A review of communication-oriented optical wireless systems', *EURASIP Journal on Wireless Communications and Networking*, vol. 2012, no. 1, p. 91.

Boukerche, A., Oliveira, H.A., Nakamura, E.F. & Loureiro, A.A. 2007, 'Localisation systems for wireless sensor networks', *IEEE wireless Communications*, vol. 14, no. 6, pp. 6-12.

Bulten, W. 2015, 'Kalman filters explained: Removing noise from RSSI signals', *Recuperado de https://www. wouterbulten. nl/blog/tech/kalman-filtersexplained-removing-noise-from-rssi-signals*.

Burzacca, P., Mircoli, M., Mitolo, S. & Polzonetti, A. 2014, '"iBeacon" technology that will make possible Internet of Things', *International Conference on Software Intelligence Technologies and Applications & International Conference on Frontiers of Internet of Things 2014*, pp. 159-65.

Chan, S. & Sohn, G. 2012, 'Indoor localisation using wi-fi based fingerprinting and trilateration techiques for lbs applications', *International Archives of the Photogrammetry, Remote Sensing and Spatial Information Sciences*, vol. 38, no. 4, p. C26.

Chen, C., Lin, S., Lin, T., Chu, Y., Jiang, J., Yang, E., Tseng, C. & Lu, F. 2007, 'Development of wireless sensor network technology-based ecological monitoring system', *Proceedings of International Seminar on Agricultural Structure and Agricultural Engineering (IS-ASAE2008), National Taiwan University, Taipei, Taiwan, December 8-9, 2007*, pp. 120-9.

Chen, Y., Lymberopoulos, D., Liu, J. & Priyantha, B. 2013, 'Indoor Localisation Using FM Signals', *IEEE Transactions on Mobile Computing*, vol. 12, no. 8, pp. 1502-17.

Chen, Y., Yang, Q., Yin, J. & Chai, X. 2006, 'Power-efficient access-point selection for indoor location estimation', *IEEE Transactions on Knowledge and Data Engineering*, vol. 18, no. 7, pp. 877-88.

Cherntanomwong, P. & Suroso, D.J. 2011, 'Indoor localisation system using wireless sensor networks for stationary and moving target', *2011 8th International Conference on Information, Communications & Signal Processing*, IEEE, pp. 1-5.

Cherntanomwong, P., Takada, J.-i. & Tsuji, H. 2009, 'Signal subspace interpolation from discrete measurement samples in constructing a database for location fingerprint technique', *IEICE transactions on communications*, vol. 92, no. 9, pp. 2922-30.

Chuenurajit, T., Phimmasean, S. & Cherntanomwong, P. 2013, 'Robustness of 3D indoor localisation based on fingerprint technique in wireless sensor networks', *2013 10th International Conference on Electrical Engineering/Electronics, Computer, Telecommunications and Information Technology*, pp. 1-6.

Conte, G., De Marchi, M., Nacci, A.A., Rana, V. & Sciuto, D. 2014, 'BlueSentinel: a first approach using iBeacon for an energy efficient occupancy detection system', *BuildSys@ SenSys*, Citeseer, pp. 11-9.

Corna, A., Fontana, L., Nacci, A.A. & Sciuto, D. 2015, 'Occupancy detection via iBeacon on Android devices for smart building management', *2015 Design, Automation & Test in Europe Conference & Exhibition (DATE)*, pp. 629-32.

Costilla-Reyes, O. & Namuduri, K. 2014, 'Dynamic Wi-Fi fingerprinting indoor positioning system', *2014 International Conference on Indoor Positioning and Indoor Navigation (IPIN)*, IEEE, pp. 271-80.

Dahlgren, E. & Mahmood, H. 2014, 'Evaluation of indoor positioning based on Bluetooth Smart technology', *Master of Science Thesis in the Programme Computer Systems and Networks*.

Davis, S.C., Diegel, S.W. & Boundy, R.G. 2009, *Transportation energy data book*, Oak Ridge National Laboratory.

Decuir, J. 2014, 'Introducing Bluetooth Smart: Part II: Applications and updates', *IEEE Consumer Electronics Magazine*, vol. 3, no. 2, pp. 25-9.

Dilger, D.E. 2013, 'Inside iOS 7: iBeacons enhance apps' location awareness via Bluetooth LE', *ed: Apple Insider.–2013.–2013*.

Ding, G., Zhang, J., l, Z. & Tan, Z. 2013, 'Overview of received signal strength based fingerprinting localisation in indoor wireless LAN environments', *2013 5th IEEE International Symposium on Microwave, Antenna, Propagation and EMC Technologies for Wireless Communications*, pp. 160-4.

Ding, R., Qian, Z. & Wang, X. 2010, 'UWB positioning system based on joint TOA and DOA estimation', *Journal of Electronics & Information Technology*, vol. 32, no. 2, pp. 313-7.

Evans, D. 2011, 'The internet of things: How the next evolution of the internet is changing everything', *CISCO white paper*, vol. 1, no. 2011, pp. 1-11.

Fang, S.-H. & Lin, T.-N. 2008, 'Indoor location system based on discriminant-adaptive neural network in IEEE 802.11 environments', *IEEE Transactions on Neural networks*, vol. 19, no. 11, pp. 1973-8.

Fang, S.-H., Lin, T.-N. & Lee, K.-C. 2008, 'A novel algorithm for multipath fingerprinting in indoor WLAN environments', *IEEE transactions on wireless communications*, vol. 7, no. 9, pp. 3579-88.

Fard, H.K., Chen, Y. & Son, K.K. 2015, 'Indoor positioning of mobile devices with agile iBeacon deployment', *2015 IEEE 28th Canadian Conference on Electrical and Computer Engineering (CCECE)*, pp. 275-9.

Feldmann, S., Kyamakya, K., Zapater, A. & Lue, Z. 2003, 'An indoor bluetooth-based positioning system: Concept, implementation and experimental evaluation', *International Conference on Wireless Networks*, vol. 272.

Fujihara, A. & Yanagizawa, T. 2015, 'Proposing an Extended iBeacon System for Indoor Route Guidance', *2015 International Conference on Intelligent Networking and Collaborative Systems*, pp. 31-7.

Gast, M.S. 2014, *Building applications with iBeacon: proximity and location services with Bluetooth low energy*, " O'Reilly Media, Inc.".

Gatesichapakorn, S., Takamatsu, J. & Ruchanurucks, M. 2019, 'ROS based Autonomous Mobile Robot Navigation using 2D LiDAR and RGB-D Camera', *2019 First International Symposium on Instrumentation, Control, Artificial Intelligence, and Robotics (ICA-SYMP)*, pp. 151-4.

Gezici, S., Tian, Z., Giannakis, G.B., Kobayashi, H., Molisch, A.F., Poor, H.V. & Sahinoglu, Z. 2005, 'Localisation via ultra-wideband radios: a look at positioning aspects for future sensor networks', *IEEE signal processing magazine*, vol. 22, no. 4, pp. 70-84.

Gonzalez, G.R., Organero, M.M. & Kloos, C.D. 2008, 'Early infrastructure of an internet of things in spaces for learning', *2008 Eighth IEEE International Conference on Advanced Learning Technologies*, IEEE, pp. 381-3.

Gu, Y., Lo, A. & Niemegeers, I. 2009, 'A survey of indoor positioning systems for wireless personal networks', *IEEE Communications surveys & tutorials*, vol. 11, no. 1, pp. 13-32.

Haeberlen, A., Flannery, E., Ladd, A.M., Rudys, A., Wallach, D.S. & Kavraki, L.E. 2004, 'Practical robust localisation over large-scale 802.11 wireless networks', *Proceedings of the 10th annual international conference on Mobile computing and networking*, ACM, pp. 70-84.

Hahnel, D., Burgard, W., Fox, D., Fishkin, K. & Philipose, M. 2004, 'Mapping and localisation with RFID technology', *IEEE International Conference on Robotics and Automation, 2004. Proceedings. ICRA'04. 2004*, vol. 1, IEEE, pp. 1015-20.

He, Z., Cui, B., Zhou, W. & Yokoi, S. 2015, 'A proposal of interaction system between visitor and collection in museum hall by iBeacon', *2015 10th International Conference on Computer Science & Education (ICCSE)*, pp. 427-30.

Hong-Shik, K. & Jong-Suk, C. 2008, 'Advanced indoor localisation using ultrasonic sensor and digital compass', *2008 International Conference on Control, Automation and Systems*, pp. 223-6.

Honkavirta, V., Perala, T., Ali-Loytty, S. & Piché, R. 2009, 'A comparative survey of WLAN location fingerprinting methods', *2009 6th workshop on positioning, navigation and communication*, IEEE, pp. 243-51.

Iglesias, H.J.P., Barral, V. & Escudero, C.J. 2012, 'Indoor person localisation system through RSSI Bluetooth fingerprinting', *2012 19th International Conference on Systems, Signals and Image Processing (IWSSIP)*, IEEE, pp. 40-3.

Ilyas, M. & Mahgoub, I. 2004, *Handbook of sensor networks: compact wireless and wired sensing systems*, CRC press.

Ji, X. & Zha, H. 2004, 'Sensor positioning in wireless ad-hoc sensor networks using multidimensional scaling', *IEEE INFOCOM 2004*, vol. 4, IEEE, pp. 2652-61.

Jiang, Y., Pan, X., Li, K., Lv, Q., Dick, R.P., Hannigan, M. & Shang, L. 2012, 'Ariel: Automatic wi-fi based room fingerprinting for indoor localisation', *Proceedings of the 2012 ACM Conference on Ubiquitous Computing*, ACM, pp. 441-50.

Johnson, L., Adams, S., Cummins, M., Estrada, V., Freeman, A. & Ludgate, H. 2013, 'The NMC Horizon Report: 2012 Higher Education Edition Austin', *Texas: The New Media Consortium*.

Kang, D., Namgoong, Y., Yang, S., Choi, S. & Shin, Y. 2006, 'A simple asynchronous UWB position location algorithm based on single round-trip transmission', *2006 8th International Conference Advanced Communication Technology*, vol. 3, IEEE, pp. 4 pp.-1461.

Karunarathna, M. & Dayawansa, L. 2006, 'Energy absorption by the human body from RF and microwave emissions in Sri Lanka', *Sri Lankan Journal of Physics*, vol. 7.

Kharidia, S.A., Ye, Q., Sampalli, S., Cheng, J., Du, H. & Wang, L. 2014, 'HILL: A Hybrid Indoor Localisation Scheme', *2014 10th International Conference on Mobile Ad-hoc and Sensor Networks*, pp. 201-6.

Kim, C. & Lee, S. 2014, 'A research on Beacon code architecture extension using category and code Beacon structure', *2014 International Conference on Information and Communication Technology Convergence (ICTC)*, pp. 187-8.

Koühne, M. & Sieck, J. 2014, 'Location-Based Services with iBeacon Technology', *2014 2nd International Conference on Artificial Intelligence, Modelling and Simulation*, pp. 315-21.

Kumagai, J. & Cherry, S. 2004, 'Sensors and sensibility', *IEEE Spectrum*, vol. 41, no. 7, pp. 22-6.

Kuo, S.-P., Wu, B.-J., Peng, W.-C. & Tseng, Y.-C. 2007, 'Cluster-enhanced techniques for pattern-matching localisation systems', *2007 IEEE International Conference on Mobile Adhoc and Sensor Systems*, IEEE, pp. 1-9.

Laoudias, C., Michaelides, M.P. & Panayiotou, C. 2011, 'Fault tolerant fingerprint-based positioning', *2011 IEEE International Conference on Communications (ICC)*, IEEE, pp. 1-5.

Li, X.-Y., Wan, P.-J. & Frieder, O. 2003, 'Coverage in wireless ad hoc sensor networks', *IEEE Transactions on computers*, vol. 52, no. 6, pp. 753-63.

Li, X. & Cao, F. 2014, 'Location based TOA algorithm for UWB wireless body area networks', *2014 IEEE 12th International Conference on Dependable, Autonomic and Secure Computing*, IEEE, pp. 507-11.

Li, Z., Dehaene, W. & Gielen, G. 2009, 'A 3-tier UWB-based indoor localisation system for ultra-low-power sensor networks', *IEEE Transactions on Wireless Communications*, vol. 8, no. 6, pp. 2813-8.

Liu, H., Darabi, H., Banerjee, P. & Liu, J. 2007, 'Survey of wireless indoor positioning techniques and systems', *IEEE Transactions on Systems, Man, and Cybernetics, Part C (Applications and Reviews)*, vol. 37, no. 6, pp. 1067-80.

Meltzer, D., Chung, J., Khalili, P., Marlow, E., Arora, V., Schumock, G. & Burt, R. 2010, 'Exploring the use of social network methods in designing healthcare quality improvement teams', *Social science & medicine*, vol. 71, no. 6, pp. 1119-30.

Misra, P. & Enge, P. 1999, 'Special issue on global positioning system', *Proceedings of the IEEE*, vol. 87, no. 1, pp. 3-15.

Moses, R.L., Krishnamurthy, D. & Patterson, R.M. 2003, 'A self-localisation method for wireless sensor networks', *EURASIP Journal on Advances in Signal Processing*, vol. 2003, no. 4, p. 839843.

Nagpal, R., Shrobe, H. & Bachrach, J. 2003, 'Organizing a global coordinate system from local information on an ad hoc sensor network', *Information processing in sensor networks*, Springer, pp. 333-48.

Ng, H., Sim, M. & Tan, C. 2006, 'Security issues of wireless sensor networks in healthcare applications', *BT Technology Journal*, vol. 24, no. 2, pp. 138-44.

Niculescu, D. & Nath, B. 2003, 'DV based positioning in ad hoc networks', *Telecommunication Systems*, vol. 22, no. 1-4, pp. 267-80.

Olule, E., Wang, G., Guo, M. & Dong, M. 2007, 'Rare: An energy-efficient target tracking protocol for wireless sensor networks', *2007 International Conference on Parallel Processing Workshops (ICPPW 2007)*, IEEE, pp. 76-.

Osterlind, F., Pramsten, E., Roberthson, D., Eriksson, J., Finne, N. & Voigt, T. 2007, 'Integrating building automation systems and wireless sensor networks', *2007 IEEE Conference on Emerging Technologies and Factory Automation (EFTA 2007)*, IEEE, pp. 1376-9.

Otsason, V., Varshavsky, A., LaMarca, A. & De Lara, E. 2005, 'Accurate GSM indoor localisation', *International conference on ubiquitous computing*, Springer, pp. 141-58.

Papamanthou, C., Preparata, F.P. & Tamassia, R. 2008, 'Algorithms for location estimation based on RSSI sampling', *International Symposium on Algorithms and Experiments for Sensor Systems, Wireless Networks and Distributed Robotics*, Springer, pp. 72-86.

Pei, L., Chen, R., Liu, J., Tenhunen, T., Kuusniemi, H. & Chen, Y. 2010, 'Inquiry-based bluetooth indoor positioning via rssi probability distributions', *2010 Second International Conference on Advances in Satellite and Space Communications*, IEEE, pp. 151-6.

Porcino, D. & Hirt, W. 2003, 'Ultra-wideband radio technology: potential and challenges ahead', *IEEE communications magazine*, vol. 41, no. 7, pp. 66-74.

Savvides, A., Han, C.-C. & Strivastava, M.B. 2001, 'Dynamic fine-grained localisation in ad-hoc networks of sensors', *Proceedings of the 7th annual international conference on Mobile computing and networking*, ACM, pp. 166-79.

Schauer, L., Dorfmeister, F. & Maier, M. 2013, 'Potentials and limitations of wifi-positioning using time-of-flight', *International Conference on Indoor Positioning and Indoor Navigation*, IEEE, pp. 1-9.

Sen, S., Chakraborty, S. & Sutradhar, A. 2015, 'Estimation of vehicle yaw rate and lateral motion for dynamic stability control using unscented Kalman filtering (UKF) approach', *Michael Faraday IET International Summit 2015*, pp. 24-9.

Shang, F., Champagne, B. & Psaromiligkos, I.N. 2014, 'A ML-based framework for joint TOA/AOA estimation of UWB pulses in dense multipath environments', *IEEE Transactions on Wireless Communications*, vol. 13, no. 10, pp. 5305-18.

Tekinay, S. 1998, 'Wireless geolocation systems and services', *IEEE Communications Magazine*, vol. 36, no. 4, pp. 28-.

Townsend, K., Cufí, C. & Davidson, R. 2014, *Getting started with Bluetooth low energy: tools and techniques for low-power networking*, " O'Reilly Media, Inc.".

Ueda, H., Lee, J.H., Okamoto, S., Byung-Ju, Y. & Yuta, S. 2011, 'People tracking method for a mobile robot with laser scanner and omni directional camera', *2011 8th International Conference on Ubiquitous Robots and Ambient Intelligence (URAI)*, pp. 503-7.

Varsamou, M. & Antonakopoulos, T. 2014, 'A bluetooth smart analyzer in iBeacon networks', *2014 IEEE Fourth International Conference on Consumer Electronics Berlin (ICCE-Berlin)*, pp. 288-92.

Varshavsky, A., De Lara, E., Hightower, J., LaMarca, A. & Otsason, V. 2007, 'GSM indoor localisation', *Pervasive and mobile computing*, vol. 3, no. 6, pp. 698-720.

Wang, J., Chen, C., Lin, T., Chuang, C., Lai, T. & Jiang, J. 2012, 'High-Precision RSSI-based Indoor Localisation Using a Transmission Power Adjustment Strategy for Wireless Sensor Networks', *2012 IEEE 14th International Conference on High Performance Computing and Communication & 2012 IEEE 9th International Conference on Embedded Software and Systems*, pp. 1634-8.

Wang, K., Nirmalathas, A., Lim, C., Alameh, K. & Skafidas, E. 2016, 'Optical Wireless-Based Indoor Localisation System Employing a Single-Channel Imaging Receiver', *Journal of Lightwave Technology*, vol. 34, no. 4, pp. 1141-9.

Wang, M., Xue, B., Wang, W. & Yang, J. 2017, 'The design of multi-user indoor UWB localisation system', *2017 2nd International Conference on Frontiers of Sensors Technologies (ICFST)*, pp. 322-6.

Wang, T., Chen, X., Ge, N. & Pei, Y. 2013, 'Error analysis and experimental study on indoor UWB TDoA localisation with reference tag', *2013 19th Asia-Pacific Conference on Communications (APCC)*, IEEE, pp. 505-8.

Wang, Y., Ye, Q., Cheng, J. & Wang, L. 2015, 'RSSI-Based Bluetooth Indoor Localisation', *2015 11th International Conference on Mobile Ad-hoc and Sensor Networks (MSN)*, pp. 165-71.

Want, R., Hopper, A., Falcao, V. & Gibbons, J. 1992, 'The active badge location system', *ACM Transactions on Information Systems (TOIS)*, vol. 10, no. 1, pp. 91-102.

Wassi, G.I., Despins, C., Grenier, D. & Nerguizian, C. 2005, 'Indoor location using received signal strength of IEEE 802.11 b access point', *Canadian Conference on Electrical and Computer Engineering, 2005.*, IEEE, pp. 1367-70.

Wymeersch, H., Maranò, S., Gifford, W.M. & Win, M.Z. 2012, 'A machine learning approach to ranging error mitigation for UWB localisation', *IEEE transactions on communications*, vol. 60, no. 6, pp. 1719-28.

Xiong, H., Wang, J., Tian, H., Yang, H. & Yi, K. 2010, 'Investigation of UWB positioning based on antenna array', *Systems Engineering and Electronics*, vol. 32, no. 2.

Yang, S. & Wang, B. 2017, 'Residual based weighted least square algorithm for Bluetooth/UWB indoor localisation system', *2017 36th Chinese Control Conference (CCC)*, IEEE, pp. 5959-63.

Yin, J., Yang, Q. & Ni, L.M. 2008, 'Learning adaptive temporal radio maps for signal-strength-based location estimation', *IEEE transactions on mobile computing*, vol. 7, no. 7, pp. 869-83.

Youssef, M. & Agrawala, A. 2005, 'The Horus WLAN location determination system', *Proceedings of the 3rd international conference on Mobile systems, applications, and services*, ACM, pp. 205-18.

Zhang, S., Han, R., Huang, W., Wang, S. & Hao, Q. 2018, 'Linear Bayesian Filter Based Low-Cost UWB Systems for Indoor Mobile Robot Localisation', *2018 IEEE SENSORS*, pp. 1-4.

Zhao, J. & Mili, L. 2019, 'A Decentralized H-Infinity Unscented Kalman Filter for Dynamic State Estimation Against Uncertainties', *IEEE Transactions on Smart Grid*, vol. 10, no. 5, pp. 4870-80.

Zhao, Y., Yang, Y. & Kyas, M. 2011, 'Comparing centralized Kalman filter schemes for indoor positioning in wireless sensor network', *2011 International Conference on Indoor Positioning and Indoor Navigation*, IEEE, pp. 1-10.

Zhou, S., Wang, B., Mo, Y. & Liu, W. 2012, 'Indoor multi-resolution subarea localisation based on received signal strength fingerprint', *2012 International Conference on Wireless Communications and Signal Processing (WCSP)*, pp. 1-6.

Appendix

Publication

Book Chapters (Published):

1. Yu Z., Chaczko Z., Shi J. (2020) Low Cost Wireless Micro-Electro-Mechanical-Systems Accelerometers Linear Sensor Model. In: Klempous R., Nikodem J. (eds) Smart Innovations in Engineering and Technology. ICACON 2017, APCASE 2017. Topics in Intelligent Engineering and Informatics, vol 15. Springer, Cham
2. Chaczko Z., Chiu C., Yu Z. (2020) Assessment of a Multi-agent RFID Platform for Industrial Logistic Operations. In: Klempous R., Nikodem J. (eds) Smart Innovations in Engineering and Technology. ICACON 2017, APCASE 2017. Topics in Intelligent Engineering and Informatics, vol 15. Springer, Cham

Papers (Published)

3. Yu Z, Chaczko Z, Optimization of IMU Indoor Localization with Wireless Sensors, 2018 4th IEEE International Conference on Computer and Communications, December 7-10, 2018.
4. Yu Z, Chaczko Z, Jiang J. Development and Optimization of Wireless Indoor Localization Error Modelling, International Conference on Systems Engineering. IEEE Computer Society, 2017:475-479.